Histological, Trace Element, and Stable Isotopic Reconstruction of Dental Development, Diet, and Weaning in Ugandan Chimpanzees (*Pan troglodytes schweinfurthii*): Implications for Studies of Hominin Life History

by

Máire A. Malone

A dissertation submitted in partial fulfillment
of the requirements for the degree of
Doctor of Philosophy
(Anthropology)
in the University of Michigan
2019

Doctoral Committee:

Professor John Kingston, Co-Chair
Professor Laura MacLatchy, Co-Chair
Professor Jacinta Beehner
Professor Gary Schwartz, Arizona State University
Dr. B. Holly Smith

Maire A. Malone

malonema@umich.edu

ORCID iD: 0000-0002-4876-0637

Acknowledgements

I am grateful to the University of Michigan's Rackham Graduate School, the African Studies Center, and the International Institute for assistance in funding this research, as well as to John Mitani and the other researchers at the Ngogo Chimpanzee Project in Kibale National Park, Robert Kityo at Makarere University's Zoology Museum, Milford Wolpoff, and Jacinta Beehner for access to specimens. Permits to export, import and sample the specimens in this study were obtained from the Ugandan Wildlife Authority and Ugandan National Center for Science and Technologies, as well as the United Stated Department of Fish and Wildlife, the Convention on International Trade in Endangered Species, and the Centers for Disease Control.

I'm eternally grateful to Laura MacLatchy for acting as my advisor and mentor, and for her patience and guidance. My thanks go also to John Kingston for his constant role as a collaborator and sounding board, to Gary Schwartz, Holly Smith, and Jacinta Beehner for their training, advice, and for acting as my committee. I'm also grateful to John Mitani for helpful feedback, to Maureen Devlin, Guillaume Girard, Steve Sostrum, and Jason Curtis, for training, sample analysis, and access to lab facilities, and to Wendy Dirks and Amon Mugume for various forms of guidance.

I am also indebted to numerous colleagues for helpful conversations and insights, espcecially Marcela Benitez, Chelsea Fisher, Rachna Reddy, Aaron Sandel, Bethany Hansen, Elizabeth Tinsley-Johnson, Julia Stuhltrager, and the MacLatchy Lab Group.

Table of Contents

List of Tables

List of Figures

Abstract

Understanding the origins of the modern human life history profile, or the scheduling of energy tradeoffs between growth, somatic maintenance, and reproduction, is a key issue in biological anthropology. In order to determine when, and in what contexts, the modern human life history profile evolved, we must look to our hominin ancestors in the fossil record to reconstruct their diets and life histories, as well as to our closest living relatives, the chimpanzees, for clues to the links between observed life history variables, such as weaning age, and hard tissue evidence for changes in diet and developmental pace that may also preserve in the fossil record. This project investigates the relationships between the dental development, the weaning process, and the diets of wild Ugandan chimpanzees (*Pan troglodytes schweinfurthii*) using three different, but interrelated methods.

The first study uses histological analysis to compare dental formation and emergence variables between individuals from several chimpanzee communities, and results suggest that the chimpanzees from the Ngogo community have delayed dental development and life history pace relative to other communities of this subspecies (*Pan troglodytes schweinfurthii*). It is also found that the range of ages at first molar emergence across these wild chimpanzee communities overlaps with that previously documented for captive chimpanzees. A final finding is that a growth spurt during first molar root formation of the Ngogo chimpanzees in this study likely coincides with the age at which this tooth comes into functional occlusion, slightly preceding inferred ages at weaning completion documented by other researchers using a fecal isotope study

of Ngogo infant chimpanzees.

The second study examines the relationship between trace elemental distributions in chimpanzee dental tissues and structural indicators of developmental pace established in the previous study, to assess whether the first molar root growth spurt shows evidence of aligning with weaning completion. This work uses laser ablation inductively coupled plasma-mass spectrometry (LA ICP-MS) to collect calcium-normalized barium (Ba/Ca) values from the first molars used in the previous study, and finds that the distribution of this apparent proxy for dietary change within the enamel and dentine of these chimpanzees' teeth supports the link between the timing of the root growth spurt and weaning completion proposed in the first study.

The third study attempts to disentangle the numerous sources of variability in chimpanzee dietary inputs, which manifest in their bodily tissues, and which inform studies of dietary reconstruction, paleoecology, and life history for extinct taxa, including fossil hominins. Stable isotope analyses of carbon ($\delta^{13}C$), oxygen ($\delta^{18}O$), and nitrogen ($\delta^{15}N$) are conducted on bone, teeth, and hair of the chimpanzees used in the previous two studies, and the variation in these isotopic outputs within an individual's tissues, between the different tissues, and between individuals is in some cases great enough that this could obscure sources of dietary variation in fossil taxa to whom these same methods are applied. Another finding is that isotopic variation in sources of dietary inputs, either from different dietary items themselves, or from the same items growing in different environments, could confound interpretations of fossil hominin diets.

Taken together, these three studies use structural markers of root growth rate and chemical markers of dietary changes to develop a proxy for weaning completion in chimpanzees, and present a refined diet-to-enamel $\delta^{13}C$ offset value to be used in future primate dietary reconstructions.

Chapter 1: Introduction

Understanding the origins of the modern human life history profile, or the scheduling of energy tradeoffs between growth, somatic maintenance, and reproduction (Stearns, 1992), is a key issue in biological anthropology. In order to understand when, and in what contexts, the modern human life history profile evolved, we must look to our hominin ancestors in the fossil record to reconstruct their life histories.

The fossil record, however, is limited to bones and teeth, and even within those hard tissues, it is only the enamel that survives the millenia relatively unchanged. Investigations of fossil hominin life history are, therefore, constrained by what these hard tissues can tell us about past growth, somatic maintenance, and reproduction, and accessing evidence for energetic tradeoffs between key life history events or parameters, such as gestation length, age at weaning, age at first reproduction, and interbirth interval, presents numerous challenges.

Since teeth preserve a structural record of their growth processes, are less succeptible than bone to diagenetic alterations, and are found with relative frequency in the fossil record, they make an ideal avenue for investigations of diet and growth in extinct taxa. An understanding of the diverse ways that development, diet, and life history manifest in the hard tissues of living apes, including our closest living relatives, the chimpanzees, is therefore critical to interpretations of these factors in fossil taxa. Diet acts as an organism's interface between its own development and the environment it inhabits, since the contents of its developing tissues come

from the food and water it ingests, and these, in turn, are products of environmental conditions surrounding them. This project investigates the relationships between the dental development, the weaning process, and the diets of wild Ugandan chimpanzees (*Pan troglodytes schweinfurthii*) using three different, but interrelated methods.

The first study uses histological analysis to measure and compare dental formation and emergence variables between individuals from several chimpanzee communities, to assess whether chimpanzees from Ngogo have delayed dental development relative to other populations, and to situate that outcome within life history theory. The second study examines the relationship between trace elemental distributions in chimpanzee dental tissues and structural indicators of developmental pace, to assess whether a peak in M1 root growth rate shows evidence of aligning with weaning completion. The third study attempts to disentangle the numerous sources of variability in chimpanzee dietary inputs, which manifest in their various bodily tissues, and which inform studies of dietary reconstruction, paleoecology, and life history for extinct taxa, including fossil hominins.

The first core chapter, entitled "Chapter 2: Histological reconstruction of dental development, stress, and life history of chimpanzees (*Pan troglodytes schweinfurthii*) from Kibale National Park, Uganda", explores the relationship between dental development and life history for members of several communities of chimpanzees from Uganda, focusing on the Ngogo community, due to their unusually large group size, low mortality rates, and consistently adundant food resources (Wood et al., 2017). The Ngogo chimpanzee community has been continuously studied since 1993, and John Mitani, David Watts, and Kevin Langergraber have been involved with the Ngogo Chimpanzee Research Project since its beginning.

Figure 1: Map of *Pan* subspecies distribution throughout African continent with locations of several long-term study sites

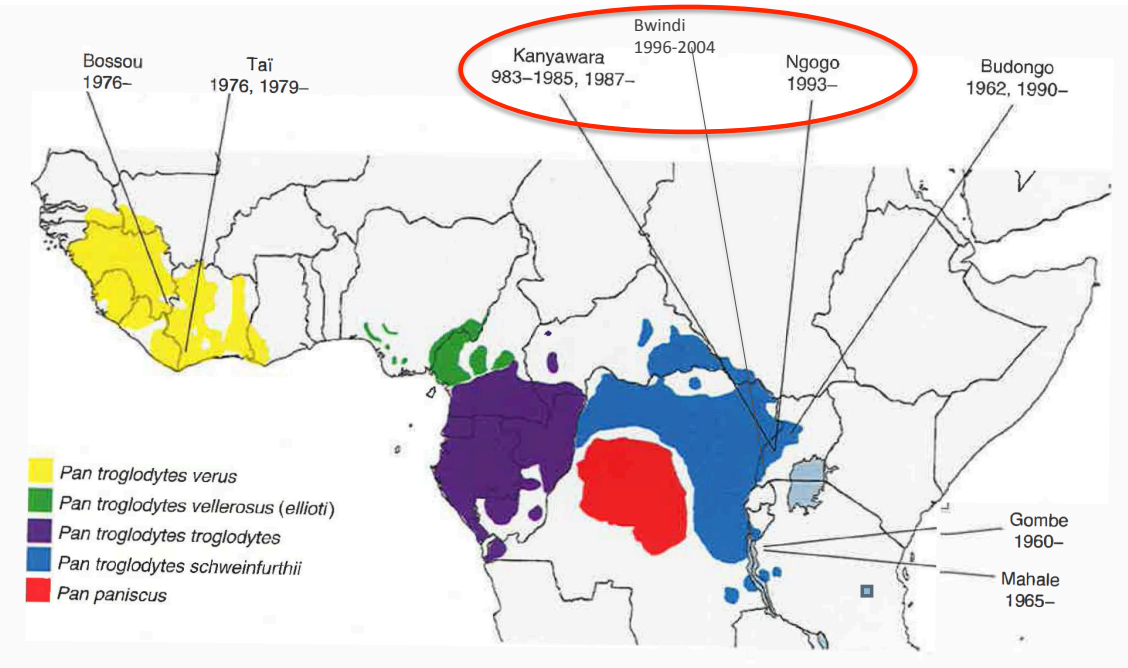

Figure 1: The above map shows the distributions of various *Pan* subspecies across the African continent, with the distribution of *Pan troglodytes schweinfurthii*, the subspecies in focus in this study, shown in blue, and the sites from which the chimpanzees in this study originate circled in red, including the individuals from Kanyawara from Machanda et al. (2015).

One of the aims of this chapter is to document variability in dental developmental parameters between the Ngogo chimpanzees and those from several other *P.t. schweinfurthii* communities, to assess how much dental developmental variability to expect within a single subspecies. Another aim is to try and disentangle the complex interplay between dental formation rates, the dental eruption process, and the weaning process for the Ngogo chimpanzees, since direct biogeochemical evidence for the weaning process in this population has been documented (Badescu et al., 2017). To accomplish this, the work of Dean and Cole (2013) was expanded upon to explore the previously reported association between the age at which the first mandibular molar (M_1) emerges through the gingiva and a growth spurt that occurs during the root formation process in chimpanzees. This growth spurt appears to occur

several months after initial emergence (Dean and Cole, 2013), which may place it closer to the isotopically inferred weaning completion age, thereby creating a precise structural proxy for this important life history variable. A final aim is to explore whether certain dental developmental parameters, such as first molar gingival emergence age, differ between captive and wild chimpanzees. Each of these aims is geared toward refining methods of characterizing dental development, and its links with the weaning process, in the closest extant relative to humans, in order to more accurately infer life history pace in fossil hominins and hominoids.

The second core chapter, entitled "Chapter 3: Calcium-normalized barium (Ba/Ca) distributions in enamel and dentine of wild Ugandan chimpanzees (*Pan troglodytes schweinfurthii):* Implications for weaning studies in fossil taxa" seeks to link structural markers of growth pace in chimpanzee first molars (M_1) with trace element evidence for dietary transitions associated with the weaning process. Previous work has demonstrated the effectiveness of using changing levels of barium throughout tooth development to indicate levels of maternal milk intake (Austin et al., 2013; Smith et al., 2017; Smith et al., 2018).

This study finds that in the first molars (M1), of most of the chimpanzees in this sample, the calcium-normalized barium (Ba/Ca) intensity increased between birth and the first three to six months of life, and then gradually decreased over the next year of formation. Occasional spikes in M1 Ba/Ca intensity occurred after that point and may indicate increases in nursing frequency within the second year of life, or if these spikes are brief, they could result from episodes of illness or nutritional deficiency in which the infant's own skeletal stores of calcium (and therefore, barium) were mobilized and incorporated into dental tissues forming at that time. Variation in enamel Ba/Ca levels from several later forming teeth are included to show spikes in Ba/Ca levels at the time of the root growth spurt, which then lower again, and stay at low levels

thereafter, except in cases where there was taphonomic damage to the enamel. In several cases, the patterns of Ba/Ca change are harder to discern, due to sampling issues, damage to enamel crowns, or extreme outlier values that drive the range of variation to be too wide to pick up subtle changes. Methods of troubleshooting these and other issues are presented.

The third core chapter is entitled "Chapter 4: Isotopic variability within the tissues of *Pan troglodytes schweinfurthii* informs efforts at fossil hominin dietary reconstruction and underscores the need for habitat-specific plant isotope studies". This chapter attempts to address how the many sources of variation in diet, and the ways that dietary items are incorporated into the tissues of the body in living taxa, complicate attempts to use stable isotopic analysis of enamel apatite to interpret and characterize the diets of fossil taxa, including hominins.

The final chapter is entitled "Chapter 5: Conclusions, Implications, Future Directions". In this chapter are summarized the main results and findings of the three core chapters, as well as their implications for advancing studies of life history and dietary reconstruction in extant and fossil taxa. The relevance of the outcomes of each study is discussed, as are common themes running throughout the chapters, and future projects related to these topics are also explored.

Works Cited

Bădescu, I., Katzenberg, M. A., Watts, D. P., and Sellen, D. W. 2017. A novel fecal stable isotope approach to determine the timing of age-related feeding transitions in wild infant chimpanzees. American Journal of Physical Anthropology, 162(2), 285–299. http://doi.org/10.1002/ajpa.23116

Dean, M. C., and Cole, T. J. 2013. Human Life History Evolution Explains Dissociation between the Timing of Tooth Eruption and Peak Rates of Root Growth. PLoS ONE, 8(1). http://doi.org/10.1371/journal.pone.0054534.

Stearns, S.C. 1992. The evolution of life histories. Oxford: Oxford University Press.

Wood, B. M., Watts, D. P., Mitani, J. C., and Langergraber, K. E. 2017. Favorable ecological circumstances promote life expectancy in chimpanzees similar to that of human hunter-gatherers. Journal of Human Evolution, 105, 41-56.

Chapter 2: Histological reconstruction of dental development, stress, and life history of chimpanzees (*Pan troglodytes schweinfurthii*) from Kibale National Park, Uganda

Abstract: Understanding the dental development of our closest living relative, the chimpanzee, is essential for providing a clearer picture of the relationships among the dental development, ecology, and life histories of fossil hominins. This study presents novel and detailed dental developmental data from the Ngogo community of wild chimpanzees (*Pan troglodytes schweinfurthii)* from Kibale National Park, Uganda. A number of dental developmental variables are compared between members of this population and those of other chimpanzee populations. Compared with previous work, this study notes increased average enamel daily secretion rates (DSR) and expands the known range of Retzius line periodicity (RP) in chimpanzees. Total crown formation times (TFT) are determined using enamel and dentine structures, and root formation times and extension rates reveal ages when rooth growth spurts occurred, which are then used as a variable to predict life history events linked with the initial gingival emergence* of the lower first molar (M_1). Episodes of stress are documented using the timing and frequency of accentuated lines in enamel and dentine, and the patterns are used to infer the timing of the weaning process. The Ngogo chimpanzees show overall later inferred ages of M_1 emergence and occlusion compared with other Ugandan chimpanzees, which may be related to their lower

*All further mentions of "emergence" in this text will refer to the initial gingival emergence stage of the eruption process, and not to alveolar emergence, nor to any time between gingival emergence and functional occlusion.

extrinsic mortality risk. Despite the small size of this sample, the data from these new individuals increase three-fold what is known about dental development in this subspecies. This expanded sample of wild chimpanzee dental developmental data also provides, for the first time, evidence that the range of variation in M_1 emergence ages represented within this single subspecies is at least as large as the variation documented thus far for captive chimpanzees. Overall, these data add to the current picture of the range of variation in wild chimpanzee dental development, they support a link between molar root extension rates, molar emergence and occlusion timing, and the weaning process, and they augment the great ape data pool with which the dental development and life history data of fossil hominins can be compared.

Introduction: A fundamental issue in biological anthropology concerns the evolution of hominin life history. The modern human pace of life history, or the scheduling of developmental milestones, is unusual, even among hominoids. We develop slowly, but wean early. We begin reproducing somewhat later in life compared with other apes, but have short interbirth intervals. In addition, we humans have a unique developmental stage called childhood, during which parental care allows for prolonged social and cognitive development (Schultz, 1960; Harvey and Clutton-Brock, 1985; Bogin, 1990). Understanding when and in what evolutionary contexts this pattern of growth and development emerged is critical for reconstructing hominin life histories (Schwartz, 2012).

Because the pace of dental development is closely linked with many aspects of life history (Smith, 1989), and because dental tissues preserve a record of their incremental growth (Risnes, 1998), teeth present an ideal tool for exploring hominin life history evolution and variation. In order to understand how dental development and life history varied among different

hominins, dental development and life history data from closely related extant taxa, specifically, humans and great apes, are used as comparative groups (reviewed in Kelley and Schwartz, 2012). Such studies aim to determine whether a particular fossil hominin's life history pace was more "ape-like" (e.g. Bromage and Dean, 1985; Anemone et al., 1996), or more "human-like" (Mann, 1987), with the majority of these studies assigning the hominins in question a more ape-like pace (e.g. Beynon and Dean, 1987; 1988), and suggesting that the modern human pace of life history evolved relatively recently (reviewed in Schwartz, 2012). However, the types of comparative dental developmental data used, as well as the sources of such data, have varied greatly, due to the limited numbers of ape specimens available for study, the often-destructive nature of analytical methods (e.g. dissection of in situ teeth from the jaws, histological sectioning, etc.), and an underdeveloped picture of the variation in dental development within and between apes at the level of species, subspecies, and population. Collecting such data from different populations of the same subspecies may reveal more of the variability to be expected for *Pan,* overall, and this, in turn, will allow for a more thoroughly representative "ape" sample to be used in comparisons with fossil hominins.

Considerable amounts of human dental developmental data are available for study (e.g., Hillson, 2005; AlQahtani et al., 2010), but similar dental developmental data from wild chimpanzees are limited (Zihlman et al., 2004; Machanda et al., 2015). Importance has been placed upon using only wild chimpanzee dental development in comparison with that of modern humans and fossil hominins, due, in part, to the proposed developmental acceleration in captive versus wild chimpanzees, resulting from the artificial conditions, food provisioning, and different energetic outputs for chimpanzees in captivity (Zihlman et al., 2004). There is some debate, however, about whether this delay manifests dentally in wild chimpanzees (Zihlman et al., 2007;

Smith et al., 2010), so additional dental developmental data from new wild chimpanzee populations will add valuable data points to the currently sparse comparative sample. This will permit more rigorous comparisons to be made between the dental development and life histories of wild and captive chimpanzees, thereby furthering our understanding of the appropriateness of using captive chimpanzee dental developmental data in comparisons with fossil hominin dental development and associated life histories.

Given the very small sample sizes available for study, it is also unknown how variable wild chimpanzee dental development can be across a species, or even for different populations within the same subspecies living in different ecological conditions. For East African chimpanzees (*Pan troglodytes schweinfurthii*), there are confidently known M_1 eruption data (from initial gingival emergence through occlusion) available for only three individuals from Kanyawara (Machanda et al., 2015). The current study produces estimated M_1 emergence and occlusion ages for seven additional *P. t. schweinfurthii* individuals: four from Ngogo, two from neighboring communities that are just outside of Ngogo (but are not Kanyawara), and one from Bwindi Impenetrable Nation Park. While ten total individuals from five different communities cannot illustrate the overall variation in East African chimpanzee dental development, these new data more than triple the size of the sample available for the subspecies.

Background: Teeth are a valuable medium for the analysis of developmental timing in extinct taxa, due to their relative abundance in the fossil record, their resistance to post-mortem alteration, and because they preserve an exact record of their development in their incremental microstructures (e.g. Risnes, 1998; Dean, 2000; Antoine et al., 2009). Such structures can be

periodic, forming at regular, consistent intervals (e.g. cross-striations and Retzius lines in enamel or von Ebner's lines and Andresen lines in dentine), or they can be aperiodic, and exist as visible

Table 1: Dental abbreviations and definitions used in this study

Abbreviation	Definition	Abbreviation	Definition	Abbreviation	Definition
ICDSR	Inner cuspal daily secretion rate	RP	Retzius line periodicity	EDJ	Enamel-dentine junction
MCDSR	Middle cuspal daily secretion rate	CFT	Cuspal formation time	M1	First molar
OCDSR	Outer cuspal daily secretion rate	RFT	Root formation time	M2	Second molar
IIDSR	Inner imbricational daily secretion rate	TFT	Total formation time	M3	Third molar
MIDSR	Middle imbricational daily secretion rate	R#	Retzius line number	P4	Fourth premolar
OIDSR	Outer imbricational daily secretion rate	APV*	Age at peak root growth velocity	IFT	Imbricational formation time
DDSR	Dentine daily secretion rate	ER	Extension rate	CEJ	Cemento-enamel junction
CI	Crown initiation age	CC	Crown completion age	IBI	Inter-birth interval

Table 1: Detailed descriptions and methods of measurement of the above abbreviations are given in Background and Methods.

*APV is the term used by Dean and Cole (2013) but which is referred to here as the root growth spurt age.

structures resulting from growth processes, but not subject to any known time-dependency (e.g. enamel prisms, dentine tubules, and Hunter-Schreger bands) (reviewed in Smith, 2008). Structures can also form as a result of disturbances to normal growth, and these form at irregular intervals influenced by any number of external and internal factors (discussed further below and also see Goodman and Rose, 1990; Bowman, 1991; Macho et al., 1996; Simpson, 1999; Guatelli-Steinberg, 2001; Thomas, 2003; Guatelli-Steinberg, 2004; Skinner and Hopwood, 2004). Each type of structure forms in all three dental tissues (enamel, dentine, and cementum), but only those in enamel will be reviewed here, with the corresponding structures in dentine included where relevant.

Periodic structures: As teeth start to develop (see Figure 2a), ameloblasts (enamel-forming cells) secrete enamel matrix as they move away from the enamel-dentine junction (EDJ) in a 24-hour (short-period) interval, thereby forming enamel prisms and thickening the enamel (Boyde, 1989). This happens first in the formation of cuspal or appositional enamel, which increases a tooth's height, and subsequently with the imbricational (lateral and cervical), enamel (Dean, 1998). Once the cuspal enamel reaches a predetermined thickness, new ameloblasts from along the EDJ are recruited to start forming additional enamel prisms, and they begin to extend the enamel-forming front cervically (away from the cusp) (Boyde, 1989). Each new cohort of recruited cells begins moving away from the EDJ in a staggered pattern, and this movement is interrupted at a longer-period regular interval, marking the progress of all the enamel-forming cells at that moment in time (Antoine et al., 2009). The two main periodic structures in enamel, cross-striations and Retzius lines (both detailed below), are left behind as evidence of the fluctuations in these interwoven rhythms of growth. Odontoblasts (dentine-forming cells) begin along the EDJ also, but they move inward toward the pulp cavity of the tooth as they secrete dentine, and they leave behind tubules as tracks of their movement that correspond to enamel prisms (Dean and Scandrett, 1996).

Cross-Striations/von Ebner's lines: As they secrete enamel, the ameloblasts leave behind evidence of their daily secretion rate (DSR) in the form of alternating dark and light bands called cross-striations (Boyde, 1989), due to the circadian rhythm of metabolic activity (Antoine et al., 2009). Von Ebner's lines are the daily-forming lines that appear in dentine (Dean and Scandrett, 1996), and DSR can also be determined for dentine using these features. Numerous studies have demonstrated this 24-hour rhythm of growth in enamel and dentine, some of which employed

experiemental means to confirm this daily cycle of formation (e.g. Schour and Hoffman, 1939b; Okada, 1943; Okada, 1945; Bromage, 1991; Ohtsuka and Shinoda,1995; Rinaldi, 1999; Ohtsuka-Isoya et al., 2001; Smith et al., 2007), and some have precisely measured the number of days of growth that could be seen in well-preserved teeth and compared this with known dates of birth and death (e.g. Antoine et al., 2009).

The exact physiological mechanisms behind the formation of alternating dark and light daily bands in enamel and dentine, when viewed using transmitted and polarized light, have not been definitively resolved, but the pattern has been thought to result from either differing pH levels in the blood circulating during day versus night (and consequently incorporated into tissues forming during those times), or from prism/tubule orientation differences, or both (Okada, 1943).

Striae of Retzius: Cross-striations, as short-period lines, are thought to represent daily increments of enamel secretion, but there are also long-period lines, called striae of Retzius or Retzius lines, which form at longer intervals and represent the location of the forming enamel front at the time of that regular disruption to the mineralization process (Retzius, 1837; Smith, 2004) (See figure 2b). In dentine, these long-period lines are known as Andresen lines, and they form with the same periodicity as do their enamel counterparts (Dean and Scandrett, 1996). The phenomena regulating the formation of these long-period structures are not clearly understood, though many mechanisms have been proposed for their origin, including episodes of hypomineralization, hypermineralization, or prism re-orientation (reviewed in Risnes, 1990). The Retzius lines in the imbricational enamel also manifest on the tooth surface as perikymata, or alternating ridges and grooves running around the outside of the crown (Boyde, 1964).

Figure 2: Cellular view of enamel formation and view of periodic structures in enamel

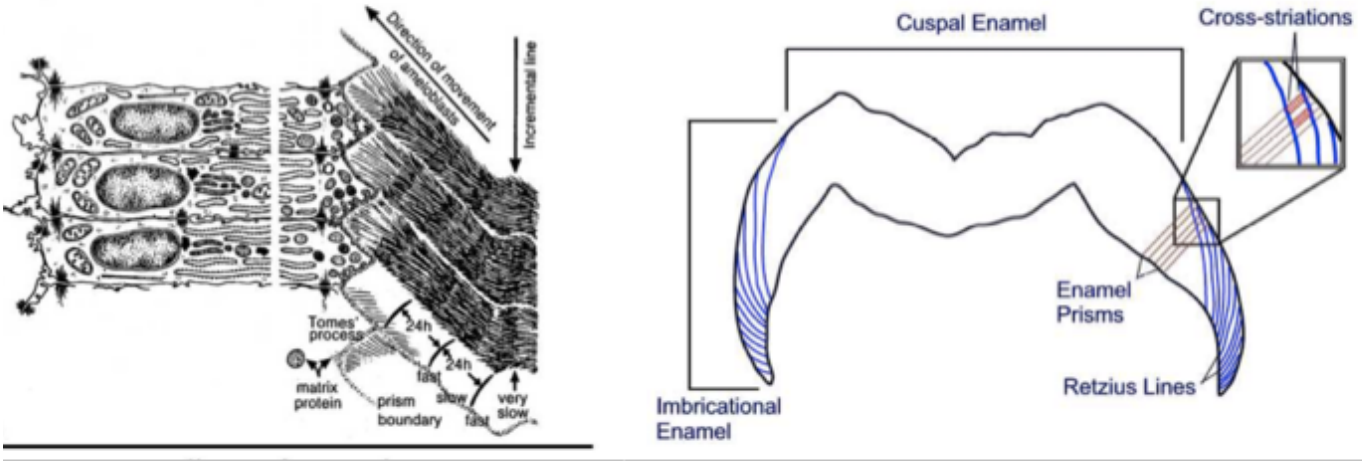

Figure 2a (left): Diagram of ameloblasts secreting enamel in 24-hour increments and forming enamel prisms containing daily cross-striations as they move toward the crown surface. EDJ is to the right of the structures pictured and the occlusal surface would be toward the top of the pictured structures (From Smith, 2004/Modified from Boyde, 1989) . **Figure 2b (right):** Schematic of the location, orientation, and general appearance of enamel prisms (gray), Retzius lines (blue), and cross-striations (red) in the enamel of a typical molar crown. (From Smith, 2004)

Periodic Variables: The regular nature with which these periodic structures form allows them to act as consistent repeating (periodic) variables that can be readily compared between areas of a tooth, between teeth of an individual, between individuals, etc.

Daily Secretion Rate (DSR): Both types of daily forming structures, cross-striations in enamel and von Ebner's lines in dentine, are visible in thin sections via polarized/transmitted light (Boyd, 1982; Smith, 2006), and they vary in their distance apart based upon the amount of daily growth taking place during the formation of a given area of the tooth. In humans, average cuspal enamel daily secretion rate (DSR) is ~4 μm/day, though this average is slightly lower and slightly higher in the innermost and outermost enamel regions, respectively (Reid and Dean, 2006; Smith et al., 2007). In chimpanzees this average cuspal daily secretion rate (CDSR) has been shown elsewhere to be 3.88-4.17 μm/day (Smith et al., 2007). DSR also increases from

inner through outer enamel and decreases from cuspal through cervical enamel (Beynon et al., 1991b; Macho and Wood, 1995; Reid et al., 1998). The DSR in dentine also increases from the earliest to latest forming areas (Dean and Scandrett, 1996).

Retzius Periodicity and Number: Counting the number of daily cross-striations between adjacent pairs of Retzius lines reveals the periodicity of these long-period structures (Shellis, 1998), and this interval is consistent between all areas of a tooth and between all teeth of an individual (FitzGerald, 1998), but can vary between six and twelve days in humans (Risnes, 1998), and has been previously shown to vary from six to nine days in chimpanzees (Schwartz et al., 2001 and Smith et al., 2007). Retzius number (R#) is the full count of how many Retzius lines make up the length of the imbricational enamel, starting at the first stria to reach the crown surface as a perikyma and ending with the last stria formed in the cervical enamel.

Cusp-Specific Total Crown Formation Time: Once the number and periodicity of the striae of Retzius have been obtained, the calculation of imbricational formation time (IFT) becomes possible (Antoine et al., 2009). To do so, cross striations are counted between adjacent Retzius lines to assess Retzius periodicity (RP), and Retzius lines are counted and multiplied by this periodicity, revealing the full number of days it took to form that area of the crown. There are many factors making this difficult, however, from identifying Retzius lines clearly, to being able to count the cross striations in a given area of a thin section. Retzius lines also sometimes converge at the tooth's surface (Dean and Scandrett, 1996), so RP is more accurately assessed in enamel that is not directly at the surface of the crown.

Hominoid Retzius periodicities (RP) range from 4-12 days, with modern humans showing a very wide range of 6-12 days, with a mean and mode of eight. Few studies have

assessed total crown formation time (TFT) directly for fossil hominins, and many use estimates obtained by counting perikymata on the crown surface and calculating formation time using the human modal RP (eight). This method can be misleading however (Smith, 2008), since a one-day difference in RP could result in an over- or underestimate of formation time of more than four months. This means that if the modal value of eight is used to estimate molar TFT using perikymata counts, but the actual periodicity is 12, this would lead to an underestimation of crown formation time of up to 1.4 years (based on a maximum R# of 126 from a chimpanzee M3 from this study). Directly measuring RP and R# of fossil hominin individuals is thus likely to yield more informative results than mean or modal estimates pooled from the data of other individuals or other taxa. Long-period lines in enamel and dentine are often easily measured in histological sections or on surface enamel, due to their distinct appearance, but other features may obscure them. For this reason, Dean (1987) suggests counting only those that reach the surface as perikymata to be true Retzius lines, though convergence at crown surfaces can complicate this.

Irregular Structures: Alongside, and often superimposed upon regular periodic structures, irregular structures can also be seen within dental tissues. Accentuated lines form in enamel in response to growth disturbances that result from dietary change, illness, physical or psychological trauma, etc. and the corresponding lines in dentine are called Owen's lines (Dean et al., 1993). The neonatal line is one such accentuated line that forms at birth (Rushton, 1933; Schour 1936), and is present in the enamel and dentine of all deciduous teeth, since they all begin forming in utero. The various cusps of the permanent M1 also start mineralizing 8-12 weeks before birth in humans (Christensen and Kraus, 1965) and 4-6 weeks before birth in

chimpanzees (Reid et al., 1998). The neonatal line is often also visible in this tooth, since its appearance may result from a decreased level of calcium in the plasma during the first 48 hours after birth (hypocalcaemia) (Nóren, 1984) and may also result from the trauma of birth itself (Gustafson and Gustafson, 1967; Eli et al., 1989). It can be recognized because it divides the prenatal enamel, which contains no striae of Retzius, from the rest of the crown (discussed in Schour, 1936). Subsequent accentuated lines, visible in enamel and dentine, can also be matched between developmentally overlapping teeth (Dean et al., 1993; Dirks, et al., 2002), allowing an accurate chronology of crown and root formation to be obtained, and the degree in overlap between crown formation ages to be determined, since the absolute ages of these irregular growth disturbances can be obtained using the periodic structures that occur alongside them (Antoine et al., 2009).

Because accentuated lines often form in response to stresses occurring at transitional times while tradeoffs take place in the allocation of energy between growth, reproduction, and somatic maintenance such as birth (Gustafson and Gustafson, 1967), weaning (Rose et al., 1978; Dirks et al., 2010), and, in humans, parturition (Dean and Elamin, 2014), these structures become important indicators of the timing of life history events as recorded in dental tissues.

Life History: Studies of life history theory in living mammals (reviewed in Bogin, 1990; Schwartz, 2012) have investigated the relationships between 1) an organism's ecological context, 2) its energy investment in growth, reproduction, and somatic maintenance, and 3) variables such as brain and body mass and dental development, which, at higher taxonomic levels, are correlated with life history events or milestones (e.g. Harvey and Clutton- Brock, 1985; Charnov, 1991). Life history events themselves (e.g. gestation length, age at weaning, age at first

reproduction, etc.) are often referred to as life history variables, while other somatic measures, such as body size, brain size, and dental development, which have been shown to be broadly linked with the life history variables, have been called life history-related variables (Robson and Wood, 2008). Life history-related variables can be used to infer the timing of life history variables in taxa or individuals for which life history cannot be directly observed, such as for fossil taxa, and dental deveopment is used most often, since teeth preserve so well in the fossil record.

Dental development, specifically the age at M_1 emergence, is correlated with age at weaning and sexual maturity in a study across 21 primates (Smith, 1989), however, within species, this relationship is not as clear. Gorillas, orangutans, and chimpanzees (Robson and Wood, 2008; Smith et al., 2013) emerge their M_1s before they have been observed to complete weaning, and even at the species level, such as between mountain and lowland gorillas (Watts, 1991; Robbins et al., 2006), there is a great deal of variation in this relationship. Directly measuring how much the weaning process itself varies within extant hominoid species, subspecies, and even populations, would go a long way toward understanding the links that can and cannot be made between dental development and the weaning process of closely related fossil hominins.

Wild versus captive life history and dental development: There has been some debate about the importance of using only wild chimpanzee dental developmental data for comparisons with fossil hominins, however, much of this debate hinges on the the fact that there are only a few estimates of M1 emergence age from wild chimpanzees, and such a small sample in unlikely to show the true range of variation in even a subspecies, much less the species. Two studies on Kanyawara

chimpanzees (Smith et al., 2013 and Machanda et al., 2015) contain most of the oberved wild chimpanzee tooth emergence data currently available. One additional study by Zihlman et al. (2004), calculated maxillary M1 emergence ages for several chimpanzees (*Pan troglodytes verus*) from the Taï Forest, but there has been some debate about the accuracy of these estimates, given the misidentification of at least one of the individuals in question, and lack of precise dates of death for several individuals (Smith et al., 2010). Reevaluations of those M1 emergence estimates that were subsequently performed by Smith and colleagues, concluded that the original M1 emergence ages were not actually significantly later than those of captive chimpanzees, as Zihlman and colleagues estimated.

Weaning: Weaning is a process consisting of multiple stages that can vary in age at onset and duration (Lee, 1996). Such variation, especially in the age at weaning completion, may be linked to later life history variables for the offspring, such as age at menarche and first reproduction (Lee, 2010), as well as somatic growth rate and adult body size (Lee, 1996), and even mortality risk due to the immunological role played by nursing (McDade, 2003; Humphrey, 2010). In sum, the age at which a mammal is fully weaned (i.e. reaches nutritional independence) can potentially affect the overall pace of its life history and ultimately its evolutionary trajectory.

The weaning process like other life history events, invariably presents a number of sources of stress. This can start early on if samples of adult foods are difficult for an infant's physiology to digest (Dirks, 2002); in addition, external water sources may contain novel pathogens; and the psychological stresses of being denied access to nursing may also take its toll (reviewed in Dirks, 2002). All such interruptions to consistent nutritional intake or processing will result in disruptions to normal growth, which are registered in all of the dental tissues

forming at that time (Boyde, 1963; Beynon et al., 1991, 1998b; Bowman, 1998; Dirks, 1998; Reid et al., 1998a).

Traditionally, mandibular first molar (M_1) emergence age has been used as a proxy for weaning age, because of the correlation between these events across 21 primate species (Smith, 1992), but recent observational studies of wild great apes have shown that nursing is far from over once the infant's first molars begin to emerge into the mouth (Smith, 2013; Macho and Lee-Thorp, 2014; Smith et al., 2017). This is the first discordance between M_1 emergence and weaning completion that needs to be considered.

The second misalignment between these events is the difference between the age that weaning completion is registered in the tissues or excreta (e.g. feces) of chimpanzee infants, and how long after that point they continue to be observed on the nipple. Badescu et al. (2017) tracked the fecal nitrogen ($\delta^{15}N$) and carbon ($\delta^{13}C$) trophic offsets between Ngogo chimpanzee mothers and infants, which revealed that a number of factors can contribute to the discordance between observational field studies of weaning and the actual nutritive intake by the infant. One complicating factor is that nipple contact can occur without suckling taking place (comfort nursing) (Martin, 1984; Badescu et al., 2017), and there can also be suckling without milk flow occurring, and with no significant nutritive transfer happening (Wolff, 1968; Woolridge, 1986). Another issue is that the mean age at which chimpanzee infant $\delta^{15}N$ trophic levels reach equilibrium with the mother (~age 4-4.5 years) – ostensibly indicating the end of the weaning process – is still many months after the mean age at M_1 emergence of 3.2 years in wild (Smith et al, 2015) and 3.3 years in captive chimpanzees (Nissen and Reisen, 1964; Conroy and Mahoney, 1991; Kuykendall et al., 1992). Due to these misalignments between the late cessation of suckling behaviors, the somewhat earlier point at physiological weaning completion, and the

much earlier age at M_1 emergence, it may be that different point in the eruption process, namely the point at which the first molars reach functional occlusion, up to six months after emergence, would serve as a useful dental proxy to mark the end of the weaning process and nutritional independence (Dean and Kelley, 2012).

Seasonal and sex-based stresses: Stresses associated with habitat seasonality (e.g. seasonal food availability and seasonal breeding), may also manifest in growth disturbances in the form of accentuated lines (Dirks, 1998: Dirks et al., 2002), although this relationship is less clear. There can also be differences in the types and timing of stresses experienced by males and females over the course of their lives, beginning with differential maternal investment during the weaning process, such as that seen in chacma baboons (Cheney et al., 2004), anubis baboons (Dirks et al., 2010), western lowland gorillas (Krishna et al., 2008), and lion-tailed macaques (Nowell and Fletcher, 2007). Disentangling the patterns of accentuated lines forming due to life history stresses, particularly when they differ based on sex, from those occurring due to seasonally-induced stress, can complicate efforts to use dental tissue structures to assess the pace and pattern of life history events (e.g., Dirks et al. 2010). This study documents accentuated line ages and frequencies for seven Ugandan chimpanzee individuals and compares their stress record and tooth growth rates with points within the eruption process, as described in the literature, to determine whether tooth emergence and occlusion ages, and associated life history events, can potentially be predicted using these structural phenomena.

Study site: Kibale National Park contains moist evergreen forest, including lowland and montane forest. The density of old growth forest differs between the two research sites in the park, known as Ngogo and Kanyawara (Struhsaker, 1997; Wood et al., 2017). This is because selective logging occurred at Kanyawara, but not at Ngogo (Struhsaker, 1997). The elevation at Ngogo is between 1250 and 1470 meters, and Kanyawara is slightly higher (Struhsaker, 1997). Ngogo and Kanyawara experience annual rainfall of approximately 1500 millimeters (Wood et al., 2017).

The 35 km^2 Ngogo study area does not experience high levels of variability in the food supply (Watts, et al., 2012) faced by other chimpanzees, e.g., Täi Forest, Côte d'Ivoire (*Pan troglodytes verus*) (Boesch and Boesch-Acherman, 2000). Even the chimpanzees at Kanyawara (also *P. t. schweinfurthii*), which are only 10 km away from Ngogo, experience longer and more frequent times of fruit scarcity than the chimpanzees at Ngogo (Wood et al., 2017). The abundance of important fruit trees relied upon by the Ngogo chimpanzees, e.g. *Pterygota mildbraedii* and *Ficus mucuso* (Struhsaker, 1997; Watts et al., 2006) remains fairly consistent, allowing the Ngogo chimpanzees to maintain a relatively uninterrupted level of nutritional input throughout the year (Wood et al., 2017). *F. mucuso* in particular, can produce a large fruit crop at any time of year from each stem, making periods of fruit scarcity a shorter and rarer occurrence than at other sites (Watts et al., 2012). This relative fruit abundance means that they are able to maintain a high level of net energy intake year-to-year (Potts et al., 2011).

There are also no large-bodied predators at Ngogo, unlike the leopards at Taï (Boesch, 1991), and lions at Mahale (Tsukahara, 1993), and as of 2016, there had also been no major documented disease outbreaks in the Ngogo community (Wood et al., 2017), again setting them apart from populations such as Mahale (Nishida et al., 2003), Gombe (Pusey et al., 2008; Williams et al., 2008; Lonsdorf et al., 2011), and Taï (Boesch and Boesch-Achermann, 2000;

Leendertz et al., 2004; Kondgen et al., 2008). All of these conditions combine to make Ngogo a high quality environment that has made the community there the largest one currently known, with over 200 individuals who display survivorship rates comparable to human hunter-gatherer groups (Wood et al., 2017).

Eastern chimpanzees (*P.t. schweinfurthii)* also live in Bwindi Impenetrable National Park (BINP), Uganda and experience different challenges than do their conspecifics at Ngogo and Kanyawara, due in part to the fact that they are sympatric with mountain gorillas (*Gorilla gorilla beringei*). Bwindi lies between 2400-2600 meters above sea level (Stanford and Nkurununngi, 2003), a much higher elevation than the chimpanzees in Kibale National Park. The area is made up of contiguous, moist tropical montane rainforest that receives between 1100-2400 millimeters of rainfall annually (Carlson and Crowley, 2016). Its two dry seasons last from May to July and from late December to February (Stanford and Nkurununngi, 2003). The chimpanzees and gorillas at Bwindi will both eat fruit when it is available to them, but they mostly avoid direct contest competition (but see Stanford and Nkurununngi, 2003) for the same fruit resources by responding to times of fruit scarcity in different ways. During periods of fruit abundance, chimpanzees forage in larger groups, feeding largely on specific fruits (mainly varieties of *Ficus,* similar to the preferred food at Ngogo). During times of fruit scarcity, they forage in smaller groups, which move far apart to minimize resource competition (Stanford and Nkurununngi, 2003).

This study addresses the following three issues:

1) How do the dental developmental variables from these different communities of *Pan troglodytes schweinfurthii* inform the current view of dental developmental variability between wild and captive apes?

Prediction: M_1 emergence ages inferred for the sample overall, including the four communities from this study and the Kanyawara chimpanzees, will fall within the range inferred from captive chimpanzees. This is to be expected because previous studies have placed the Kanyawara chimpanzee M_1 emergences ages squarely within the mean captive values (Smith et al., 2013; Machanda et al., 2015), instead of several years later, as was assumed to be the norm for wild chimpanzees overall, based upon several individuals from the Taï Forest (Zihlman et al., 2004). Ages at death and M1 emergence ages were later remeasured for those Taï chimpanzees, and found to fall within the captive range (Smith et al., 2010; Smith and Boesch, 2011).

Significance: This study will add several much needed data points to the debate over whether there is a substantive difference in dental development, particularly emergence ages, between wild and captive chimpanzees (See Zihlman et al., 2004; Smith et al., 2013), since the majority of data currently available for the dental formation and eruption processes comes from captive chimpanzees (Smith et al., 2007) or from musuem collections of mixed or unknown attribution and origin. Understanding the level of variability in dental developmental parameters to be expected among members of the same subspecies that developed in different ecological conditions is a critical factor for understanding life history variability among fossil hominins from their dental remains.

2) Does the M1 root growth spurt in the chimpanzees in this sample appear to coincide with M1 emergence or occlusion?

Prediction: If M_1 root growth spurt coincides with reaching functional occlusion, and not with emergence, the growth spurt of the Ngogo chimpanzee M_1s should fall after the known age range of M_1 emergence for the Kanyawara individuals. If, instead, the growth spurt coincides with

emergence, it is likely that there would be a certain amount of overlap between the root growth spurt ages in the Ngogo chimpanzees and the Kanyawara range of M_1 emergence.

A second prediction is that the Ngogo chimpanzees from this sample will show overall later estimated M_1 emergence ages than the range for known Kanyawara chimpanzees, and the extra-group Kibale males will not. This is due to the low extrinsic mortality and consistent, high quality resource base at Ngogo (Wood et al, 2017), compared with those of the other neighboring communities.

Significance: Being able to link chimpanzee M_1 root growth spurt with occlusion opens up numerous possibilities for future studies seeking to untangle dental development and life history. On the one hand, if chimpanzee M_1s reach occlusion just prior to weaning completion, as this study predicts, then being able to locate the growth spurt presents a direct structural proxy for chimpanzee weaning completion that can be measured simply by sectioning and imaging the M_1, even if that tooth is not in the mandible and is the only tooth found.

On the other hand, even if age at M_1 emergence is still found to be a better predictor of weaning completion age than the growth spurt turns out to be, (once we have an appropriate sample in which to test this), then M_1 emergence age ranges can still be inferred from the root growth spurt in individuals for whom emergence can no longer be directly observed or measured (i.e. adults). Either way, it greatly increases the number of individuals for which we will be able to link dental emergence and the weaning process, which would be quite beneficial for studies of life history in living apes, and possibly even for fossil taxa.

3) How do the M1 root growth spurt ages of the Ngogo chimpanzees relate to the mean age at weaning completion determined for current Ngogo infants using a fecal isotope study?

Prediction: If the M1 root growth spurt in the Ngogo chimpanzees coincides with, or slightly preceeds, the age at weaning completion, then we would expect their growth spurts to fall just before 4.0-4.5 years, since this is the age range for Ngogo chimpanzee nutritional independence determined by Badescu et al. (2017) using fecal $\delta^{15}N$ and $\delta^{13}C$ values.

Significance: Recent studies show a discordance between observed weaning behaviors and records of nutritional input in various tissues of wild great apes (i.e. "weaning completion" is often defined as "cessation of nipple contact" or "last successful suckle" (Sellen, 2007; 2009), whereas stable isotope studies of hair and feces show gorillas and chimpanzees reaching nutritional independence long before they cease actions (e.g. latching on) that are classified as nursing behaviors (e.g. Reitsema, 2012; Badescu et al., 2017)). From this it follows that observed time spent nursing is not a reliable indicator of when the weaning process is complete, and a different proxy must be used for this important life history milestone. The fecal isotope study of the Ngogo chimpanzee mothers and infants provides a way to precisely measure the timing of the changes in an infant's diet that indicate it is no longer receiving nutritional input from its mother, whether it appears to be nursing or not (Badescu et al., 2017).

If the root growth spurt data from the Ngogo chimpanzees in this study support the weaning completion age range estimate from the fecal isotope study, this suggests that this growth spurt age could potentially be used to infer weaning completion age in additional Ngogo individuals for whom infant fecal isotope data is unavailable, once they are adults or deceased.

Materials: The dentitions of eight adult chimpanzees (*Pan troglodytes schweinfurthii)* were analyzed in this study. Seven of the chimpanzees were from Kibale National Park, Uganda, and one was from Bwindi Impenetrable National Park, Uganda. The remains of all individuals were housed at Makerere University's Zoology Museum (MUZM) in Kampala, Uganda. In

chimpanzees, the first through third molar crowns (M1-M3) are known to overlap in the timing of their formation (Anemone et al., 1996; Kuykendall and Conroy, 1996; Reid et al., 1998). Those three teeth were thus extracted on site from all individuals except three, and exported to the U.S. for processing and analysis. For one individual (NG003) there is no M1 present, and so the P4, M2, and M3 were selected, however, only relative ages could be determined for this individual's accentuated lines as absolute ages would require the presence of an M1. For two other individuals, there is no M2 present, so the P4 was used instead, since it has been shown to form over approximately the same period as the M2 in chimpanzees (Reid et al., 1998).

Identifying information exists for seven of the eight individuals in the sample (see Table 2). Each individual's sex is known. Approximate dates of death are known for seven of the eight chimpanzees. Dates of birth have been estimated for the five Ngogo chimpanzees using genetic data, which provides geneological information regarding individual relationships, combined with observations of the behavior and physical condition of animals when first observed (Wood et al., 2017). Six of the eight individuals are male, while one Ngogo chimpanzee and the single individual from Bwindi are female. All of the individuals died between 2002 and 2014. NG001 and NG002 are unnamed extragroup males killed by the Ngogo males during episodes of intergroup aggression (Watts et al., 2006). Another male "Grappelli" (NG003), died as a result of a within-group coalitionary attack (Watts, 2004). "Stravinsky" (NG004) was an Ngogo male who was a victim of intergroup aggression, and he was the maternal brother of "Tatum" (NG005), whose cause of death is unknown (Ngogo Chimpanzee Project unpublished data). "Webster" (NG013) may have died from respiratory disease (Wood et al., 2017). Causes of death for the Bwindi female (MUZM2625) and the single Ngogo female "Carmen" (NG012) are not known.

Table 2: Chimpanzee individuals included in this study

Individual	Origin	Sex	Name	Estimated age at death	Date and cause of death	Teeth Used
NG001	Northeastern community, Kibale National Park, Uganda[2]	M	Unknown	Adult	6-1-02/ intergroup aggression[2]	M1, M2, M3
NG002	Wantabu community, Kibale National Park, Uganda[2]	M	Unknown	Adult	11-23-02/ intergroup aggression[2]	M1, M2, M3
NG003	Ngogo, Kibale National Park, Uganda[3]	M	"Grappelli"	20	10-30-02/within-group aggression[3]	P4, M2, M3
NG004	Ngogo, Kibale National Park, Uganda[1]	M	"Stravinsky"	32	1-25-06/ intergroup aggression[1]	M1, M2, M3
NG005	Ngogo, Kibale National Park, Uganda[1]	M	"Tatum"	23	2009/unknown[1]	M1, P4, M3
NG012	Ngogo, Kibale National Park, Uganda[1]	F	"Carmen"	51	Sept 2013/ unknown	M1, M2, M3
NG013	Ngogo, Kibale National Park, Uganda[1]	M	"Webster"	26	March 2014/ respiratory disease?[3]	M1, M2, M3
MUZM2625	Bwindi Impenetrable Forest, Uganda	F	Unknown	Adult	Unknown/unknown	M1, P4, M3

Table 2: Identifying information for all eight chimpanzees used in this study. In cases where dates of birth are unknown, a general age category is used (i.e., "Adult"). The "NG" indicates an individual from or associated with the Ngogo population, while "MUZM" refers to the Makarere University's Zoology Museum. "?" indicates reported uncertainty about the cause of death. ([1]Ngogo Chimpanzee Project unpublished data (1995-2016), [2]Watts et al. (2006), [3]Wood et al. (2017))

The fact that these were all adult individuals, and many were older adults, means that many of their teeth were lightly to moderately worn, making them less than ideal for histological sectioning. However, in each individual selected, at least one cusp, usually the mesiobuccal (mb) or mesiopalatal (mp), is much less worn than the others. Since these mb and mp cusps have previously been shown to begin mineralizing earliest and complete formation latest in the mandibular and maxillary molars of chimpanzees, respectively (Reid et al., 1998), the presence of one or the other of these cusps meant that most of the early forming enamel from each tooth could be documented, and in the case of the M1, it meant that the neonatal line could be identified in most cases. Several other individuals are present in this collection but were not

selected for analysis due to a lack of the specific teeth needed for this study. The work of Reid et al. (1998) provided a framework for the amount of overlap between various simultaneously forming crowns that should be expected, which maximized the number of individuals from this collection that could be used. Their findings, that chimpanzee M1 crowns overlap in formation timing not just with the M2, but also with the P3 and P4 (Reid et al., 1998), meant that if the M2 was missing, one of the other two teeth could be used as a substitute and still allow the creation of an overlapping crown formation timeline. The only individuals excluded were those that were missing those intervening teeth (or, in a few cases, those missing their M1s and/or M3s).

Methods: *Embedding, sectioning, and imaging:* The three selected teeth of all eight chimpanzees were histologically sectioned through the mesial cusps, using modified established methods (Schwartz et al., 2006): Once the teeth were gently cleaned using dental tools and distilled water (dH_20), and then dried and photographed, the ideal plane of section for each tooth was identified and marked in order to capture the earliest forming enamel at the tip of the dentine horn, and as much of the cuspal and cervical ends of the crown as was present. The teeth were then embedded in Epo-Tek epoxy and cured overnight.

Each tooth was sectioned as directly as possible through the ideal plane in order to create two thin sections – one from each sectioned half – that mirrored each other as closely as possible. A certain amount of section obiquity often still results from this process (Dean and Kelley, 2012), but care was taken to avoid it as much as possible. To minimize the amount of material lost, a 150 micron-thick diamond embedded saw blade was used on an Isomet 1000 high-speed precision cutting saw. The two halves were lightly lapped to eliminate blade marks, removing as little material as possible, and then highly polished in a 3-micron (μm**)** aluminum oxide particle

suspension, ultrasonicated to remove aluminum particles, and dried. The half that captured the greatest extent of crown and root formation was chosen for imaging and the other half was kept for the later stage of the study. The chosen tooth half was then mounted with epoxy to a microscope slide under pressure, with care taken to avoid the creation of bubbles, which can obscure important microstructures. Thin sections were then created from each mounted tooth half, again using the thin saw blade. The mounted thin sections were then ground and lapped to a thickness of ~100±10 microns (μm**)** and again polished in an aluminum oxide suspension and ultrasonicated, however coverslips were not applied with mounting medium. Instead, a cover slip was temporarily applied using a drop of dH_20 and removed after imaging.

Sections were imaged in the University of Michigan Department of Anthropology using a Nikon NIU polarized light microscope in conjunction with Bioquant Osteo 2016 imaging software. Counts and measures of microstructures were made visually using the microscope itself, and on photomontages created by the Bioquant software.

Daily secretion rate: DSR was determined for various areas of the crown (referred to in this study as "zones"), since this rate differs between inner, middle and outer enamel, as well as between cuspal, lateral, and cervical enamel (Smith, 2008) (see Figure 2a). In each crown zone (e.g. inner cuspal, cuspal middle, etc.), distances between consecutive daily cross-striations were measured using a 40x objective, often by measuring the length of a stretch of these daily increments (See Figure 4a and 4b) and dividing by the number of cross-striations, minus one. This was done in at least three places in each zone to obtain average DSR values for each zone in μm. These measurements were then compared separately in order to show how these rates change between different zones, but were also averaged to obtain overall DSR for the cuspal and

imbricational enamel (CDSR and IDSR). DSR was also measured within similar zones in the dentine, but extended to include all areas of the root where these structures could be identified (See Appendix for raw data.)

Retzius periodicity (RP): This value was obtained first by eye, using the 20x objective to count the number of daily cross-striations between adjacent Retzius lines to obtain the number of daily increments of growth. This process was repeated in as many areas of the imbricational enamel where the daily cross-striations could be clearly discerned and counted between Retzius lines (usually between three and five different areas). Once established by direct counts, the RP was confirmed by measuring the distance between adjacent pairs of Retzius lines (Figure 4c) and dividing this distance by the local DSR (e.g. if the lines were visible in the middle imbricational zone, the MIDSR was used). These values were compared with the counts taken by eye, and then compared between cusps of the same tooth and between different teeth from the same individual to ensure intra- and intertooth consistency.

Retzius line number (R#): This value was determined by eye using the microscope, with both the 4x and 10x and objectives. Starting with the first Retzius line to reach the lateral crown surface as a perikyma (to which line 1b extends in Figure 3b), all Retzius lines that subsequently reached the crown surface were counted, moving cervically (See Figure 4d). This total number was determined on three occasions and the results were averaged to minimize intra-observer error.

Total formation time (TFT): Using the previous three enamel variables, the minimum cusp-specific formation times were determined for each tooth. This was done by first multiplying the

RP by the R# to obtain the total number of days it took to form the imbricational enamel (IFT). This was then added to the total cuspal formation time (CFT). CFT was determined by locating the first Retzius line to reach the crown surface and by picking an enamel prism intersecting it that was clear enough that it could be traced back to the point on the EDJ where it originated (line 1b in Figure 3b, modified from Reid et al., 1998). This prism length was measured and then divided by the average CDSR to determine the number of days it took to form this prism before the formation of that first imbricational Retzius line.

Figure 3a-b: Diagrams illustrating general periodic and accentuated variable measurement guides

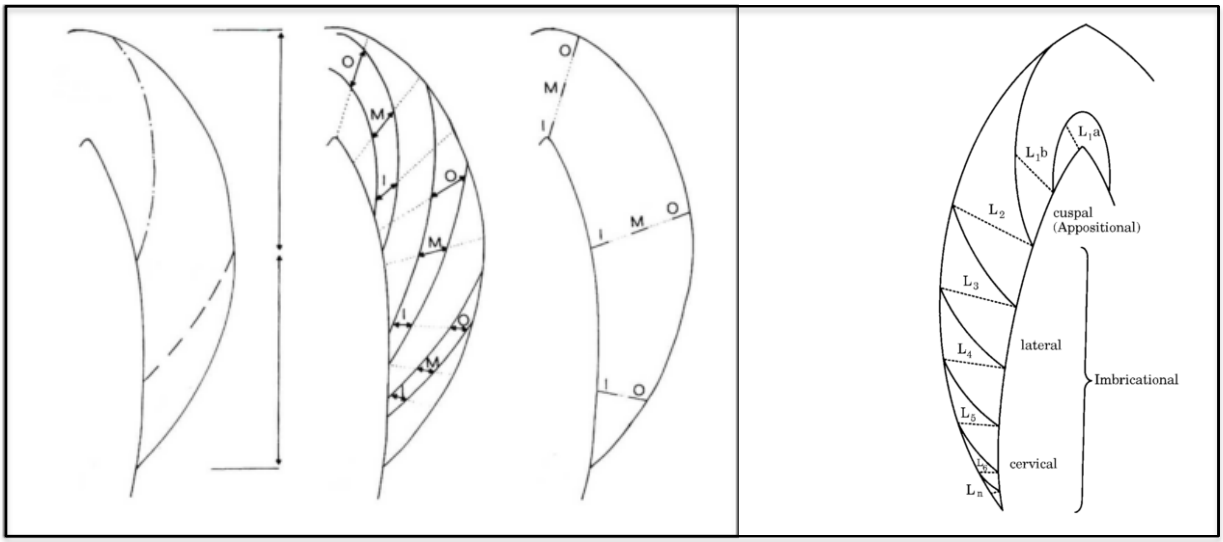

Figure 3a: The "zones" dividing up cuspal, lateral, and cervical enamel (left) and **Figure 3b**: method used to age accentuated lines (right) (Both modified from Reid et al., 1998)

However, it was also necessary to include the formation time of the earliest forming enamel, which would not have been included by only measuring the length of a prism intersecting the first imbricational Retzius line. To account for this, starting at the point on the EDJ where the line 1b prism originated, a line was drawn up and over the dentine horn to include the earliest forming enamel, including any prenatal enamel in the case of the M1. The length of a

prism stretching between the tip of the dentine horn and the occlusal-most extent of this line was then measured (line 1a in Figure 3b) and divided by the ICDSR to determine the number of days it took that area to form, and this number was added to the remaining CFT to obtain the total number of days it took to form all cuspal enamel captured from that particular section. When this CFT was added to the IFT, the TFT could be estimated.

To account for prism decussation, or the wavy, undulating path enamel prisms take within certain areas of enamel, total linear cuspal thickness is usually multiplied by 1.15, as per the standard method (Risnes, 1998), however the measuring tools available in Bioquant Osteo allowed for the entire length of the prism to be measured, and prisms showing little decussation were chosen wherever possible, so value transformations were not performed in such cases. It is also unknown how much decussation is actually present in non-human primate molar cuspal enamel, and the standard used by Risnes may only be useful for human cuspal enamel (Smith et al., 2007).

In several of the teeth, small portions of the cervical enamel were broken off, so the final forming Retzius lines could not be counted in these individuals. To offset this lack, estimates can be made for the number of missing Retzius lines, but the final IFTs reported here are based only upon what was actually present, so the final TFTs reported in Table 3 are minimum estimates. Variation in each of these developmental variables was compared between the eight individuals, but results must be interpreted with caution due to this damage and missing material.

Accentuated lines: Once the periodic structures were measured and the resulting developmental variables were determined, they were used to age the accentuated lines. The neonatal line in the M1 (Figure 4e) supplied a "zero point" from which to count up and thereby assess chronological

age ranges in later forming areas of the tooth crown and in subsequently forming teeth. The next accentuated line to appear in the M1 was aged by measuring the maximum distance along a prism, or a tubule in dentine, between the neonatal line and that first accentuated line (Figure 4f). This distance was divided by the local DSR to obtain the number of days since birth that passed before the formation of that line, since a continuous sequence of cross striations could rarely be counted between these lines. The next accentuated line to form could then be aged by following the first accentuated line to its origin on the EDJ (line 3 in Figure 3b) and measuring the length of a prism (line 4 in Figure 3b) from that point to the next forming accentuated line and repeating the process of dividing the length by the local DSR. That number of days could then be added to the age of the first accentuated line to obtain the absolute age of the second line, and this process could then be repeated for all other accentuated lines in the enamel and the dentine.

Cross-matching: All subsequent accentuated lines in the M1 were then aged (see Figure 9), and when a recognizable sequence of these lines could be identified in the earlier forming enamel of the subsequent tooth (M2 or P4), those areas of the two teeth could be cross-matched (registered) to one another, so that the chronology could be continued into M2 formation, and the process repeated between M2 and M3. In this way, a complete developmental chronology of these teeth was created for seven of the eight individuals, and the minimum amount of enamel developmental overlap was estimated. The corresponding variables in dentine were also assessed in several cases where the accentuated lines were more visible in dentine than in enamel (See Figure 4g).

Figure 4: Periodic and accentuated enamel variables obtained from chimpanzee molars in this study

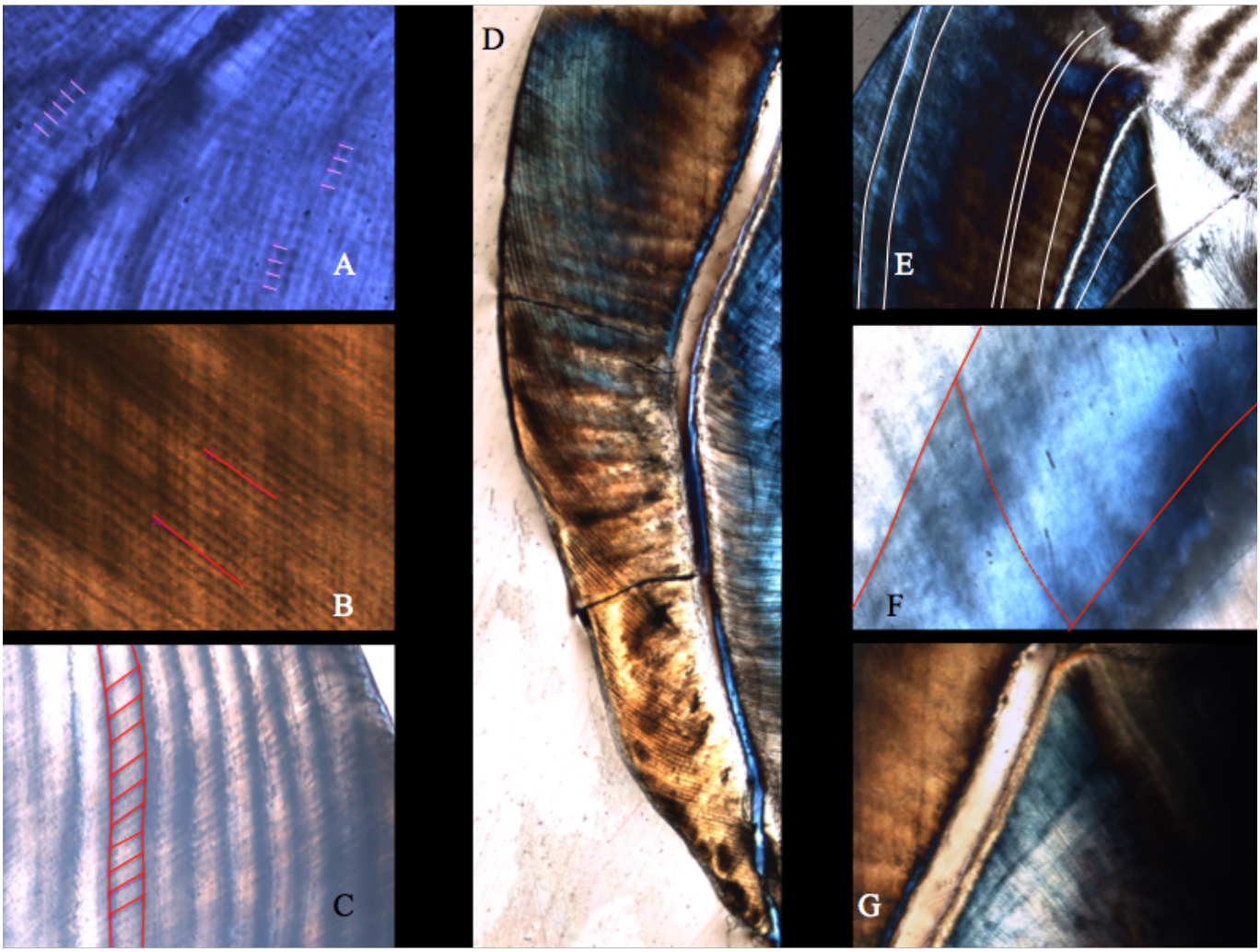

Figure 4: a-highlighted daily cross-striations, **b**-each red line is one border of a single enamel prism, from which enamel daily secretion rates (DSR) can be obtained by measuring the length of that stretch of prism and dividing the length by the number of daily growth increments that can be seen along it, **c**-measured Retzius line periodicity (RP), **d-** Retzius line number (R#), **e**-highlighted accentuated lines in the M1 of NG001, including the neonatal line, and numerous accentuated lines, **f**-measured distance along a prism between neonatal line and first accentuated line in NG005 M1, **g**-corresponding accentuated lines in enamel (brown) and dentine (blue) in NG001 M2.

Extension rate (ER): In several of the crowns, it was not possible to count all of the Retzius lines of the lateral enamel due to cracking or breaking away of portions of the enamel, and/or a certain amount of the cuspal enamel had been worn away, making full estimates of cuspal and/or imbricational formation time problematic. In these cases, the extension rate was determined for the crown and root dentine. Strictly speaking, the extension rate refers to the rate at which new

enamel-forming and dentine-forming cells differentiate along the EDJ, or inner root surface, and are activated each day (Shellis, 1998). Practically speaking, within dentine, the extension rate refers to the amount of formation taking place toward the the pulp cavity versus the growth occuring apically, or toward the root tip.

To measure the ER, starting at the dentine horn, a dentine tubule was measured to a distance of ~200 μm into the root, or to where it intersected with an Andresen line or an accentuated line of Owen in that area, and that line was then followed back to the EDJ, or the inner root surface. (The tubule length was followed along any curvature it showed, in order to capture the full number of days of growth along it, as opposed to a straight-line measure, which would have overestimated the growth distance, perhaps intersecting with a stria significantly more than 200 μm into dentine growth.) Measuring how much EDJ length there was between the tubule's and stria's intersections with the EDJ, or the inner root surface, provided the amount of newly extended crown or root that had formed during however many days passed passed within that 200 μm interval. The measured tubule length (~200 μm) was then divided by the previously established local DSR to get the number of days of formation within that interval, and then the extension length was divided by the number of days associated with that interval to obtain the extension rate for that interval of crown or root dentine. This was continued all the way down the crown until the apical end was reached (See Figure 5).

By adding together the formation times for each interval all the way down the crown and root, the TFT could then be estimated a second time, and this TFT also included root formation time (RFT). These estimates were preferentially used to measure TFTs because formation times obtained using enamel were limited by the damage and wear to the crowns, and because this

alternate method has been shown to produce accurate estimates of formation time efficiently, especially in teeth like these that are not ideal for sectioning, (Dean and Kelley, 2012).

In addition to permitting more robust estimates of TFTs, the extension rate also varies over the course of crown and root formation (Boyde, 1963), peaking at a particular point during root formation (Gleiser and Hunt, 1955; Moorees et al., 1963; Dean and Kelley, 2012), that is thought to be associated with either M_1 emergence or functional occlusion age in chimpanzees (Dean and Kelley, 2012; Dean and Cole, 2013). The age at which this peak ER occurs, referred to here as the root growth spurt age, can then be measured and compared between individuals. Remeasuring the root ERs, starting at a consistent point in each M1, the cemento-enamel junction (CEJ), allowed this changing ER to be compared between individuals. The ages of these new intervals had to be obtained using the ages of the original 200 μm intervals that began in the crown dentine, since those could be absolutely aged using the neonatal line.

Analysis: Ages at which the accentuated lines formed, numbers of accentuated lines, and regularity of accentuated lines (i.e., do they form with regular time intervals or more randomly), were all documented for members of this study, and the periodic variables used to measure them were compared with those of chimpanzee populations from other studies. Crown and root extension rates were also compared for these individuals, as well as ages at which rooth growth spurts occurred. Crown formation times obtained using extension rates were compared between individuals and with other chimpanzee populations from the literature for which this has been documented. Analysis of these variables were assessed qualitatively and using descriptive statistics, since the sample sizes were small.

Figure 5: Dentine extension rate measurement method in the M1 of male chimpanzee "NG001"

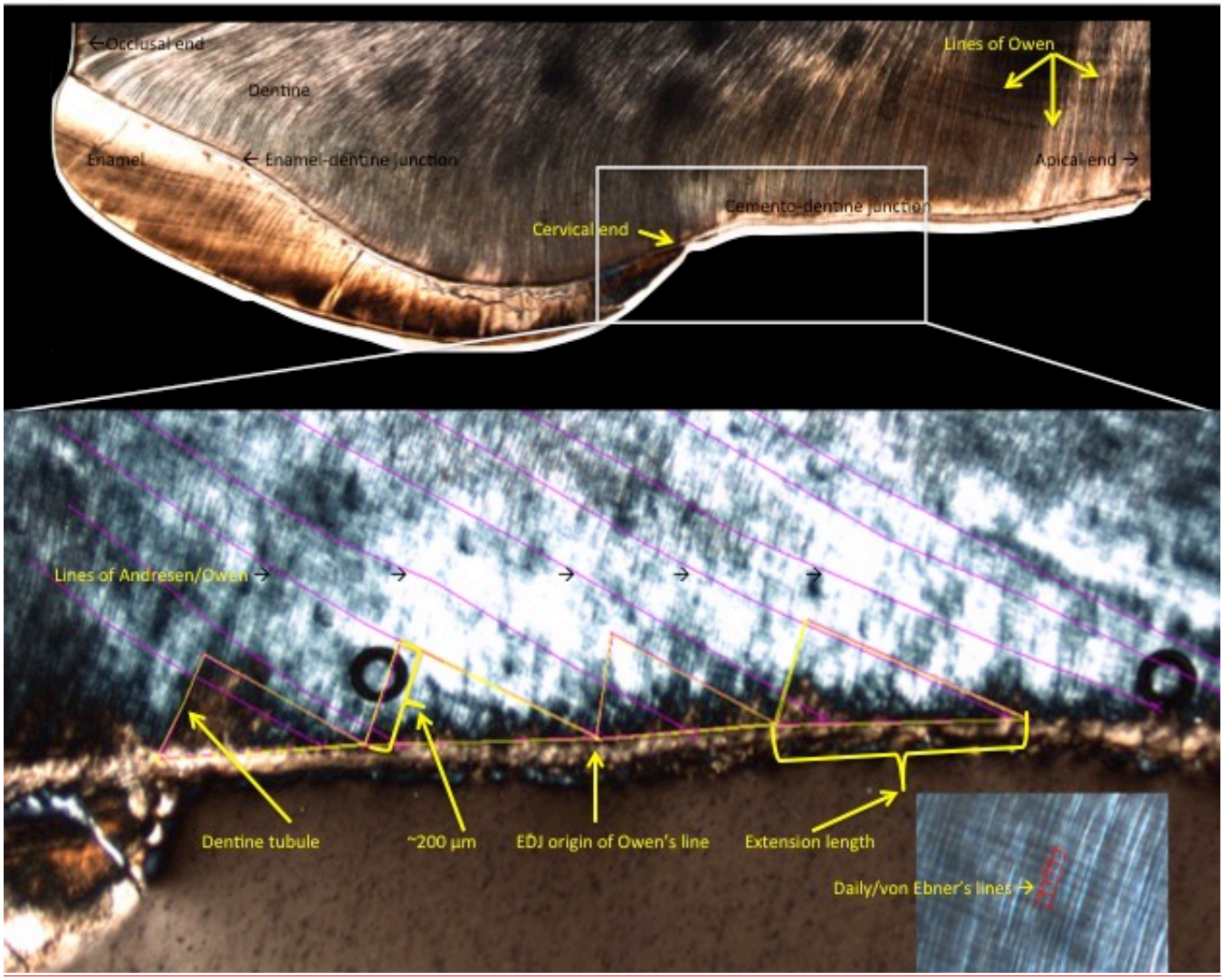

Figure 5: The top panel shows the mesiobuccal cusp of "NG001"'s left M_1 at low power through transmitted/polarized light. The portion highlighted and enlarged on the bottom is the cervical end of the enamel – dentine junction (EDJ) and the beginning of the root dentine at the cemento-dentine junction (CDJ). Several dentine tubules are highlighted showing their growth up to 200 µm away from the CDJ, and the Andresen lines with which they intersect are followed back to their origin lower down on the CDJ.The distance between the tubule start point and the Andresen line origin is also highlighted along the CDJ. The inset on the bottom shows a high-powered (20x) view of the daily lines in dentine, called von Ebner's lines, and these were measured to obtain DSR in dentine.

Along with dental developmental variables, I collected all available life history variables for the Ngogo and Kanyawara chimpanzee communities from the Kibale National Park, as well as for chimpanzees from Bwindi Impenetrable National Park. These are compared in Table 7.

Results: Tables 3-6 present cusp-specific measures of all dental developmental variables being compared between the three teeth of each of the eight chimpanzee individuals, as well as descriptive statistics for the most salient variables. Additional raw values are included in the Appendix. Figures 5-9 contain charts of the developmental variables and their distributions, as well as histological images of some of the incremental and periodic structures used to construct the crown formation chronologies for these individuals. For some variables, means from this study are compared to overall means from other studies to determine how these individuals fit within the overall variability in *Pan*. (Raw values in the Appendix)

Enamel DSR: Overall DSR ranged from 3.15-6.75 μm/day, (See Appendix) with a general increase in values from inner to outer zones. Average CDSR for all teeth in the sample was 4.64 ± 0.39 μm/day, average IDSR was 5.0 ± 0.49 μm/day with standard deviations ranging from 0.29-0.57 μm/day (n=24). (Table 3). For M1s considered separately, the mean CDSR value was 4.65 μm/day (±0.36, n=7) and the mean ICDSR value was 5.45 μm/day (±0.48, n=7). The mean CDSR and IDSR values for the three P4s that were included (4.48 μm/day ±0.39) also fell within the range of these values for the three molar types.

RP: Retzius periodicity for all teeth in the sample ranged from 5-6 days, with a mean of 5.38 and a mode of 5 (n=24). Between multiple cusps of the same tooth and between multiple teeth from the same individual, the periodicity was consistent. The RP in both female individuals was 6 while the male values were 5, 5, 5, 5, 6, and 6.

R#: Retzius number varied widely, especially since some teeth were missing some of their final cervical growth increments due to breakage, so these have not been directly compared. However, those counts varied the least in the M1 (=82 ± 11) and the most in the M2 (=101 ± 25).

TFT: Average total formation time tended to increase from the M1-M3, though the lowest standard deviation appeared in the M2. (Separate values listed by tooth and by individual included in the Appendix) These TFTs were also minimum estimates, due to the enamel damage and wear, so these must be interpreted with caution.

Table 3: Descriptive statistics for periodic variables in enamel of all teeth of this study's chimpanzees

		CDSR (µm)			**IDSR (µm)**			**RP (days)**			**TFT (days)**	
Tooth	$\bar{x}$	range	σ	$\bar{x}$	range	σ	$\bar{x}$	range	σ	$\bar{x}$	range	σ
M1	4.65 n=7	4.19-5.13	0.36	5.45	4.60-6.03	0.48	5.38 n=8	5-6	0.52	646	502-776	85.29
M2	4.40 n=6	4.06-4.88	0.29	4.50	4.03-5.05	0.39	""	""	""	781	661-857	72.9
M3	4.87 n=8	4.20-5.63	0.50	5.06	4.20-5.81	0.53	""	""	""	963	885-1111	82.62
P4	4.48 (n=3)	4.17-4.91	0.39	4.64	4.28-5.30	0.57	""	""	""	N/A	N/A	N/A
Grand Mean	4.64	3.15-6.75	0.39	5 (σ= 0.43)	N/A	0.49	5.38	N/A	N/A	N/A	N/A	N/A

Table 3: Means ($\bar{x}$), ranges, and standard deviations (σ) for each measure are given for each tooth, and then the grand mean (χ) is given for all the teeth combined from all individuals. CDSR=cuspal daily secretion rate, IDSR=imbricational daily seretion rate, RP=Retzius line Periodicity, TFT=total cusp-specific formation time

Accentuated Lines: The neonatal line, as the first visible accentuated line to form in the M1, varied greatly in appearance, but was identifiable as the first line to appear in the inner cuspal enamel, close to the dentine horn. Additional accentuated lines are documented throughout M1

formation in Figure 9, and their frequencies and distribution throughout the crown and root are compared with root extension rates and M1 emergence ages. The relationship between the root growth spurt age and accentuated line frequency can also be seen in Figure 9.

Figure 6: Cross-matching of chimpanzee M1-M3 crown development using accentuated lines in enamel and dentine

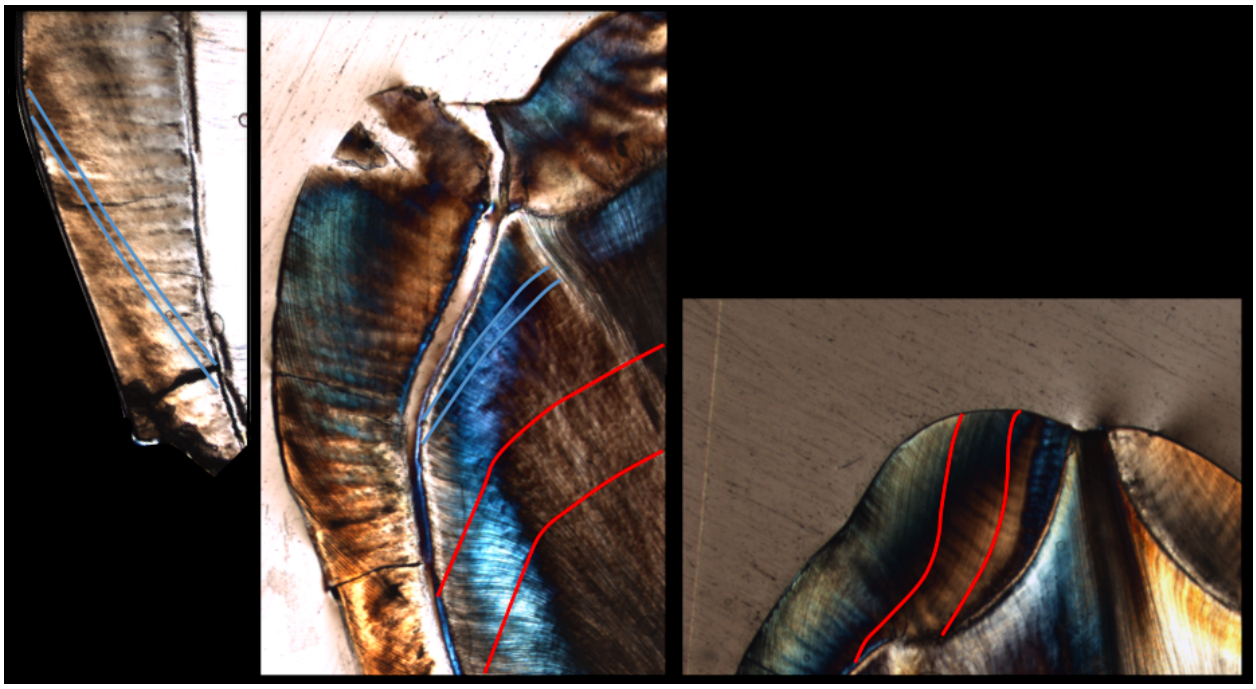

Figure 6: Photomontages taken at 40x of ~100 µm-thin sections from the mesial cusps of the RM_1 (left), RM_2 (middle) and RM_3 (right) of individual NG001. Prominent accentuated striae are visible in the late-forming enamel and early-forming dentine of RM_1 and RM_2 (blue lines), while another set of accentuated striae can be seen in the late-forming dentine of RM_2 and early-forming enamel of RM_3 and even in the very late-forming root dentine of RM_1 (not pictured). These sets of striae were used to cross-match these teeth and determine the extent of crown formation overlap.

Cross-matching: Prominent accentuated lines forming late in the M1 were cross-matched with their simultaneously forming counterparts in the M2 (or the P4), and repeated for later accentuated lines in M2 and M3 (e.g. Figure 6). Cross-matching accentuated lines enables charting the extent of crown formation overlap, but because the periodic structures and variables were more reliably seen and measured in the dentine of many of these individuals, dentine extension rates were used in order to obtain the remainder of the data for the chimpanzees in this study.

Table 4: Dentine extension rate variables in the M1s of all chimpanzees in this study

Individual	Dentine daily secretion rate (μm/day)	Peak root ER (μm/day)	Root growth spurt age (days)	Rooth growth spurt age (years)	Total dentine formation (years)
NG001	2.50	14.07	966	2.65	7.07
NG002	2.60	11.18	1004	2.75	6.35
NG004	2.40	7.96	1251	3.43	4.11**
NG005	2.10	11.97	1441	3.95	5.52
NG012	2.50	7.36	1617	4.43	5.33
NG013	2.20	9.52	1569	4.30	6.84
Ngogo mean/ range	2.30/ 2.10-2.50	9.20/ 7.36-11.97	1470/ 1251-1617	4.03/ 3.43-4.43	5.45**
Kibale mean/ range	2.40/ 2.10-2.60	10.34/ 7.36-14.07	1308/ 966-1617	3.59/ 2.65-4.43	5.87**/ 4.11-7.07
MUZM2625	2.10	12.11	1346	3.69	4.22**
Overall mean/ range	2.30/ 2.10-2.60	10.60/ 7.36-14.07	1313/ 966-1617	3.60/ 2.65-4.43	5.63/ 4.11-7.07**
Other study mean* n=14	2.30/ N/A	8.70/ 6.10-10.20	1387/ N/A	3.8/ 3.0-4.7	N/A

Table 4: Dentine daily secretion rates (DDSR) and peak root extension rates (ER) in μm/day are used to obtainroot growth spurt ages in days and years, and total crown and root formation time in years. *Taken from Dean and Kelley, 2012 **full root ER measurements couldn't be made due to damage at the root apex, so total formation time is incomplete and means are affected by this.

Dentine DSR: For of these chimpanzees' M1s, the DSR in the 200 μm of root dentine closest to the EDJ and the root surface ranged from 2.1-2.6 μm/day, increasing from more cervical to more apical areas of the root.

Dentine extension rate: The overall dentine extension rate in the M1s ranged from 3.08-14.32 μm/day. This rate varied between different stages of dentine formation throughout the crown and the root (e.g. Figure 6). In stage one there was an initial velocity increase in the crown dentine, decreasing toward the region of the cemento-dentine junction (CDJ) in stage two, then increasing in stage three to a peak velocity around midway down the root, once again decreasing thereafter in stage four. Peak root extension rate/velocity averaged 10.6 μm/day, ranging from 7.36-14.07. This is compared with the average peak extension rates (8.70) from 14 chimpanzee M1s from Dean and Kelley (2012) in Table 4 below. The changing extension rate was measured in two different trials, and the pattern of change compared between the two trials, in order to ensure the

peak in root growth rates lined up, and that the pattern of change was consistent (see charts in Figure 7). Conducting two separate trials also minimized intra-observer error and demonstrated the reproducibility of the results.

Root growth spurt age: The age at which the root growth spurt occurred in the M1 root dentine averaged 3.60 years, with a range of 2.65 - 4.43 years in this sample overall. If the Kibale chimpanzees are examined separately, they still show a mean root growth spurt age of 3.59 years (range = 2.65 - 4.43 years) and the Ngogo chimpanzees themselves have a mean root growth spurt age of 4.03 (range = 3.43 - 4.43 years). Root growth spurt ages of the chimpanzees used by Dean and Kelley (2012) are also listed in Table 4 (3.80 years, n = 14). All three dentine variables were similar between studies.

Figure 7: Extension rate variation over crown and root formation in seven chimpanzee M1s

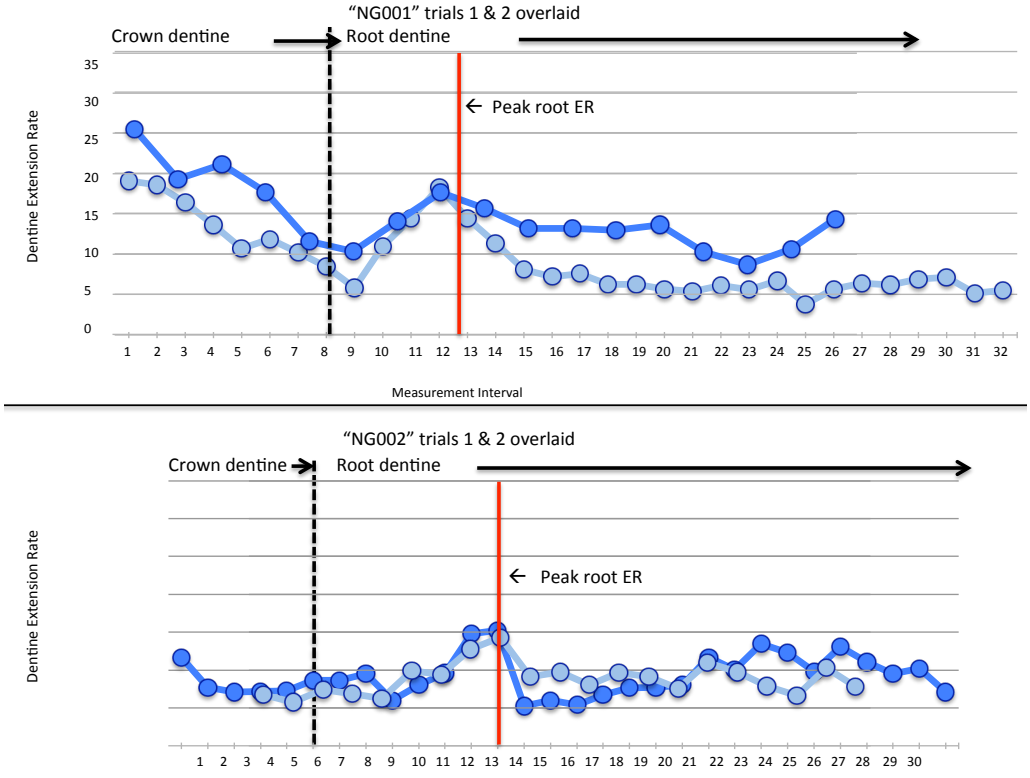

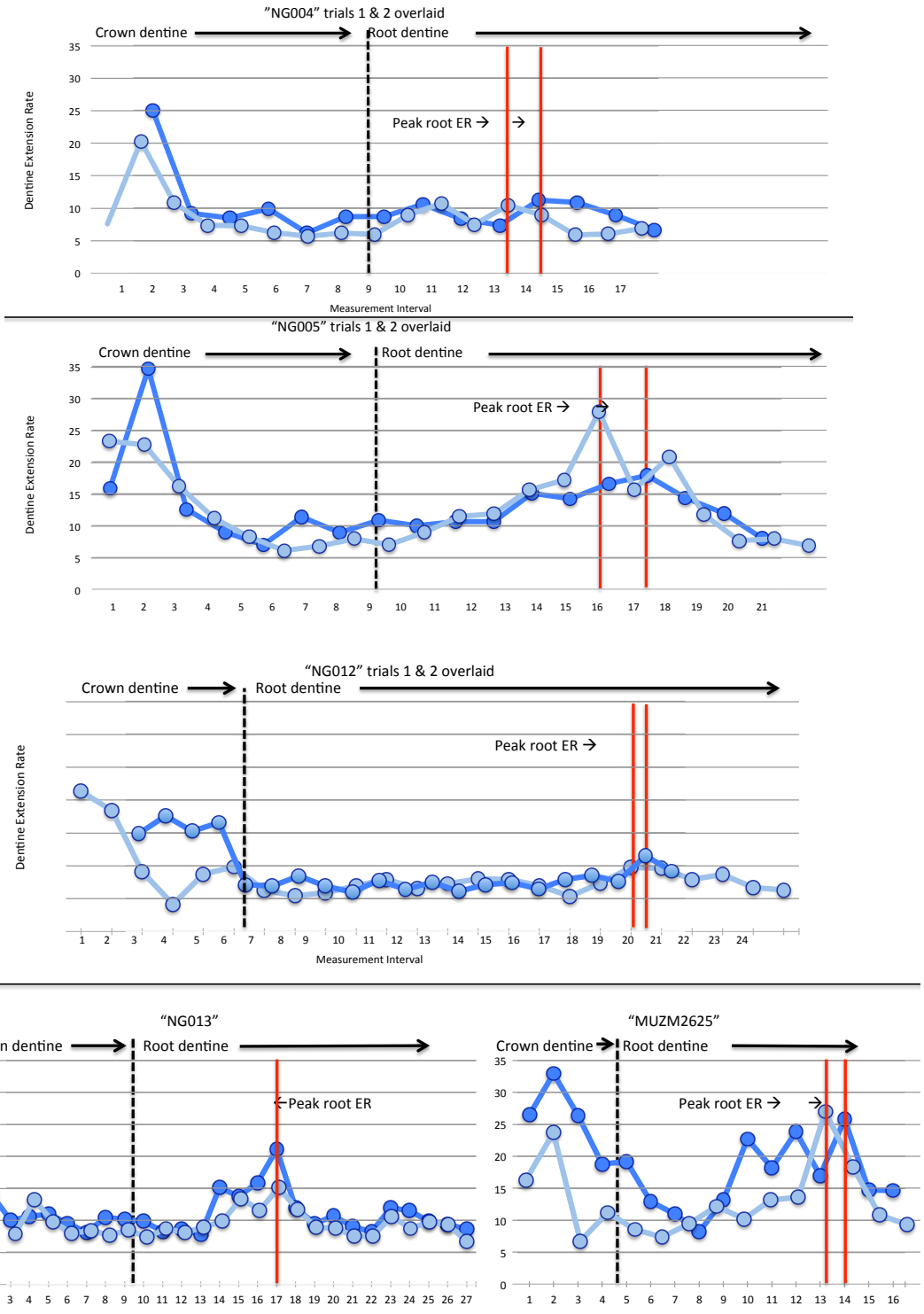

Figure 7: Crown and root extension rates (in µm/day) were measured on two different days in order to minimize intra-observer error, and the two trials are overlaid in light and dark blue to show their similarity in pattern. The x-axis shows each successively measured 200 µm interval taken from earliest forming dentine in the crown (interval 1) to the latest forming area of the root that was preserved and measurable. Intervals have not been compared to absolute age in this figure, instead they have been arranged to show similarity in the pattern of extension rate change between the two trials. The y-axis shows the dentine extension rates in µm/day. Crown and root dentine areseparated by the dashed line and the peak in the root dentine extension rate is highlighted by a red line. The peaks in the two trialswere compared for consistency. Charts are for the M1s only.

The root growth spurt and M1 emergence vs. occlusion: The root growth spurt in half of these chimpanzees fell after or on the high end of the range of M_1 emergence ages taken from captive chimpanzees (2.14 - 3.99 yrs (Kuykendall, 1992)), and the growth spurt for the Bwindi chimpanzee and three out of four of the Ngogo chimpanzees fell 2-12 months after the full range of M_1 emergence ages documented for wild Kanyawara chimpanzees (2.80 - 3.30 yrs, n=3 (Smith et al, 2013)). To obtain M1 emergence age estimates, a range of 2.5 – 6.0 months was subtracted from the growth spurt age, since that is the estimated time between emergence and attainment of full functional occlusion in the M_1s of the Kanyawara chimpanzees (Smith et al., 2013; Machanda et al., 2015). This resulted in M1 emergence age ranges seen in Table 5 and Figure 8.

The M1s used in this study, however, were a mix of maxillary and mandibular teeth, and maxillary M1s (M^1) have been shown to have delayed formation and emergence relative to their mandibular counterparts (Reid et al., 1998; Machanda et al., 2015). It was thus necessary to further infer the estimated M_1 emergence age by subtracting that time delay (~six months) from the estimated M^1 emergence age, in those three individuals whose maxillary M1s were analyzed here. This resulted in the "Estimated M_1 emergence age" seen in Table 5. The final M_1 emergence age range for the entire sample from this study is 2.15 - 4.10 years, with a range of 2.43 - 4.10 years for the Ngogo individuals and a 3.19 - 3.49 year age range estimated for the single Bwindi individual. The Kanyawara M_1 emergence age range (2.50 - 3.30 years) is included in Figure 8 to show where this range falls within the overall *P.t. schweinfurthii* M_1 emergence ranges from this study, including the earlier ages for the extra-group males, the later ages for the Ngogo sample overall, and the single Bwindi M_1 emergence age estimate falling in the middle of the Ngogo range.

Table 5: Estimated M_1 emergence ages for the seven chimpanzees in this study based on root growth spurt/occlusion age

Individual	Root growth spurt/Occlusion age (years)	Estimated M1 Emergence age range (years)	Final estimated M_1 emergence age ranges and means (years)
NG001	2.65	2.15-2.45	2.15-2.45 (mean=2.30)
NG002	2.75	2.25-2.55	2.25-2.55 (mean=2.40)
NG004	3.43	*2.93-3.23*	2.43-2.73 (mean=2.58) (spurt=2.93)
NG005	3.95	*3.45-3.75*	2.95-3.25 (mean=3.10) (spurt=3.45)
NG012	4.43	*3.93-4.23*	3.43-3.73 (mean=3.58) (spurt=3.93)
NG013	4.30	3.80-4.10	3.80-4.10 (mean=3.95)
Ngogo mean	**4.03**	n/a	**3.30**
Kibale mean	**3.59**	n/a	**2.99**
MUZM2625	3.69	3.19-3.49	3.19-3.49 (mean=3.34)
Overall mean	**3.60**	n/a	**3.04**

Table 5: 2.5-6.0 months was subtracted from each root growth spurt age to obtain the "Estimated M1 emergence age ranges", and a further six months was subtracted from the three M^1 emergence age ranges to obtain the full ranges of possible "Estimated M_1 emergence age". tMaxillary M1 emergence ages are seen in italics and means are in bold.

Figure 8: Estimated M_1 emergence age ranges by community

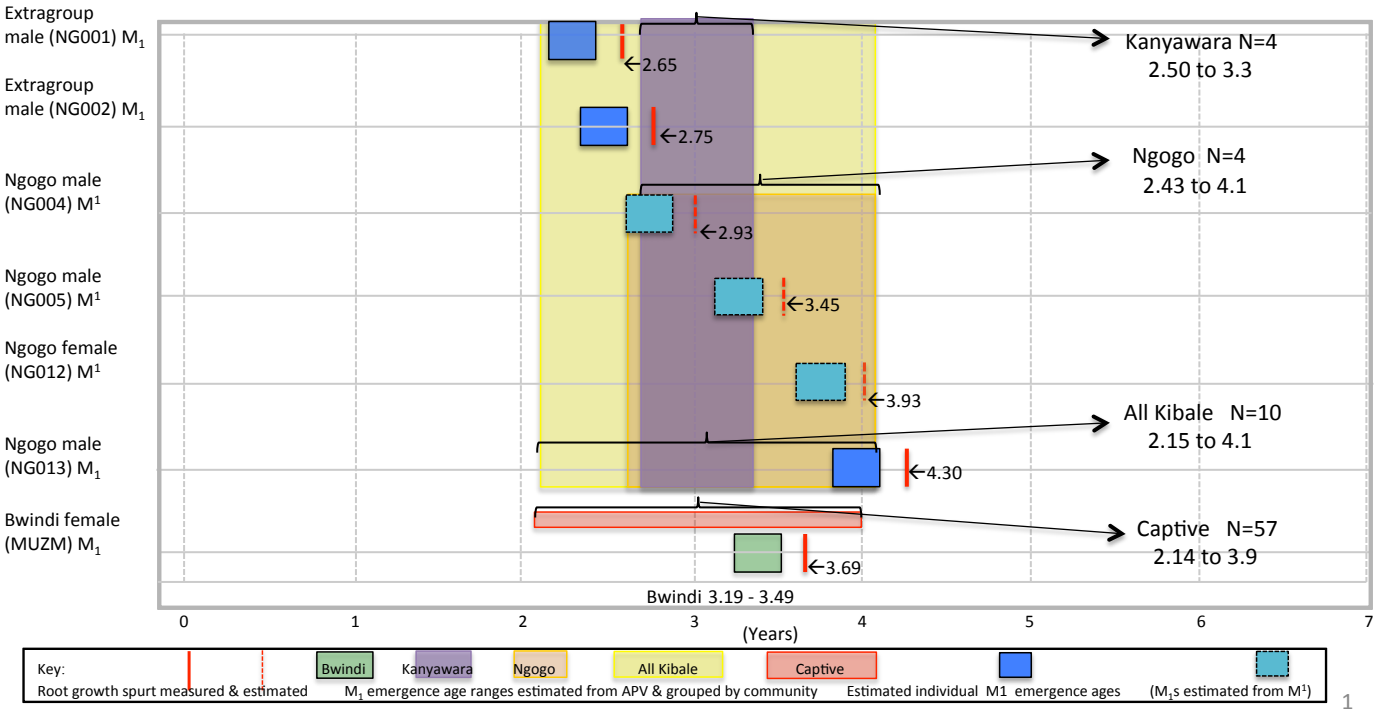

Figure 8: Arrows point to each community's estimated M_1 emergence age range on the right

The original paper (Machanda at al., 2015) only included the three M_1 values in their final age range, but here, their additional earlier M_1 emergence age of ≤2.50 years was used to push the

Kanyawara range backward to its greatest extent, since the M_1 had already emerged in this individual before observation began, but how much before was unknown. (Figure 8). The full currently known range of M_1 emergence ages for all wild *P.t. schweinfurthii* individuals is now 2.15 – 4.10 years, which overlaps almost perfectly with the full M_1 emergence age range inferred for captive individuals of 2.14 – 3.99 years (Kuykendall et al., 1992).

Discussion: One constraint on the available chimpanzee dental developmental data is the fact that many collections are made up of mixed wild and captive chimpanzees, as well as individuals of unknown sex, provenience, or subspecies. In the absence of background information on the individuals being studied, it is difficult to determine the underlying causes of variability seen in dental development and the life history variables linked to them. The *Pan* sample used by Smith (2004) consists of five individuals of known sex but unknown subspecies or area of origin, and ten individuals of unknown sex, unknown subspecies, and unknown wild vs. captive origin, all from the London Natural History Museum collection. The study did include teeth from 47 wild *P.t. verus* individuals from Liberia (from Peabody Museum, Harvard University), but these were mostly of unknown sex. A subset of seven of these individuals was used by Reid et al. (1998). Also included were 13 additional individuals of unknown sex, unknown subspecific attribution, and unknown wild versus captive status from various other collections. With a total of 75 individuals, the Smith (2004) study was the largest of its kind representing chimpanzees, however, while it significantly increased the amount of detailed dental developmental data available from chimpanzees, understanding the sources of dental developmental variability between individuals is made difficult when sex, status, attribution, and area of origin are unknown. The author notes, however, that many of the histological slides available for study and

reanalysis were made from teeth selected by the original researchers specifically because of their unknown status, allowing them to minimize damage done to specimens about which more information was known (Smith, 2004). As more data from wild populations are collected and added to this growing body of work, it will be possible to clarify the sources of variability in chimpanzee dental development, whether attributable to taxon, sex, ontogeny, or ecology.

Ngogo Dental Developmental Variables: Previous studies of chimpanzee molar enamel have shown DSR increasing from the enamel-dentine junction (EDJ) to the crown surface in both the cuspal and the imbricational enamel and decreasing from cusp to cervix, with Smith et al. (2007) reporting statistically significant trends in these directions for a mixed *Pan* samples of 69 individuals (mixed in terms of sex, in wild vs. captive origin, and in subspecific attribution). The results presented here support that trend (see Table 6). Mean overall enamel CDSR estimates for *Pan* are reported elsewhere as 4.17 μm/day (n = 69) (Smith et al., 2007), however, the mean of the data presented here – 4.82 μm/day (n = 24) – shows an increase from the average described in the literature. Comparing just the M1s reveals a CDSR mean of 4.65 μm/day from this study (n = 7, range = 4.19 - 5.13), and 4.06 μm/day from the Smith et al. (2007) study (n = 7, range = 3.49 - 4.52), allowing comparisons between equal sample sizes and within the same tooth type. This would mean a 0.59 μm/day difference in M1 CDSR between the two studies. When the Ngogo M1 values are examined alone, they exhibit a mean CDSR of 4.83 μm/day, placing the CDSR from this population 0.77 μm/day above the M1 data from the Smith et al. (2007) study, which appears to be a noticable increase, but it is not known whether the difference is statistically or biologically significant. Data from additional individuals will allow more rigorous statistical testing to be performed.

Mean RP of the Smith et al. (2007) sample was 6.4 with a range of 6 - 7 (n = 61), and Schwartz et al. (2001) reported a range of 6-9 for the periodicity of *Pan* teeth. This study's RP range of 5-6 increases this overall species range of variation in RP to 5-9. DSR and RP from this study and several others are compared in Table 6. Smith (2004) notes, however, that several of the chimpanzees in that sample had RP values that could have been either 5 or 6, but since it was not able to be confirmed, the RP value of 5 was omitted from the final range in that study.

Table 6: Comparisons of periodicity and DSR for the chimpanzees in this study along with other studies of *Pan*

	RP	**ICDSR**	**MCDSR**	**OCDSR**	**AVG CDSR**	**Male RP**	**Female RP**
***This Study* N**	24	24	24	24	24	18	6
Mean	5.38	4.15	4.62	5.07	4.62	5.17	6
Range	5-6	3.2-5.18	4.0-6.1	4.26-6.36	4.06-5.63	5-6	6
***Smith et al., 2007* N**	61	69	69	69	69	N/A	N/A
Mean	6.4	3.62	4.28	4.61	4.17	N/A	N/A
Range	6-7	N/A	N/A	N/A	3.15-6.75	N/A	N/A
Schwartz et al., 2001 N	20	54	N/A	4	58	10	10
Mean	6.95	3.37	N/A	4.39	3.88	7.0	6.9
Range	6-9	2.69-4.34	N/A	3.75-5.29	2.69-5.29	6-9	6-8

Table 6: N/A=no data were available for this value in that particular study; N varies even within each study since not all individuals could be used for all measures, and sex was unknown for the chimpanzees in the Smith et al., 2007 study.

Dentine, root growth spurt, and life history: In addition to the variety of enamel developmental variables observed in these chimpanzee molars, dentine formation variables in the M1 were examined, to more reliably track full tooth development in samples with enamel damage or areas of the crown where no periodic variables could be seen. The dentine extension rates were particularly useful, since previous studies have shown that, in chimpanzees, the age at which the

M1 root dentine peaks in its extension rate, happens just after its age at emergence (Dean and Kelley, 2012; Dean and Cole, 2013). This is especially helpful for estimating M1 emergence in individuals whose teeth are fully formed or no longer in the jaw.

This study found that the root growth spurt in five out of seven of the chimpanzees occurred after the observed age ranges at M1 emergence in other wild chimpanzees. Studies of the chimpanzees at Kanyawara, located 10 km northwest of Ngogo, have shown a 2.5-6.0 month delay between emergence into the oral cavity and full functional occlusion (Smith et al., 2013; Machanda et al., 2015). This lends support to the idea that the root growth spurt in chimpanzee molars coincides with reaching functional occlusion, several months after emergence (Dean and Kelley, 2012; Dean and Cole, 2013). If this is the case, it could represent a more accessible life history-related variable than M_1 emergence, since being able to use teeth in chewing could be considered more biologically relevant than initial emergence through the gingiva, and since the root growth spurt can be measured in adult and isolated teeth. Once the M_1s reach functional occlusion, there is still a six month lag between M_1 and M^1 emergence (Machanda et al., 2015), which means that the upper molar would just be starting to emerge when the lower one reaches full occlusion, thus providing an opposing occlusal surface against which to chew. This would mean that a direct proxy for an important life history variable, attainment of nutritional independence (commonly known as weaning completion), can be documented in the structure of fully adult teeth, greatly increasing the numbers of individuals for whom this life history variable can be estimated.

The link between chimpanzee root growth spurt and the M1 eruption process, however, is not seen in modern humans (Dean and Cole, 2013). This dental growth spurt does occur in all teeth in modern humans, but it is disconnected from that tooth's emergence age. This makes it

even more imperative to develop secondary indicators of the weaning process that can be used to show that a given fossil hominin either completed weaning at the same time as its late root growth spurt, as would be expected if its life history were more chimpanzee-like, or if the root growth spurt and other indicators of weaning completion occurred long before M1 emergence and occlusion, which would be more similar to the modern human pattern. One such potential secondary indicator of the weaning process is the distribution of stress lines.

Stress frequency and weaning: To link the root growth spurt and M1 functional occlusion with the weaning process, ages and frequencies of stress-associated accentuated lines must also be considered. It is apparent from Figure 9 that the majority of accentuated lines in these chimpanzees' M1s formed prior to when the growth spurt was reached, with greatest frequency occurring during the estimated age of M1 emergence. Thereafter, they occurred much more infrequently.

The frequency and timing of accentuated line occurrences in the M1 dentine provide a potential way forward for exploring the idea that peak M_1 root growth occurs just prior to attaining functional occlusion, andjjust prior to weaning completion. Early weaning-related stresses that an infant would experience are likely to be related to the inability to fully digest the new adult foods as it tries to incorporate them into its diet. This initial adult food sampling has been observed in Ngogo infants starting as early as three months old, and evidence for this early incorporation of some adult foods has also been seen in the relatively early beginnings of convergence between mother and offspring $\delta^{15}N$ and $\delta^{13}C$ trophic levels (Badescu et al., 2017). Novel pathogens from non-nursing water sources are another potential reason for stress lines to appear early in the weaning process (Dirks et al., 2002). Between age one and two, the relative

contribution of milk to the diet gradually decreases in Ngogo chimpanzees, as inferred from infant fecal $\delta^{15}N$ values (Badescu et al., 2017), perhaps coinciding with initial rejection by mothers of infants' attempts to nurse. This rejection may represent a psychological stress that would certianly create accentuated lines. The types of stress an infant would experience most frequently in the time just prior to attainment of M_1 functional occlusion are likely to be nutritional stresses due to not yet having full dental capabilities for processing a largely adult qdiet, alongside increased nutritional demands due to a peak in somatic growth (Dirks et al., 2010).

Figure 9: Kibale chimpanzee M1 dentine accentuated line frequency curves

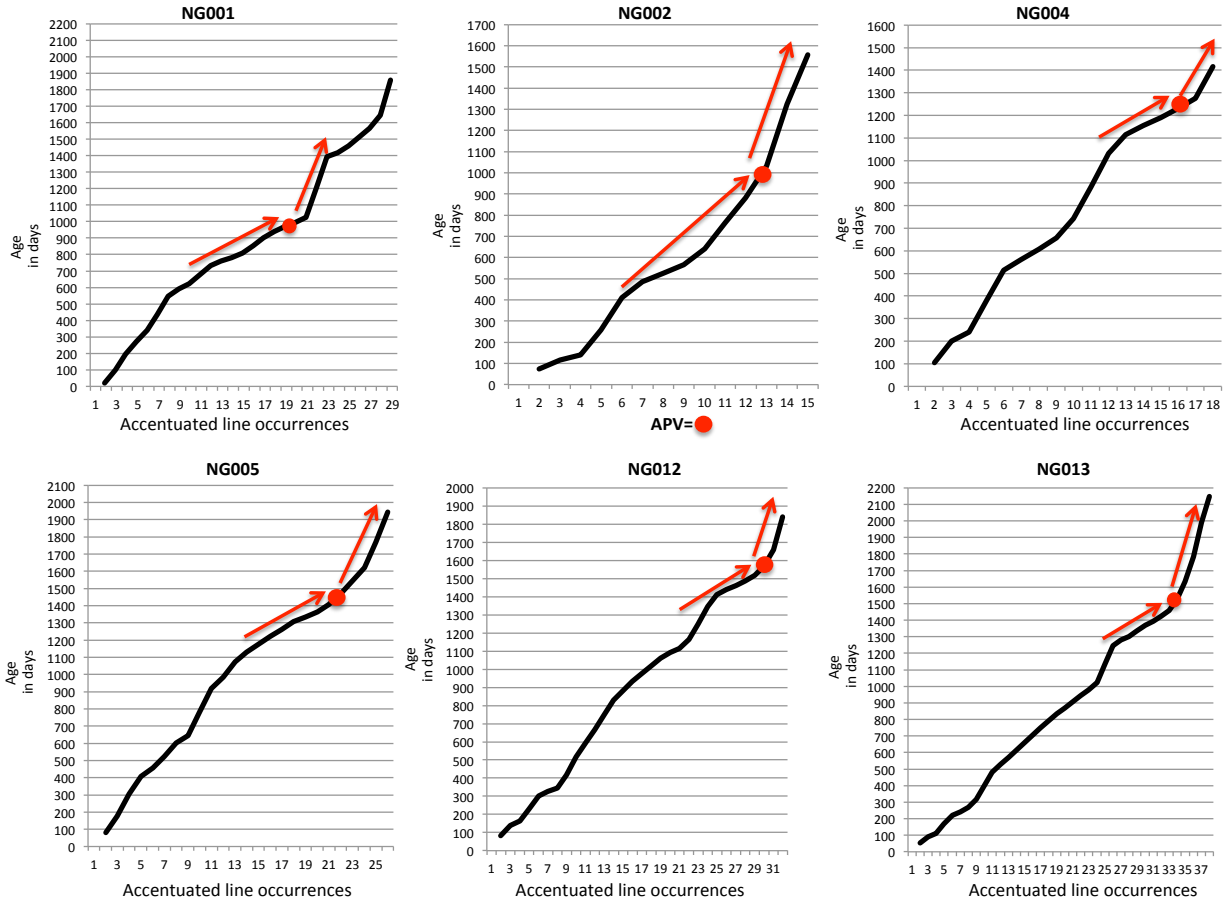

Figure 9: These graphs show the accentuated line frequency curves in the M1s of the six Kibale chimpanzees. Each accentuated line is listed on the x-axis, and the ages in days at which they formed are on the y-axis. Steepness of frequency curve is overlaid in black with red arrows to show periods of time in which more numerous stresses occurred (flatter curve) versus those in which fewer stresses took place (steeper curve). The root growth spurt age is also indicated on each curve by a red circle.

Weaning from M1 emergence, observations, and isotopes: Smith et al. (2013) describe how Kanyawara chimpanzees continue to suckle long after their M_1s have emerged, and often beyond the age of functional occlusion. They note that the offspring are likely receiving little nutritional input from nursing at this point, as evidenced by the change in insulin rates from breastmilk produced by mothers after infants are around two years old, despite increased time spent on the nipple (Emery Thompson et al., 2012).

Badescu et al. (2017) found a similar discordance between the "age at weaning completion," as assessed using field observations of time spent on the nipple, and the same age estimated using the convergence of fecal $\delta^{15}N$ trophic offsets between Ngogo chimpanzee mothers and infants over time. This would mean that observed time spent nursing is not an accurate indicator of the true energetics of the weaning process. Instead, the nitrogen and carbon offset data from feces provide a framework for describing the timing of the weaning process in the Ngogo chimpanzees.

Based upon the results in the current study (see Figure 8), the Ngogo chimpanzees in this sample emerged their M_1s between age 2.43 and 4.0 years (as inferred by backtracking 2.5-6.0 months from the root growth spurt age), then, at age 3.03-4.60 years, they experienced peak root growth rates just before their M_1s reached functional occlusion (according to the duration of M_1 eruption as measured in several Kanyawara chimpanzees (Machanda et al., 2015)). The proposal that they reached weaning completion just after they experienced their M1 root growth spurt and attained functional occlusion, is consistent with the timeframe of weaning completion by age 4-4.5 years for current Ngogo chimpanzee infants, that has been established through mother-infant fecal $\delta^{15}N$ and $\delta^{13}C$ trophic offsets (Badescu et.al, 2017).

The two extragroup males in the current study appear to have gone through these same steps at slightly earlier ages. This is consistent with the life history theory precept that differential extrinsic mortality risk exerts the greatest influence over developmental pace, and these two males are more likely than the Ngogo males to have been subject to such risks. While little is known about the communities to which these males belonged, numerous instances of lethal intergroup aggression (many described in Watts et al., 2006) have resulted in the deaths of many males from groups that border Ngogo, and this alone would seem to be a form of greater extrinsic mortality for extra-group males compared with Ngogo males. This is in addition to the fact that extra-group individuals would have less access to the abundant food resources of Ngogo, likely subjecting them to increased levels of density-dependent mortality risk, which could result in an accelerated life history pace.

The small sample sizes being compared here, preclude saying something definitive about this relationship, and the lack of any observed early life history data from these individuals means that caution should be used in interpretations; nonetheless, the patterns, even in this small sample are suggestive.

Table 7: Life history variables for the *Pan* communities compared in this study

Community	Population size	Ages at dispersal/first birth (years)	Weaning completion age Observed/measured (years)	Inter-birth interval (IBI) Means/ranges/N (years)
Ngogo	>200 (204 as of May, 2016)[1]	13/14[1]	5.5-6/4.0-4.5[2]	Mean=5.42, S.D. ±0.97, Range- 3.25-8.21 (N=48 females, 85 births*)
Kanyawara	~60 (56 as of 2013)[7]	12.9[5]	4.3-6.1[6] /?	Mean=5.96 Range=3.3-10.9 (N=7 females/23 births*[6])
Bwindi	>30 as of 2003[4]	?	?	?

[1]from Wood et al., 2017; [2]from Badescu, 2017; [3]from Ngogo Chimpanzee Project unpublished data; [4]from Stanford and Nkurunungi, 2003; [5]Stumpf et al., 2009; [6]Machanda et al., 2015; [7]Muller and Wrangham, 2014; *IBIs only included when successive offspring survived.

Ngogo chimpanzee ecology and life history: Across chimpanzee sites, it is females who disperse at reproductive maturity, in order to avoid inbreeding with close male kin (Mitani et al., 2002; Nishida and Kawanaka 1972; Pusey 1979).). At Kanyawara and Ngogo, female dispersal occurs around age 13 (Table 7). While still uncommon, female chimpanzees stay in their natal community with somewhat greater frequency at Ngogo compared with other populations (J. Mitani, pers. comm.), perhaps due in part to the reduced risk that they might breed with a close male relative in such a large community, and perhaps due also to the reduced risk of female feeding competition in an environment with such consistent, high-quality food availability (Watts et al., 2012; Badescu et al., 2017).

Ngogo females generally first reproduce around age 14 (Wood et al., 2017), and exibit inter-birth intervals that are more or less consistent with the means of those observed at other chimpanzee sites. The Ngogo mean is 5.42 years (S.D. ±0.97 years) for 85 successful consecutive births, with a range of 3.25 - 8.21 years (Ngogo Chimpanzee Project unpublished data).

Extrinsic mortality: The chimpanzees of the Ngogo community experience very little density-dependent mortality risk due to the abundance of consistent, high-quality food resources in their territory (Wood et al., 2017). Extrinsic mortality risk refers to sources of mortality such as predation by large predators (including human poachers), infanticide and disease outbreaks. In contexts where extrinsic mortality risk is high, the logical life history strategy is to accelerate maturation in order to reach reproductive maturity early enough to avoid dying before reproducing. Many cercopithecoid primates employ this life history strategy, and manage to remain reproductively successful, even when extrinsic mortality risk is high (Dirks and Bowman,

2007). The Ngogo chimpanzees, as noted above, are exposed to no large predators in their territory, and while there are instances of infanticide, the disease outbreaks that have sometimes devastated other chimpanzee populations (and appeared for the first recorded time at Ngogo early in January of 2017 (Negrey et al., 2019)), did not affect this community during the time when the chimpanzees in this sample were developing. All of these factors could result in the later M_1 emergence and occlusion ages, and inferred weaning completion, among the Ngogo chimpanzees in this sample.

By contrast, the Kanyawara community is also relatively free of disease or predators, but they do experience density dependent mortality risk (Muller and Wrangham, 2014), due to the less abundant food supply in that area, and especially the lack of the *Ficus mucuso* tree, so widespread at Ngogo (Potts and Watts, 2011). This increased mortality risk could explain the somewhat earlier M_1 emergence age of the Kanyawara individuals. The same sorts of risks, in addition to high levels of lethal intergroup aggression, could explain the even earlier estimated ages of M_1 emergence for the two extragroup males in the sample, although the small sample size make such inferences provisional.

Comparatively less is known about the Bwindi chimpanzee life history, but the estimated M_1 emergence age for the single individual in this sample (3.19 – 3.49 years), falls at the late end of the Kanyawara range and in the middle of the Ngogo range. This female chimpanzee's M_1 root growth spurt/occlusion age is 3.69 years, which puts her inferred weaning completion age later than all of the Kanyawara individuals and right in the middle of the weaning age range inferred for the Ngogo chimpanzees in this sample. Dental developmental data from additional Bwindi individuals is needed to determine where the developmental pace of this population fits within the overall range for *Pan troglodytes schweinfurthii.*

Hominin life history evolution: The use of the root growth spurt as a life history-related variable provides a tantalizing way forward for assessing life history pace in more fossil hominin individuals, thus enabling comparisons between populations and taxa. This is due in part to the fact that adult M_1s can be analyzed using this method, as opposed to being limited to the small number of fossil juvenile dental remains to reconstruct M_1 gingival emergence from alveolar emergence (which is when the tooth first pushes through the bone of the jaw), which is only retrievable from teeth still in the mandible (e.g. Kelley and Smith, 2003; Schwartz et al., 2006; Kelley and Schwartz, 2010). Using the root growth spurt to reconstruct occlusion age, and perhaps weaning completion age, allows even isolated M_1s to be analyzed in this way. Using adult teeth also limits the amount of compromised dental developmental data from individuals that died young, and may have experienced pathologies that would have influenced their growth rate (Smith et al., 2010; Smith and Boesch, 2011), thus confounding studies of "typical" developmental pace for that taxon.

The results of the current study suggest that, at least in the case of M1 root formation and emergence/occlusion ages, values from captive individuals could be just as appropriate as wild data for use in comparisons with fossil hominins. This was demonstrated by the fact that, within the single subspecies of *Pan troglodytes schweinfurthii* this study found as much variation in M_1 emergence ages as there is in the entire known captive chimpanzee data pool, which speaks to the possibility that we still know very little about the true extent of chimpanzee variability in dental developmental parameters or in certain life history parameters. It has been suggested, however, that this pattern is unlikely to hold for M2s and M3s, since these later-forming and emerging teeth seem to be more responsive to different ecological and energetic conditions, such as those that would differ between wild and captive individuals (Machanda et al., 2015).

The methods employed here could be used to measure the M_1 root growth spurt age in any number of fossil taxa, and the limiting factor is the preservation of the dentine periodic and accentuated microstructures. If these structures are sufficiently preserved, it may even be possible to image them non-invasively using techniques such as phase contrast X-ray synchrotron microtomography (e.g. Tafforeau and Smith, 2008; Tafforeau et al., 2012; Le Cabec et al., 2015), thereby circumventing the need to destructively process extremely rare fossil teeth using more conventional histological methods. In cases when dentine structures cannot be visualized non-invasively, however, careful histological section preparation could still yield informative M_1 root growth rate data.

It has been proposed elsewhere (Wood et al., 2017) that a chimpanzee-like last common ancestor (LCA) of humans and chimpanzees could potentially have made the transition to a life history pattern more like that of *Homo sapiens* without needing all of the socioecological adaptations (maternal and/or infant provisioning, social structure, cooperation, etc.), commonly cited as requisite conditions for the evolution of the modern human life history profile, if they experienced the food abundance, and lack of predation and disease seen at Ngogo. Cases like the Ngogo community are therefore important to consider when investigating modern human life history evolution, as they offer an expanded view of what "typical" chimpanzee life history is like, as well as how variable life history can be in closely related groups, in this case among different communities of the same subspecies, if even one ecological variable, such as food abundance, differs between them.

Conclusions: Collecting weaning-related data for extant primates presents a number of challenges, regardless of the method, but it seems clear that using observational data alone

overestimates the duration of the weaning process. In order to address changes in weaning ages and behaviors in fossil hominoids and hominins, we need to find an accurate marker for whatever threshold within the weaning process must be crossed by living hominoids for them to be considered somatically and nutritionally weaned, even if not behaviorally weaned.

The estimated M_1 emergence age range of 2.15-4.10 years in our chimpanzee sample, and the range of 2.14-3.99 years for the known captive chimpanzee sample, supports the first prediction that the similarity and overlap in these ranges suggests that captive chimpanzee M_1 emergence data can be used as a comparative sample in studies of fossil hominin dental development and life history. The second prediction was that this new sample, made up of small numbers of individuals from four different *P.t. schweinfurthii* communities, would help illustrate the dental developmental variability to be expected within a single *Pan* subspecies, and this was achieved by increasing the known M_1 emergence age range from 9.6 months in the four previously documented Kanyawara chimpanzees, to an estimate of almost two years for the full sample that now includes all five communities.

For the Ngogo chimpanzees in this study, the M_1 root growth spurts all fell considerably after the age range of Kanyawara M_1 emergence, which supported the third prediction that M_1 root growth spurt is most likley to coincide with its attainment of occlusion several months after emergence. The fourth prediction was upheld by the result that most of the Ngogo chimpanzees also emerged their M_1s somewhat after those at Kanyawara, or on the late end of their range.

The fifth prediction, that the growth spurt and M_1 occlusion age slightly preceed, weaning completion, was supported by the root growth spurt age range = 3.03 - 4.60 years in the Ngogo chimpanzees in this sample, and the inferred ages at weaning completion (4.0-4.5 years) from fecal isotope data of Ngogo infant-mother pairs.

Results overall suggest that the M1 root growth spurt, likely coinciding with the attainment of functional occlusion, followed by an abrupt drop in stress episode frequency, may represent a structural proxy for the threshold of nutritional independence/weaning completion in these Ugandan chimpanzees.

Future Directions: In future work seeking to resolve the issue of the co-occurrence of the M_1 root growth spurt and occlusion, it would be beneficial to assess root growth spurt ages on the intact dental remains of as many juvenile chimpanzees as possible. This would permit the root growth spurts and M_1 emergence ages to be measured on the same individuals, to avoid using pooled M_1 emergence data in favor of direct comparisons, so as to verify the 2.5-6.0 month emergence-to-occlusion delay, instead of inferring one parameter from the other and introducing error at each step.

It has been noted that the age at first reproduction may be a highly effective indicator of overall life history pace as well (Dean, 2016), and so it would be useful to assess whether parturition lines from female chimpanzee first births can be located at the end of M3 root formation, since they finish forming between age 13-14 in some chimpanzees (Dean and Cole, 2013; Machanda et al., 2015), and such lines have been observed and validated with known parturition dates in human M3s (Dean and Elamin, 2014). Future work should seek to assess whether dentally determined ages at chimpanzee nutritional independence could relate to age at first birth by using M3 parturition lines. This would be especially effective by looking only at natal Ngogo females, since they, and not immigrant females, would have had their early life history influenced by the conditions at Ngogo.

This is the first study to document the M1 root growth spurt in a wild population of chimpanzees, and to use it to reconstruct estimated M_1 emergence and occlusion ages in order to link M_1 formation and eruption processes with the weaning process. Future such studies would benefit from incorporating additional lines of evidence for dietary changes, such as stable isotope and trace element analyses, into investigations of wild primate dental development and life history evolution. In addition, in order to more accurately compare weaning age data between chimpanzee populations and subspecies, further fecal isotope studies should be carried out in populations such as the Taï Forest chimpanzees, those at Mahale and Gombe, as well as at Bwindi and Kanyawara. Doing so will allow consistent measures of "weaning completion" to be compared to see whether the Ngogo chimpanzees do, in fact, wean later than other populations.

Works Cited

AlQahtani, S.J., Hector, M.P., Liversidge, H.M. 2010. The London atlas of human tooth development and eruption. American Journal of Physical Anthropology 142:481–490.

Anemone, R. L., Mooney, M. P., and Siegel, M. I. 1996. Longitudinal study of dental development in chimpanzees of known chronological age: implications for understanding the age at death of Plio-Pleistocene hominids. American Journal of Physical Anthropology, 99(1), 119–33.

Antoine, D., Hillson, S., Dean, M.C. 2009. The developmental clock of dental enamel: A test for the periodicity of prism cross-striations and an evaluation of the likely sources of error in histological studies of this kind. Journal of Anatomy, 214:45-55.

Bădescu, I., Katzenberg, M. A., Watts, D. P., and Sellen, D. W. 2017. A novel fecal stable isotope approach to determine the timing of age-related feeding transitions in wild infant chimpanzees. American Journal of Physical Anthropology, 162(2), 285–299. http://doi.org/10.1002/ajpa.23116

Beynon, A.D., Dean, M.C., Reid, D.J. 1991. Histological study on the chronology of the developing dentition in gorilla and orangutan. American Journal of Physical Anthropology 86:189-203.

Beynon, A.D., Dean, M.C., Reid, D.J. 1991. On thick and thin enamel in hominoids. American Journal of Physical Anthropology. 86, 295-309.

Boesch, C., Boesch-Achermann, H. 2000. The Chimpanzees of the Taï Forest: Behavioural Ecology and Evolution. Oxford University Press, Oxford.

Bogin, B. 1990. The evolution of human childhood. BioScience 40:16-25.

Boyde, A. 1963. Estimation of age at death of young human skeletal remains from incremental lines in the dental enamel. In: Third International Meeting in Forensic Immunology, Medicine, Pathology, and Toxicology, London, April 1963, pp. 16-24.

Boyde, A. 1964. The structure and development of mammalian enamel. Ph.D. Dissertation, The London Hospital Medical College.

Boyde, A. 1989 Enamel. In Teeth. Handbook of Microscopic Anatomy (eds Berkovitz BKB, Boyde A, Frank RM, Höhling HJ, Moxham BJ, Nalbandian J, Tonge CH), pp. 309–473. New York: Springer Verlag.

Bromage, T.G., Dean, M.C. 1985. Re-evaluation of the age at death of immature fossil hominids. Nature 31:525-528.

Bromage, T.G. 1991. Enamel incremental periodicity in the pig-tailed macaque: a polychrome fluorescent labeling study of dental hard tissues. American Journal of Physical Anthropology 86, 205-214.

Carlson, B. A., and Crowley, B. E. 2016. Variation in carbon isotope values among chimpanzee foods at Ngogo, Kibale National Park and Bwindi Impenetrable National Park, Uganda. American Journal of Primatology, 78, 1031–1040.

Charnov E.L. 1991. Evolution of life history variation among female mammals. Procedings of the National Academy of Sciences of the United States of America, 88:1134-37 21.

Dean, M.C. 1987. Growth layers and incremental markings in hard tissues; a review of the literature and some preliminary observations about enamel structure in *Paranthropus boisei*. Journal of Human Evolution,16, 157-172.

Dean, M.C. 1998. A comparative study of cross-striation spacings in cuspal enamel and of four methods of estimating the time taken to grow molar cuspal enamel in *Pan, Pongo,* and *Homo*. Journal of Human Evolution, 35, 449e462.

Dean, M.C. 2000. Progress in understanding hominoid dental development. Journal of Anatomy. 197, 77-101.

Dean, M.C., Beynon, A.D., Thackeray, J.F., Macho, G.A. 1993. Histological reconstruction of dental development and age at death of a juvenile *Paranthropus robustus* specimen, SK 63, from Swartkrans, South Africa. American Journal of Physical Anthropology, 91, 401-419.

Dean, M.C., Scandrett, A.E. 1996. The relation between long-period incremental markings in dentine and daily cross-striations in enamel in human teeth. Archive of Oral Biology, 41, 233-241.

Dean, M. C., and Kelley, J. 2012. Comparative dental development in *Hispanopithecus laietanus* and *Pan troglodytes*. Journal of Human Evolution, 62(1), 174–178. http://doi.org/10.1016/j.jhevol.2011.10.003.

Dean, M. C., and Cole, T. J. 2013. Human Life History Evolution Explains Dissociation between the Timing of Tooth Eruption and Peak Rates of Root Growth. PLoS ONE, 8(1). http://doi.org/10.1371/journal.pone.0054534.

Dean, M. C., and Elamin, F. 2014. Parturition lines in modern human wisdom tooth roots : do they exist , can they be characterized, and are they useful for retrospective determination of age at first reproduction and / or inter-birth intervals? Annals of Human Biology, 4460. http://doi.org/10.3109/03014460.2014.923047.

Dirks, W. 1998. Histological reconstruction of dental development and age of death in a juvenile gibbon (*Hylobates lar*). Journal of Human Evolution, 35, 411-425.

Dirks, W., Bowman, J.E. 2007. Life history theory and dental development in four species of catarrhine primates. Journal of Human Evolution, 53, 309-320.

Dirks, W., Reid, D. J., Jolly, C. J., Phillips-Conroy, J. E., and Brett, F. L. 2002. Out of the mouths of baboons: stress, life history, and dental development in the Awash National Park hybrid zone,

Ethiopia. American Journal of Physical Anthropology, 118(3), 239–52. http://doi.org/10.1002/ajpa.10089.

Dirks, W., Humphrey, L. T., Dean, M. C., and Jeffries, T. E. 2010. The relationship of accentuated lines in enamel to weaning stress in juvenile baboons (*Papio hamadryas anubis*). Folia Primatologica; International Journal of Primatology, 81(4), 207–23. http://doi.org/10.1159/000321707.

Emery Thompson, M., Muller, M., Wrangham, R. 2012. The energetics of lactation and the return to fecundity in wild chimpanzees. Behavioral Ecology, 23(6):1234–1241.

FitzGerald, C.M., 1998. Do enamel microstructures have regular time dependency? Conclusions from the literature and a large-scale study. Journal of Human Evolution, 35, 371-386.

Gleiser, I., Hunt, E. E. 1955. The Permanent Mandibular First Molar: Its Calcification, Eruption, and Decay, American Journal of Physical Anthropology 13:253-84.

Goodman, A. H., and Rose, J. C. 1990. Assessment of Systemic Physiological Perturbations From Dental Enamel Hypoplasias and Associated Histological Structures, Yearbook of Physical Anthropology, 110, 59–110.

Guatelli-Steinberg, D. 2001. What can developmental defects of enamel reveal about physiological stress in nonhuman primates? Evolutionary Anthropology, 10, 138-151.

Guatelli-Steinberg, D. 2004. Analysis and significance of linear enamel hypoplasia in Plio-Pleistocene hominins. American Journal of Physical Anthropology 123, 199-215.

Gustafson, A. 1959. A morphological investigation of certain variations in the structure and mineralization of human deciduous dental enamel. Odontologisk Tidskrift 67, 365-472.

Gustafson, G., and Gustafson., A. G. 1967. Microanatomy and histochemistry of enamel. In Structural and Chemical Organization of Teeth, A. E. W. Miles, ed. London: Academic Press, 75–134.

Harvey P.H., Clutton-Brock TH. 1985. Life history variation in primates. Evolution 39: 559-81.

Hillson, S. W. 2005. Teeth. 2nd Ed. Cambridge: Cambridge University Press.

Humphrey, L. T. 2010. Weaning behaviour in human evolution. Seminars in Cell & Developmental Biology, 21, 453–461.

Kelley, J., and Smith, T.M. 2003. Age at first molar emergence in early Miocene *Afropithecus turkanensis* and life-history evolution in the Hominoidea. Journal of Human Evolution, 44, 307-329.

Kelley, J., and Schwartz, G. T. 2010. Dental development and life history in living African and Asian apes. Proceedings of the National Academy of Sciences of the United States of America, 107(3), 1035–40. http://doi.org/10.1073/pnas.0906206107.

Kelley, J., and Schwartz, G. T. 2012. Life-History Inference in the Early Hominins *Australopithecus* and *Paranthropus*, International Journal of Primatology, 33, 1332–1363. http://doi.org/10.1007/s10764-012-9607-2.

Köndgen, S., Kühl, H., N'Goran, P.K., Walsh, P.D., Schenk, S., Ernst, N., Biek, R., Formenty, P., Mätz-Rensing, K., Schweiger, B., Junglen, S., Ellerbrok, H., Nitsche, A., Briese, T., Lipkin,W.I., Pauli, G., Boesch, C., Leendert, F.H. 2008. Pandemic human viruses viruses cause decline of endangered great apes. Current Biology, 18, 260-264.

Krishna BA, Singh, M., Singh, M., Kaumanns W 2008. Infant development and weaning in *Macaca silenus* in the natural habitats of the Western Ghats, India. Current Science 94: 347–355.

Kuykendall, K.L., Mahoney, C.J., Conroy, G.C. 1992. Probit and survival analysis of tooth emergence ages in a mixed-longitudinal sample of chimpanzees (*Pan troglodytes*). American Journal of Physical Anthropology, 89, 379-399.

Kuykendall, K. L., and Conroy, G. C. 1996. Permanent tooth calcification in chimpanzees (*Pan troglodytes*): Patterns and polymorphisms. American Journal of Physical Anthropology. 99: 159–174.

Lee, P. C. 1996. The meanings of weaning: Growth, lactation, and life history. Evolutionary Anthropology, 5,87–96.

Lee, P. C. 2010. Growth and Investment in Hominin Life History Evolution: Patterns, Processes, and Outcomes. International Journal of Primatology, 33(6), 1309–1331. http://doi.org/10.1007/s10764-011-9536-5.

Leendertz, F.H., Ellerbrok, H., Boesch, C., Couacy-Hymann, E., Mätz-Rensing, K., Hakenbeck, R., Bergmann, C., Abaza, P., Junglen, S., Moebius, Y., Vigilant, L., Formenty, P., Pauli, G. 2004. Anthrax kills wild chimpanzees in a tropical rainforest. Nature, 430, 451-452.

Machanda, Z., Brazeau, N. F., Bernard, A. B., Donovan, R. M., Papakyrikos, A. M., Wrangham, R., and Smith, T. M. 2015. Dental eruption in East African wild chimpanzees. Journal of Human Evolution, 2015, 2–9. http://doi.org/10.1016/j.jhevol.2015.02.010.

Macho, G. A., Reid, D. J., and Beynon, A. D. 1996. Climatic effects on dental development of *Theropithecus oswaldi* from Koobi Fora and Olorgesailie. Journal of Human Evolution, 30, 57–70.

Macho, G. a, and Lee-Thorp, J. a. 2014. Niche partitioning in sympatric *Gorilla* and *Pan* from Cameroon: Implications for life history strategies and for reconstructing the evolution of hominin life history. PloS One, 9(7), e102794. http://doi.org/10.1371/journal.pone.0102794.

Mann, A.B., LampI, M., Monge, J. 1987. Maturational patterns in early hominids. Nature 328:673-75

Martin, P. 1984. The meaning of weaning. Animal Behaviour, 32, 1257– 1259.

McDade, T. W. 2003. Life history theory and the immune system: steps toward a human ecological immunology. American Journal of Physical Anthropology, Supplement *37*, 100–25. http://doi.org/10.1002/ajpa.10398.

Moorees, C. F. A., Fanning, E. A., and Hunt, E. E. 1963, Age variation of formation stages for ten permanent teeth, Journal of Dental Research, 42, 1490–502.

Muller, M. N., and Wrangham, R. W. 2014. Mortality rates among Kanyawara chimpanzees. Journal of Human Evolution, 66(1), 107–114. http://doi.org/10.1016/j.jhevol.2013.10.004.

Negrey, L.D., Reddy, R.B., Scully, E.J., Phillips-Garciad, S., Owens, L.A., Langergraber, K.E., Mitani, J.C., Emery Thompson, M., Wrangham, R.W., Muller, M.N., Otali, E., Machanda, Z., Hyerobag, D., Grindle, K.A., Pappas, T.E., Palmenberg, A.C., Gerne, J.E., and Goldberg , T.L. 2019. Simultaneous outbreaks of respiratory disease in wild chimpanzees caused by distinct viruses of human origin. Emerging Microbes & Infections, VOL. 8 https://doi.org/10.1080/22221751.2018.1563456.

Nissen, H.W., Riesen, A.H. 1964. The eruption of the permanent dentition of chimpanzees. American Journal of Physical Anthropology 22: 285–294.

Noren, J.G. 1984. Microscopic study of enamel defects in deciduous teeth of infants of diabetic mothers. Acta Odontologica Scandanavia, 42:153-156.

Nowell, A.A., Fletcher, A.W. 2007. Development of independence from the mother in *Gorilla gorilla gorilla*. International Journal of Primatology, 28(2):441–55.

Ohtsuka, M., Shinoda, H. 1995. Ontogeny of circadian dentinogenesis in the rat incisor. Archives of Oral Biology, 40:481–485.

Okada, M. 1943. Hard tissues of animal body: highly interesting details of Nippon studies in periodic patterns of hard tissues are described. The Shanghai Evening Post, pp. 15-31.

Potts, K. B., Watts, D. P., and Wrangham, R. W. 2011. Comparative Feeding Ecology of Two Communities of Chimpanzees (Pan troglodytes) in Kibale National Park, Uganda. International Journal of Primatology, 32(3), 669–690. http://doi.org/10.1007/s10764-011-9494-y

Pusey, A.E. 1979. Intercommunity transfer of chimpanzees in Gombe National Park. In: Hamburg, D., McCown, E. (Eds.), The Great Apes. Benjamin Cummings, Menlo Park, pp. 465-479.

Reid, D.J., Schwartz, G.T., Dean, C., Chandrasekera, M.S. 1998. A histological reconstruction of dental development in the common chimpanzee, *Pan troglodytes*. Journal of Human Evolution,. 35, 427-448.

Reid, D., Dean, M.C. 2006. Variation in modern human enamel formation times. Journal of Human Evolution, 50, 329-346.

Reitsema, L. J. 2012. Introducing fecal stable isotope analysis in primate weaning studies. American Journal of Primatology, 74, 926–939.

Retzius, A. 1837. Bemerkungen uber den innern Bau der Zahne, mit besonderer Ruchsicht auf den im Zahnknochen vorkommenden Rohrenbae. Mullers Archiv fur Anatomie und Physiologyie, pp. 486.

Rinaldi, C. 1999. A record ofhibernation in the incisor teeth ofRecent and fossil marmots (*Marmota flaviventris*). In: Mayhall, J. (Ed.) 11th International Symposium on Dental Morphology. Oulu University Press, Oulu, Finland, pp. 112–119.

Risnes, S. 1990. Structural characteristics of staircase-type Retzius lines in human dental enamel analyzed by scanning electron microscopy. Anatomy Records, 226, 135–146.

Risnes, S. 1998. Growth tracks in dental enamel. Journal of Human Evolution, 35, 331-350.

Robbins, M.M., Nkurunungi, J.B., McNeilage, A. 2006. Variability of the feeding ecology of eastern gorillas. In: Hohmann, G., Robbins, M.M., Boesch, C. (Eds.), Feeding Ecology of Apes and Other Primates. Cambridge University Press, Cambridge, pp 25-47.

Robson, S. L., Wood, B., Shea, B. T., Arnold, C., … Soligo, C. 2008. Hominin life history: reconstruction and evolution. Journal of Anatomy, 212(4), 394–425. http://doi.org/10.1111/j.1469-7580.2008.00867.

Rose, J. C., Armelagos, G. J., and Lallo, J. W. 1978. Histological enamel indicator of childhood stress in prehistoric skeletal samples. American Journal of Physical Anthropology, 49:511–516.

Rushton, M.A. 1933. On the fine contour lines of the enamel of milk teeth. Dental Records, 53, 170-171.

Schour, I. 1936. The neonatal line in the enamel and dentin of human deciduous teeth and first permanent molar. J. Am. Dent. Assoc. 23, 1946-1955.

Schour, I., Hoffman, M.M. 1939. Studies in tooth development: II. The rate of apposition of enamel and dentin in man and other mammals. Journal of Dental Research, 18, 161-175.

Schultz, A.H. 1960. Age changes in primates and their modification in man. In Human Growth, ed. JM Tanner, pp. 1-20. Oxford: Pergamon.

Schwartz, G. T. 2012. Growth, Development, and Life History throughout the Evolution of Homo. Current Anthropology, 53(S6), S395–S408. http://doi.org/10.1086/667591.

Schwartz, G.T., Reid, D.J., Dean, C. 2001. Developmental aspects of sexual dimorphism in hominoid canines. International Journal of Primatology, 22, 837-860.

Schwartz, G.T., Reid, D.J., Dean, M.C., Zihlman, A.L. 2006. A faithful record of stressful life events preserved in the dental developmental record of a juvenile gorilla. International Journal of Primatology, 22, 837-860.

Sellen, D. W. 2007. Evolution of infant and young child feeding: Implications for contemporary public health. Annual Review of Nutrition, 27, 123–148.

Sellen, D. W. 2009. Evolution of human lactation and complementary feeding: Implications for understanding contemporary cross-cultural variation. In G. Goldberg, A. Prentice, A. Prentice, S. Filteau, & K. Simondon (Eds.), Breast-feeding: Early influences on later health (pp. 253–282). Dordrecht: Springer.

Shellis, R.P. 1998. Utilization of periodic markings in enamel to obtain information on tooth growth. Journal of Human Evolution, 35, 387-400.

Skinner, M.F., Hopwood, D. 2004. Hypothesis for the causes and periodicity of repetitive linear enamel hypoplasia in large, wild African (*Pan troglodytes* and *Gorilla gorilla*) and Asian (*Pongo pygmaeus*) apes. American Journal of Physical Anthropology, 123, 216-235.

Smith, B.H. 1989. Dental development as a measure of life history in primates. Evolution, 43:683-88.

Smith, T.M. 2004. Incremental development of primate dental enamel. Ph.D. Dissertation. Stony Brook University.

Smith, T.M. 2006. Experimental determination of the periodicity of incremental features in enamel. Journal of Anatomy, 208, 99-114.

Smith, T. M. 2008. Incremental dental development : Methods and applications in hominoid evolutionary studies. Journal of Human Evolution, 54(2), 205–224. http://doi.org/10.1016/j.jhevol.2007.09.020.

Smith, T. M. 2013. Teeth and Human Life-History Evolution*. Annual Review of Anthropology, 42(1), 191–208. http://doi.org/10.1146/annurev-anthro-092412-155550.

Smith, T.M., Reid, D.J., Dean, M.C., Olejniczak, A.J., Ferrell, R.J., Martin, L.B. 2007. New perspectives on chimpanzee and human dental development. In: Bailey, S.E., Hublin, J.- J. (Eds.), Dental Perspectives on Human Evolution: State of the Art Research in Dental Paleoanthropology. Springer, Dordrecht, pp. 177-192.

Smith, T. M., Smith, B. H., Reid, D. J., Siedel, H., Vigilant, L., Hublin, J. J., & Boesch, C. 2010. Dental development of the Taï Forest chimpanzees revisited. Journal of Human Evolution, 58(5), 363–73. http://doi.org/10.1016/j.jhevol.2010.02.008.

Smith, T. M., Machanda, Z., Bernard, A. B., Donovan, R. M., Papakyrikos, A. M., Muller, M. N., and Wrangham, R. 2013. First molar eruption, weaning, and life history in living wild chimpanzees. Proceedings of the National Academy of Sciences of the United States of America, 10(8) 2787-2791. http://doi.org/10.1073/pnas.1218746110.

Smith, T. M., Tafforeau, P., Le Cabec, A., Bonnin, A., Houssaye, A., Pouech, J., … Menter, C. G. 2015. Dental ontogeny in Pliocene and early Pleistocene hominins. PLoS ONE, 10(2), 1–20. http://doi.org/10.1371/journal.pone.0118118.

Smith, T. M., Austin, C., Hinde, K., Vogel, E. R., and Arora, M. 2017. Cyclical nursing patterns in wild orangutans, Science Advances, (May), 1–9.

Smith, B. H., and Boesch, C. 2011. Mortality and the magnitude of the "wild effect" in chimpanzee tooth emergence. Journal of Human Evolution, 60(1), 34–46. http://doi.org/10.1016/j.jhevol.2010.08.006.

Stanford, C. B., and Nkurunungi, J. B. 2003. Behavioral Ecology of Sympatric Chimpanzees and Gorillas In Bwindi Impenetrable National Park, Uganda : Diet, International Journal of Primatology, 24(4).

Struhsaker, T. T. 1997. Ecology of an African rainforest. Gainesville: University Press of Florida.

Stumpf, R. 2007. Chimpanzees and bonobos: Diversity within and between species. In: Campbell, C., Fuentes, A., MacKinnon, K., Bearder, S., Stumpf, R. (Eds.), Primates mates in Perspective. Oxford University Press, New York, pp. 321-344.

Tafforeau, P.T., Smith, T.M. 2008. Nondestructive imaging of hominoid dental microstructure using phase contrast X-ray synchrotron microtomography. Journal of Human Evolution, 54, 272-278.

Tafforeau, P., Zermeno, J. P., and Smith, T. M. 2012. Tracking cellular-level enamel growth and structure in 4D with synchrotron imaging. Journal of Human Evolution, 62(3), 424–8. http://doi.org/10.1016/j.jhevol.2012.01.001.

Thomas, R.F. 2003. Enamel defects, well-being and mortality in a medieval Danish village. Ph.D. Dissertation, Pennsylvania State University.

Tsukahara, T. 1993. Lions eat chimpanzees: the first evidence of predation by lions on on wild chimpanzees. American Journal of Primatology, 29, 1-11.

Watts DP. 1991. Mountain gorilla reproduction and sexual behaviour. American Journal of Primatology 24:211-226.

Watts, D.P. 2004. Intracommunity coalitionary killing of an adult male chimpanzee at at Ngogo, Kibale National Park, Uganda. International Journal of Primatology, 25, 507-521.

Watts, D. P., Muller, M. N., Amsler, S. J., Mbabazi, G., and Mitani, J. C. 2006. Lethal Intergroup Aggression by Chimpanzees in Kibale National Park , Uganda, American Journal of Primatology, 180 (February 2005), 161–180. http://doi.org/10.1002/ajpa.

Watts, D.P., Potts, K.B., Lwanga, J.S., Mitani, J.C. 2012. Diet of chimpanzees (*Pan troglodytes schweinfurthii*) at Ngogo, Kibale National Park, Uganda, 1. Diet composition and diversity. American Journal of Primatology, 74, 114-129.

Williams, J., Lonsdorf, E., Wilson, M., Schumacher-Stankey, J., Goodall, J., Pusey, A. 2008. Causes of death in the Kasekela chimpanzees of Gombe National Park, Tanzania. American Journal of Primatology 70, 766-777.

Wolff, P.H. 1968. The serial organization of sucking in the young infant. Pediatrics, 42(6):943- 956.

Wood, B. M., Watts, D. P., Mitani, J. C., and Langergraber, K. E. 2017. Favorable ecological circumstances promote life expectancy in chimpanzees similar to that of human hunter-gatherers. Journal of Human Evolution, 105, 41-56. http://doi.org/10.1016/j.jhevol.2017.01.003

Woolridge, M.W. 1986. The 'anatomy' of infant sucking. Midwifery, 2:164-171.

Zihlman, A., Bolter, D., Boesch, C. 2004. Wild chimpanzee dentition and its implications for assessing life history in immature hominin fossils. Procedings of the National Academy of Sciences. 101, 10541-10543.

Zihlman, A.L., Bolter, D.R., Boesch, C. 2007. Skeletal and dental growth and development in chimpanzees (*Pan troglodytes*) of the Taï National Forest, Cote d'Ivoire. Journal of Zoology, 273, 63-73.

Chapter 3: Calcium-normalized Barium (Ba/Ca) Distributions in Enamel and Dentine of Wild Ugandan Chimpanzees (*Pan troglodytes schweinfurthii)*: Implications for Weaning Studies in Fossil Taxa

Abstract: Calcium-normalized barium ratios (Ba/Ca) in tooth enamel and dentine have been shown to be correlated with dietary transitions associated with life history events such as birth, and the onset and completion of weaning in numerous primates. This study uses the histologically assessed timing of the changes in Ba/Ca ratios in the teeth of wild chimpanzees, to verify whether these changes coincide with weaning completion age, as inferred from the ages at which the first molar (M_1) root growth spurt occurred, based on a previous study of these individuals. Similar data from a sample of yellow baboons and red-tailed monkeys are also considered here to verify the method.

This study finds that in the first molars (M1) of most of the chimpanzees in our sample, the calcium-normalized barium (Ba/Ca) ratio increased between birth and the first three to six months of life, and then gradually decreased over the next year of formation. Occasional spikes in the M1 Ba/Ca ratio occurred after that point and may indicate increases in nursing frequency or intensity within the second year of life, or could result from episodes of illness in which the infant's own skeletal stores of calcium (and therefore, barium) were mobilized and incorporated into dental tissues forming at that time. Patterns in enamel Ba/Ca levels from the later-forming teeth of several of the chimpanzees are also analyzed, and these show spikes in Ba/Ca levels at the same ages as when the root growth spurt occurs in the M1. This is significant because it suggests that a dietary transition was indeed occurring alongside this structural marker of a peak

in growth rate, supporting the proposition that weaning completion follows close on the heels of the M1 growth spurt in chimpanzees. Following the growth spurt, Ba/Ca levels decrease again, and stay at low levels thereafter, except in cases where there was damage to the enamel. This suggests that nutritive intake from nursing ceases just after this point, since breast milk is the only source of heightened levels of Ba/Ca in early development (Smith et al., 2017, 2018). In some samples, the patterns of Ba/Ca change are more difficult to discern, due to sampling issues, damage to enamel crowns, or extreme outlier values that drive the range of variation to be too wide to pick up subtle changes. Methods of troubleshooting these and other issues are presented.

Introduction: While other skeletal sources of life history information, like body size and brain size, can be used to infer relative measures of life history pace (Robson and Wood, 2008), dental developmental data are particularly relied upon when assessing the life history pace of fossil apes (hominoids) and human ancestors (hominins), since teeth are more abundant and more durable than anything else in the fossil record, and because they preserve a real-time record of their development within their incrementally forming tissues. The age at which the first mandibular molar (M_1) emerges through the gingiva into the jaw has been used to infer weaning age in extant and fossil primates, due to the correlation between weaning age and M_1 emergence across the order Primates (Smith, 1989; Smith, 1991; Smith and Tompkins, 1995). However, recent studies have found that the age at M_1 emergence in wild, as well as in captive chimpanzees, is well before they cease nursing (Smith et al., 2013; Machanda et al., 2015), and it has been suggested that the end of the weaning process may align closely with the age at which the M_1 attains functional occlusion (Malone, Chapter 1), 2.5-6.0 months after emergence (Machanda et al., 2015). Several studies have also found that chimpanzee M_1 roots show

evidence of a growth spurt at a point after emergence, (Dean and Kelley, 2012; Dean and Cole, 2013), and this root growth spurt may occur as M1s are reaching functional occlusion (Dean and Kelley, 2012). A previous study by the author documented enamel and dentine formation variation, and stress episode distribution, in the teeth of wild chimpanzees (*Pan troglodytes schweinfurthii*) from the Ngogo population in Kibale National Park, as well as one individual from Bwindi Impenetrable National Park, Uganda (Malone, Chapter 1). The study found that the M_1 root growth spurt for the Ngogo chimpanzees in the sample occurred 2-12 months after the M_1 emergence ages previously known for the chimpanzees from the neighboring community of Kanyawara (Machanda et al., 2015), supporting a link between the root growth spurt and the projected time of attainment of M_1 functional occlusion, rather than one between the growth spurt and M_1 emergence, per se. To link this structural marker of formation rate and inferred occlusion age to the weaning process, however, an additional source of information about Ngogo chimpanzee weaning ages was needed. The work of Badescu et al. (2017), tracking changes in fecal isotopes of Ngogo infants, provided this source. It was determined that the root growth spurt for the chimpanzees from Ngogo (Malone, Chapter 1) aligned closely with the mean inferred weaning completion age of 4.0 - 4.5 years determined for infants using the changing offsets between mother and infant fecal $\delta^{15}N$ and $\delta^{13}C$ values over time (N=52 Badescu et al., 2017). However, since the time of weaning of the chimpanzees in the dental study is unknown, the application of an additional proxy for dietary input/weaning is needed to confirm the relationship between the root growth spurt and weaning.

Calcium-normalized barium (Ba/Ca) distributions have been used in several studies to document the transition from gestational diet to nursing to adult foods in the teeth of wild orangutans (Smith et al., 2017), humans and macaques with recorded weaning histories and a

juvenile Neanderthal (Austin et al., 2013), and a fossil human molar and several Neanderthal molars from the same site (Smith et al., 2018). Ba/Ca distributions are therefore used here as a chemical proxy for weaning-related dietary transitions, to explore how the trace element distributions in enamel and dentine relate to the inferred link between chimpanzee M_1 root growth spurt and weaning completion. Comparative data from a study of yellow baboons (*Papio cynocephalus*) by the author is also used here to validate the link between structural and chemical indicators of the weaning process, taking into account their much more abbreviated weaning process compared with that of chimpanzees (Altmann et al., 1977; Altmann, 1980; Altmann et al., 1981).

Background: Teeth are a valuable medium for the analysis of developmental timing in extinct taxa, due to their relative abundance in the fossil record, their resistance to post-mortem alteration, and because they preserve an exact record of their development in their incremental microstructures (e.g. Risnes, 1998; Dean, 2000; Antoine et al., 2009). Such structures can be periodic, forming at regular, consistent intervals, such as cross-striations and Retzius lines in enamel or von Ebner's lines and Andresen lines in dentine (Antoine et al., 2009), or they can be aperiodic, and exist as visible structures resulting from growth processes, but not subject to any known time-dependency, as with enamel prisms, dentine tubules, and Hunter-Schreger bands (reviewed in Smith, 2004). Structures can also form as a result of disturbances to normal growth, and these form at irregular intervals influenced by any number of external and internal factors (see below). Each type of structure forms in all three dental tissues (enamel, dentine, and cementum), and those present in the enamel and dentine of the chimpanzees in this study have been used to document their periodic variables (i.e. daily secretion rate, Retzius/Andresen line

periodicity, Retzius line number, crown and root extension rates) and then in order to estimate crown formation time. Only the structures relevant to this study will be reviewed here, though all dental periodic, aperiodic, and irregular structures, and the variables that result from them, have been reviewed elsewhere (e.g. Smith, 2008).

Irregular Structures: In addition to regular periodic structures, irregular structures can also been seen within dental tissues. Accentuated lines in enamel can form in response to growth disturbances resulting from dietary change, illness, physical or psychological trauma, etc. and these are often visible in thin sections viewed under polarized light (Boyde, 1990; Goodman and Rose, 1990; Molnar and Ward, 1975; Rose, 1977, 1979; Rose et al., 1978; Skinner and Anderson, 1991; Teivens et al., 1996).

The neonatal line is one such accentuated line that forms at birth (Rushton, 1933; Schour 1936), and is present in all deciduous teeth as well as the first permanent molar (M1). Since the various cusps of the M1 start forming 8-12 weeks before birth in humans (Christensen & Kraus, 1965) and 4-6 weeks in chimpanzees (Reid et al., 1998), the neonatal line appearance may result from a decreased level of calcium in the plasma during the first 48 hours after birth (hypocalcaemia) (Nóren, 1984) and may also result from the trauma of birth itself (Gustafson & Gustafson, 1967; Eli et al., 1989). It can be recognized because it divides the smooth prenatal enamel, which contains no striae of Retzius, from the rest of the crown. Because accentuated lines appear to form in response to stresses occurring at transitional times such as birth (Gustafson, 1967), weaning (Rose et al., 1978; Dirks et al., 2010), and, in humans, parturition (Dean and Elamin, 2014), these structures become important indicators of the timing of life history events as recorded in dental tissues.

Stresses associated with habitat seasonality (e.g. seasonal food availability and seasonal breeding), may also manifest in growth disturbances in the form of accentuated lines (Dirks, 1998: Dirks et al., 2002), although this relationship is less clear. There can also be differences in the types and timing of stresses experienced by males and females over the course of their lives, beginning with differential maternal investment during the weaning process, such as that seen in chacma baboons (Cheney et al., 2004), anubis baboons (Dirks et al., 2010), western lowland gorillas (Krishna et al., 2008), and lion-tailed macaques (Nowell and Fletcher, 2007). Disentangling the patterns of accentuated lines forming due to life history stresses, particularly when they differ based on sex, from those occurring due to seasonally-induced stress, can complicate efforts to use dental tissue structures to assess the pace and pattern of life history events (e.g., Dirks et al. 2010).

Accentuated lines in enamel (which correspond to Owen's lines in dentine) occur alongside periodic features, which means they can be aged, but they also form at the same time within enamel and dentine as well as between simultaneously forming parts of different teeth. This synchrony in accentuated line formation allows consecutively forming teeth to be registered to one another by cross-matching these lines to determine how much crown and root formation overlap there is between consecutively forming teeth (e.g., Dean et al., 1993b; Reid et al., 1998a). It also allows periods of time in M2 or M3 crown or root formation to be aged by using an absolute timeline that starts with the neonatal line in a deciduous tooth or the M1, and continues in the next tooth using cross-matched accentuated line as reference points (e.g., Beynon et al., 1998b; Dirks, 1998; Reid et al., 1998a,b; Dirks et al., 2002; Thomas, 2003; Smith, 2004; Schwartz et al., 2006; Smith et al., 2007b; Antoine et al., 2009).

Extension rate: In previous work on these chimpanzee teeth (Malone, Chapter 1), it was not possible, in some cases, to count all of the Retzius lines in the lateral and cervical enamel due to cracking or breaking away of portions of the enamel. This prevented the total crown formation time (TFT) from being measured by using the enamel alone. To alleviate this problem, the extension rate (ER) was determined for the dentine within the crown and the root. The extension rate, in both enamel and dentine, refers to the amount of formation taking place toward the crown surface (or the pulp cavity, in the case of the root) versus the growth occurring cervically (or apically, in the root), and strictly speaking, is an expression of the rate at which new enamel-forming and dentine-forming cells differentiate along the EDJ or the inner root surface, and are activated each day (Shellis, 1998).

To measure the ER (Figure 10), starting at the dentine horn, a dentine tubule was measured to a distance of ~200 μm into the root, or to where it intersected with an Andresen line or an accentuated line of Owen in that area. That line was then followed back to the EDJ, or the inner root surface. (If the dentine horn was not present due to wear, as seen in Figure 10, the tubule closest to where the dentine horn would have been was used as the starting point.) The tubule length was followed along any curvature it showed, in order to capture the full number of days of growth along it, as opposed to a straight-line measure, which would have overestimated the growth distance, perhaps intersecting with a stria significantly more than 200 μm into dentine growth. Measuring how much EDJ length there was between the tubule's and stria's intersections with the EDJ, or the inner root surface, provided the amount of newly extended crown or root that had formed during however many days passed within that 200 μm interval. The measured tubule length (~200 μm) was then divided by the previously established local DSR to get the

Figure 10: Dentine extension rate measurement method in the M_1 of male chimpanzee "NG001"

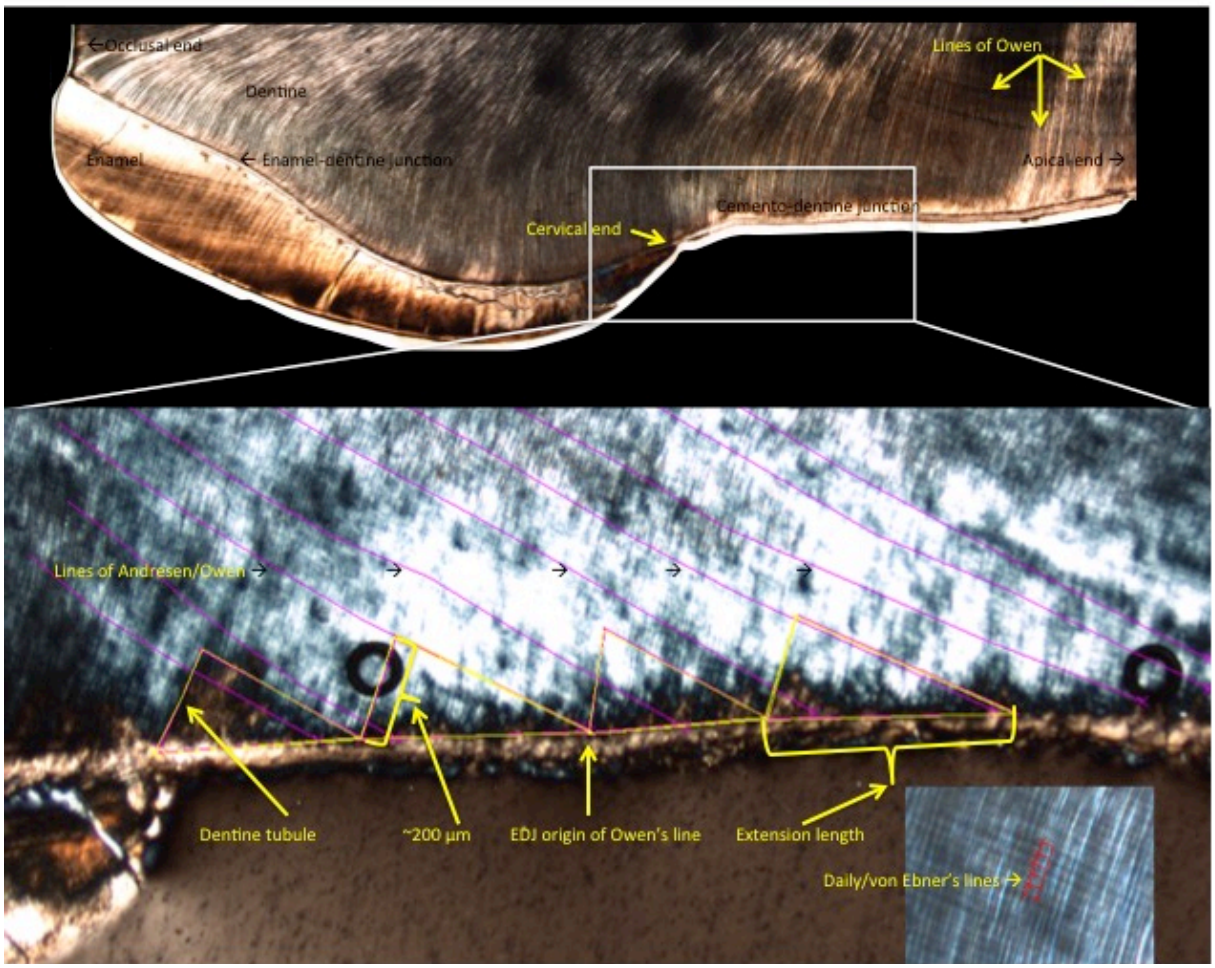

Figure 10: The top panel shows the mesiobuccal cusp of "NG001"'s left M_1 at low power through transmitted light. The portion highlighted and enlarged on the bottom is the cervical end of the enamel–dentine junction (EDJ) and the beginning of the root dentine at the cemento-enamel junction (CEJ). Several dentine tubules are highlighted along the first 200 µm of growth from the root surface, and the Andresen lines with which they intersect are followed back to their origin lower down on the root. The distance between the tubule start point and the Andresen line origin is also highlighted along the root surface. The inset on the bottom shows a high-powered (20x) view of the daily lines in dentine, called von Ebner's lines, and these were measured to obtain DSR in dentine.

number of days of formation within that interval, and then the length of the newly extended crown or root was divided by the number of days associated with that interval to obtain the extension rate for that interval of crown or root dentine. This was continued all the way down the crown until the apical end was reached.

By adding together the formation times for each interval all the way down the crown and root, the TFT could then be estimated a second time. This TFT also included root formation time (RFT). These estimates were preferentially used to measure TFTs because the formation times obtained using enamel were limited by the damage and wear to the crowns, and because this alternate method has been shown to produce accurate estimates of formation time quite efficiently, especially in teeth like these that are less than ideal for sectioning, (Dean and Kelley, 2012). Results of CFT estimates using enamel compared with the CFT and TFT estimates using dentine are compared in Malone (Chapter 1)

Root growth spurt: In addition to permitting estimates of TFTs, the extension rate varies over the course of crown and root formation (Boyde, 1963), peaking at a particular point during root formation (Gleiser & Hunt, 1955; Moorees et al., 1963; Dean & Kelley, 2012), thought to be associated in chimpanzees with emergence age, or possibly with attaining functional occlusion at the end of the eruption process (Dean & Kelley, 2012; Dean & Cole, 2013). The age at which this peak extension rate occurs, which represents a root growth spurt (Dean & Cole, 2013), can then be measured and compared between individuals.

Life History: Studies of life history theory in living mammals (reviewed in Bogin, 1990; Schwartz, 2012) have investigated the relationships between 1) an organism's ecological context, 2) its energy investment in growth, reproduction, and somatic maintenance, and 3) variables such as brain and body mass and dental development, which, at higher taxonomic levels, are correlated with life history events or milestones (e.g. Harvey and Clutton- Brock, 1985; Charnov, 1991). Life history parameters themselves (e.g. gestation length, age at weaning, age at first reproduction, etc.) are referred to by some as life history variables, while other somatic measures, such as body size, brain size, and dental development, which have been shown to be

broadly linked with the life history variables, are called life history-related variables (Robson and Wood, 2008). Life history-related variables are used to infer the timing of life history variables in taxa or individuals for which life history cannot be directly observed, such as for fossil taxa, and dental deveopment is the proxy most often used for such inferences, since teeth preserve so well in the fossil record.

Dental development, specifically the age at M_1 emergence, is correlated with age at weaning and sexual maturity in a study across 21 primates (Smith, 1989), however, within and between species, this relationship is not as clear. Gorillas, orangutans, and chimpanzees (Robson and Wood, 2008; Smith et al., 2013) emerge their M_1s before they have been observed to complete weaning, and even at the species level, such as between mountain and lowland gorillas (Watts, 1991; Robbins et al., 2006), there is a great deal of variation in this relationship. Directly measuring how much the weaning process itself varies within extant hominoid species, subspecies, and even populations, would go a long way toward understanding the links that can and cannot be made between dental development and the weaning process of closely related fossil hominins. It may also be that another point in the eruption process, namely the point at which the first molars reach functional occlusion, is an appropriate milestone to mark the end of the weaning process.

Weaning: Weaning is a process consisting of multiple stages that can vary in duration, as well as age at initiation and completion (Lee, 1996). Such variation, especially in the age at weaning completion, may be linked to later life history variables for the offspring, such as age at menarche and first reproduction (Lee, 2010), as well as somatic growth rate and adult body size (Lee, 1996), and even mortality risk due to the immunological role played by nursing (McDade, 2003; Humphrey, 2010). In short, the age at which a mammal is weaned can potentially affect

the overall pace of its life history and ultimately its evolutionary trajectory.

The weaning process like other life history events, invariably presents a number of sources of stress. This can start early on if samples of adult foods are difficult for an infant's physiology to digest (Dirks, 2002); in addition, external water sources may contain novel pathogens; and the psychological stresses of being denied access to nursing may also take its toll (reviewed in Dirks, 2002). All such interruptions to consistent nutritional intake or processing will result in disruptions to normal growth, which are registered in all of the dental tissues forming at that time (Beynon et al., 1991, 1998b; Bow- man, 1991; Boyde, 1963, 1990; Dirks, 1998; Reid et al., 1998a).

Study site: Kibale National Park contains moist evergreen forest, including lowland and montane forest (Wood et al., 2017). The density of old growth forest differs between the two research sites in the park, known as Ngogo and Kanyawara (Struhsaker, 1997; Wood et al., 2017), because selective logging occurred at Kanyawara, but not at Ngogo (Struhsaker, 1997). The elevation at Ngogo is between 1250 and 1470 meters, while Kanyawara is slightly higher (Struhsaker, 1997). Ngogo and Kanyawara both experience annual rainfall of approximately 1500 millimeters (Wood et al., 2017).

The 35 km^2 Ngogo study area does not experience the high levels of variability in the food supply documented for other chimpanzee populaitons, such as those in the Täi Forest, Côte d'Ivoire (*Pan troglodytes verus*) (Boesch and Boesch-Acherman, 2000; Watts, et al., 2012). The abundance of important fruit trees relied upon by the Ngogo chimpanzees, e.g. *Pterygota mildbraedii* and *Ficus mucuso* (Struhsaker, 1997; Watts et al., 2006) remains fairly consistent, allowing the Ngogo chimpanzees to maintain a relatively uninterrupted level of nutritional input throughout the year (Wood et al., 2017). *F. mucuso* in particular, can produce a large fruit crop at

any time of year from each stem, making periods of fruit scarcity a shorter and rarer occurrence than at other sites (Watts et al., 2012). This relative fruit abundance means that they are able to maintain a high level of net energy intake year-to-year (Potts et al., 2011). In contrast, the chimpanzees at Kanyawara, which are only 10 km away, experience longer and more frequent times of fruit scarcity than the chimpanzees at Ngogo (Wood et al., 2017).

There are also no large-bodied predators at Ngogo, unlike the leopards at Taï (Boesch, 1991), and lions at Mahale (Tsukahara, 1993), and up until 2016, there were no major documented disease outbreaks in the Ngogo community (Wood et al., 2017), setting them apart from populations such as Mahale (Nishida et al., 2003), Gombe (Pusey et al., 2007, 2008; Williams et al., 2008; Lonsdorf et al., 2011), and Taï (Boesch and Boesch-Achermann, 2000; Leendertz et al., 2004; Kondgen et al., 2008). (Although, this changed in January of 2017 with an outbreak of a two types of respiratory disease; one called human metapneumovirus and the other called human respirovirus 3. These outbreaks resulted in the deaths of 25 chimpanzees from Ngogo (Negrey et al., 2019)). All of these conditions combine to make Ngogo a high quality environment supporting a community of over 200 individuals, with survivorship rates comparable to those of human hunter-gatherer groups (Wood et al., 2017).

Eastern chimpanzees (*P.t. schweinfurthii)* also live in Bwindi Impenetrable National Park (BINP), Uganda and experience different challenges than do their conspecifics at Ngogo and Kanyawara, due in part to the fact that they are sympatric with mountain gorillas (*Gorilla gorilla beringei*). Bwindi lies between 2400-2600 meters above sea level (Stanford and Nkurunungi, 2003), a much higher elevation than the chimpanzees in Kibale National Park. The area is made up of contiguous, moist tropical montane rainforest that receives between 1100-2400 millimeters of rainfall annually (Butynski, 1984; Carlson and Crowley, 2016). Its two dry seasons last from

May to July and from late December to February (Stanford and Nkurunungi, 2003). The chimpanzees and gorillas at Bwindi will both eat fruit when it is available to them, but they mostly avoid direct contest competition (but see Stanford and Nkurunungi, 2003) for the same fruit resources by responding to times of fruit scarcity in different ways. During periods of fruit abundance, chimpanzees forage in relatively larger groups, feeding largely on specific fruits (mainly varieties of *Ficus,* similar to the preferred food at Ngogo). During times of fruit scarcity, they forage in smaller groups, which move far apart to minimize resource competition (Stanford and Nkurunungi, 2003).

Sampling stable isotopes in tooth enamel: Stable isotopes and their uses in paleodietary reconstruction, among other things, have been extensively reviewed elsewhere (Crowley, 2012; Malone, Chapter 3, and refs therein), so in this study, only their relevance regarding the use of trace elemental analysis will be discussed.

The three elements whose isotopes are most commonly used in studies of paleodiet and paleoclimate are carbon, nitrogen, and oxygen, and these can inform us about an organism's total dietary content (Froehle, 2010), their protein intake (Krueger and Sullivan, 1984; Ambrose and Norr, 1993; Tieszen and Fagre, 1993; Froehle et al., 2012), and their sources of water (Luz et al., 1984; Luz and Kolodny, 1989; Bryant and Froelich, 1995).

The challenge with using these isotope values to track changing food and water sources, however, is that their analysis using the standard GC-IRMS (isotope ratio mass spectrometry) method requires powdered enamel samples to weigh at least 500-600 micrograms (μg). In small, thin-enameled teeth like those of many primates, including chimpanzees, this only allows for a few samples per tooth. This required large sample size means that the fine scale temporal shifts that can be seen structurally in histological sections cannot be assessed isotopically, because the

amount of time covered by each sample obscured such variation. This is because the samples are not spatially distinct enough from one another to represent separate time periods, and they represent time periods too large to track changes on even a six-month scale, much less the month-to-month changes that might reveal a transition from prenatal diet to exclusive nursing or from nursing to a transitional or fully adult diet.

In addition to the issue of sample intermixture, and its effect upon reducing the isotopic variability that can be detected from drilled enamel samples, there is the problem of the two-phase enamel formation process. In the initial phase of mineralization, the structures of the enamel (enamel prisms, cross striations, Retzius lines, etc.) are laid down as a sort of scaffolding comprised of only about 30% of its final mineral content (see Suga, 1982; Balasse, 2002; Passey and Cerling, 2002). During the second phase, known as maturation, nearly all of the remaining organic components of enamel are removed and replaced by the remaining highly mineralized hydroxyapatite content that makes up fully mature enamel, and ultimately ends up being ≥96% hydroxyapatite by weight. However, there is a delay between when the initial structures are laid down, and when much of the mineral content of the enamel is incorporated into the crown (Smith, 1998). This means that in any given area of mature enamel, the content is made up of not just enamel from the original mineralization phase, whose microstructures we use to age the area, but also the fully mature enamel that was added to that enamel area during maturation, which may take up to several additional months, depending upon the taxon and tooth in question (Traylor and Kohn, 2017). This maturation front also moves through the enamel in a somewhat different orientation and path than that of the initially mineralized structures (Green et al., 2018), however, several studies suggest that the innermost enamel just along the enamel-dentine junction (EDJ) may reach maturation soonest after it is initially mineralized (Passey and Cerling,

2008). If so, this is the area to which we should look to obtain the isotopic signal that is least attenuated due to the mineralization-maturation delay. However, as previously discussed, traditional sampling methods cannot access and isolate this area of enamel by drilling in from the outside of the crown, and certainly could not obtain enough enamel powder from just that area to separate out multiple samples of sufficient weight to identify dietary transitions during molar enamel formation. Trace elemental analysis using laser ablation, however, is capable of reaching this small and somewhat sequestered sampling area (see below).

Trace elements: One way researchers have tried to overcome the limit to the isotopic variability that can be accessed via traditional sampling methods is by turning to laser ablation to obtain smaller samples of enamel apatite, whose contents can then be analyzed using either isotope ratio-mass spectrometry (IR-MS) to obtain $\delta^{13}C$ values, or by using inductively coupled plasma-mass spectrometry (ICP-MS) to detect the quantities of trace elements incorporated into the enamel (and dentine) along with calcium (reviewed in Tsutaya and Yoneda, 2014).

Strontium and barium belong to the same alkaline earth elements group as calcium (Humphrey, 2007), and they have each been found to differ in their concentrations, relative to calcium, in pre- and post-natal regions of tooth enamel and dentine (Dolphin et al., 2006). Since calcium values remain fairly constant throughout enamel, it can be used to normalize the amount of these trace elements, by using the ratio of the fluctuating trace element (Ba or Sr) to the more constant calcium (reviewed in Tsutaya and Yoneda, 2014). These ratios are expressed as Ba/Ca or Sr/Ca. Strontium and barium atoms are routed from the whole diet into the developing tissues, but less is known about the mechanisms for how barium is routed into tissues through the digestive tract (Comar et al., 1957; Sillen and Kavanagh, 1982; Burton et al., 1999).

A number of processes are at work to regulate the amount of strontium or barium, relative to calcium, that is incorporated into forming tissues, and these processes are collectively known as biopurification (Elias et al., 1982). Strontium is taken into the maternal diet through food items that contain varying amounts of strontium. However, the levels of strontium in maternal tissues are lower than those in the plant food themselves, since the adult human digestive tract discriminates against strontium, although the plants containing them do not (Humphrey, 2014). In utero, the strontium level in a fetus' developing tissues is slightly lower than its mother's level (Comar, 1963; Sillen and Kavanagh, 1982), since the transfer of calcium across the placenta and mammary gland is a process of active transport, and strontium transfer instead follows a gradient (Krachler et al., 1999; Rossipal et al., 2000). The Sr/Ca ratio becomes even lower at birth and remains low through the period of exclusive breastfeeding (Humphrey et al., 2007; Austin et al., 2013). When an infant first begins to incorporate non-milk foods into its diet, the strontium levels begin to increase in the tissues forming during that time (Tsutaya and Yoneda, 2014). They continue to increase as the infant's diet becomes increasingly reliant on non-milk foods, and only begins falling to normal adult levels once its digestive system is fully mature and can filter strontium effectively (Lough et al., 1963; Humphrey et al., 2007). Calcium-normalized strontium ratios (Sr/Ca) have been used to demonstrate possible indicators of weaning behavior in baboons (Humphrey, 2008), but the distribution of strontium in enamel may be more diffuse than barium, making estimates of dietary transitions more difficult. Austin et al. (2013) found that changes in Sr were proportionately smaller across transitions than those of Ba were, making it harder to discern pattern of change using Sr.

Due to its low bioavailability in non-milk foods (and unlike strontium), barium in breast-milk and in forming infant tissues, does not appear to be linked with the types foods being eaten,

as much as it does with maternal mobilization of calcium stores from within the skeleton during lactation (Smith et al., 2017). As calcium is released from a mother's bones to be incorporated into breast-milk, the barium already present at low levels along with her calcium, is also released into the milk being produced. This means that all of the barium that is routed into a breastfeeding infant's forming tissues comes from its mother's milk, and does not vary based on changes in her diet, but varies instead with changing amounts of milk ingestion (Smith et al., 2017).

Previous work using Ba/Ca to access weaning signals: Strategic sampling of certain trace elements found to be associated with dietary changes, such as strontium (^{88}Sr) and barium (^{138}Ba), has been quite successful at tracking the timing of dietary changes associated with the weaning process in the enamel and dentine of numerous primates.

Dietary transitions during the weaning process have been tracked in the teeth of humans, macaques, orangutans, and even a Neanderthal juvenile (See Austin et al., 2013; Smith et al., 2017), using the distribution of the calcium-normalized barium (Ba/Ca) present in different parts of the tooth. These studies conducted LA ICP-MS across the entire surface of thin sections of these teeth, noting the changing absolute Ba/Ca values in enamel versus dentine, as well as in areas of the crown possibly subject to diagenesis. They also noted the more diffuse pattern of Ba/Ca variability in enamel compared with the fairly distinct banding of these changing levels within the dentine (Austin et al., 2013; Smith et al., 2017). Histological analysis of these teeth prior to ablation allowed them to map the changing Ba/Ca values onto the image of the thin-sectioned tooth, permitting ages at dietary transitions to be estimated from the periodic and accentuated structures recorded within the section. Most recently, Smith and colleagues (2018) conducted a study that combined histological imaging of periodic tooth structures, Ba/Ca and Pb(lead)/Ca analysis, and $\delta^{18}O$ analysis of enamel phosphate, using both silver phosphate micro-

precipitation with IRMS, and secondary ion mass-spectrometry (SIMS). SIMS was able to analyze such small amounts of enamel that samples were taken from the innermost enamel layer, to demonstrate the relationships between weaning behavior, seasonal climatic fluctuations, and cyclical lead exposure in the teeth of two Neanderthals and a modern human from southeastern France (Smith et al., 2018).

Previous Ngogo chimpanzee dental development results: In a prior study by the author, an M_1 emergence age range of 2.15 - 4.10 years was estimated for the wild chimpanzee (*P.t. schweinfurthii*) sample, consisting of individuals from the five communities of Ngogo, Bwindi, Wantabu, and an unnamed community to the northeast of Ngogo (n=7 Malone, Chapter 1), and Kanyawara (n=3 Machanda et al., 2015). The new *P.t. schweinfurthii* data helped to illustrate how variable dental emergence ages can be within a single *Pan* subspecies, by increasing the known M_1 emergence age range from 9.6 months in the three previously documented Kanyawara chimpanzees, to an estimated almost two years for the sample containing all five communities. In addition, this range of M_1 emergence ages is very close to the previously documented range of 2.14 - 3.99 years for captive chimpanzee M_1 emergence (reviewed in Smith et al., 2007). For the Ngogo chimpanzees in this study, the M_1 root growth spurts all fell somewhat after the age range of Kanyawara M_1 emergence (Machanda et al., 2015), which supported the assertion that the M_1 root growth spurt was most likely to coincide with attaining functional occlusion several months after emergence. Most of the Ngogo chimpanzees were also eatimated to have emerged their M_1s somewhat after those at Kanyawara, or on the late end of their range of 2.8-3.2 years (n=3 Machanda et al., 2015), which further reinforced the connection made between the M_1 root growth spurt and occlusion.

The final finding of the study was that the M_1 root growth spurt and occlusion age likely

slightly preceded weaning completion, according to the root growth spurt age range of 3.03 - 4.60 years in these Ngogo chimpanzees, and the inferred mean age at weaning completion (4.0-4.5 years) from fecal isotope data of Ngogo infant-mother pairs (Badescu et al., 2017).

Results overall suggested that the M_1 root growth spurt coincided with the attainment of functional occlusion, followed by an abrupt drop in stress episode frequency (Malone, chapter 1 page 40), just prior to the attainment of nutritional independence/weaning completion in these chimpanzees. However, to more robustly link the root growth spurt/occlusion age to weaning completion, another proxy for weaning in these specific individuals was needed.

The current study addresses this need for a proxy of dietary change by determining the variation in Ba/Ca intensities within the inner M1 enamel and dentine of these Ugandan chimpanzees, since this variation has been linked to the transition from nursing to adult foods in the teeth of multiple extant and fossil hominoids.

The following questions will be addressed:

1) Do the changes in Ba/Ca intensity (that presumably reflect dietary changes) show the same general patterns of increase and decrease through developmental time in chimpanzees as in other primates for which this has been assessed?

Prediction: Orangutans, humans, macaques, and Neanderthals all seem to show at least some evidence of a Ba/Ca signal that begins low in prenatal enamel, rises to varying degrees in enamel formed during exclusive nursing, begins to fall as adult foods are introduced, and only rises again if the individual continued through cycles of frequent nursing during times of fruit scarcity, or if it mobilized Ca (and also Ba) from its own skeletal stores during times of serious illness or starvation (Austin et al., 2013; Smith et al., 2017; Smith et al., 2018). Due to the general pattern

seen in all of these taxa, it would be expected that something similar will be seen in chimpanzees, though the ages at which these changes occur, and the duration of those stages will differ, while the absolute values of Ba/Ca itself will vary among individuals.

2) What are the patterns of Ba/Ca changes during the ages when weaning completion has been inferred from formation and eruption data?

Prediction: It was proposed in a previous study (Malone, Chapter 1) that the consistent drop-off in stress episodes after the root growth spurt could indicate that the weaning process was completed around that time. If this is the case, then we would expect to see Ba/Ca patterns also become lower after that point, as demonstrated for orangutans once they were presumed to have finished weaning (Smith et al., 2017) and for macaques with known weaning histories (Austin et al., 2013).

3) Do patterns of dietary change as inferred from trace elements correspond with age at nutritional independence as inferred from fecal isotope studies of Ngogo chimpanzees?

Prediction: It has been shown (Malone, Chapter 1) that the M_1 root growth spurt for the chimpanzees in this study slightly precedes the mean age at which Ngogo chimpanzees complete the weaning process (Badescu, et al., 2017). Thus, if the Ba/Ca values drop off at the same ages (between 3.03-4.60 years, depending upon the individual), then the trace element values can be seen as support for the hypothesis that the M1 root growth spurt/occlusion age slightly precedes weaning completion in these chimpanzees.

Materials: The first molars and either the second molars (five individuals) or the fourth premolar (two individuals) from seven chimpanzees (*Pan troglodytes schweinfurthii)* were used

in this study. The M1s were used in a previous study by the author to collect incremental developmental data and measure crown and root extension rates and those individuals are listed in Table 8.

Table 8: Chimpanzee individuals included in this study

ID #	Origin	Sex	Name	Estimated Age	Date of death/cause of death	Teeth used
NG001	Northeastern community, Kibale National Park, Uganda[2]	M	Unknown	Adult	6-1-02/ intergroup aggression[2]	M1, M2, M3
NG002	Wantabu community, Kibale National Park, Uganda[2]	M	Unknown	Adult	11-23-02/ intergroup aggression[2]	M1, M2, M3
NG003	Ngogo, Kibale National Park, Uganda[3]	M	"Grappelli"	20	10-30-02/within-group attack[3]	P4, M2, M3
NG004	Ngogo, Kibale National Park, Uganda[1]	M	"Stravinsky"	32	2006/ intergroup aggression[1]	M1, M2, M3
NG005	Ngogo, Kibale National Park, Uganda[1]	M	"Tatum"	23	2008/unknown[1]	M1, P4, M3
NG012	Ngogo, Kibale National Park, Uganda[1]	F	"Carmen"	51	Sept 2013/unknown	M1, M2, M3
NG013	Ngogo, Kibale National Park, Uganda[1]	M	"Webster"	26	March 2014/ respiratory disease?[3]	M1, M2, M3
MUZM 2625	Bwindi Impenetrable National Park, Uganda	F	Unknown	Adult	Unknown/unknown	M1, P4, M3

Table 8: Identifying information for all eight chimpanzees used in this study. ID # refers to the individual's accession number. In cases where dates of birth are unknown, a general age category is used (i.e., "Adult"). The "NG" indicates an individual from or associated with the Ngogo population, while "MUZM" refers to the Makarere University's Zoology Museum.

Previous work (Malone, unpublished data) explored dental development and diet in a sample of six yellow baboons (*Papio cynocephalus*) from Kenya and one hybrid Hamadryas baboon (*Papio anubis-hamadryas)* from Ethiopia, and data from that study was used for comparative purposes here, with those individuals listed in Table 9. Another comparative sample came from seven red-tailed monkeys (*Cercopithecus ascanius*) that were also from Kibale National Park (Table 10).

Table 9: Yellow baboon individuals included in the comparative sample

ID #	Species/Subspecies	Area of origin	Sex	Age category	Teeth used
UM152	*Papio cynocephalus*	Loboi, Kenya	F	Adult	M1, C
UM112	*Papio cynocephalus*	Loboi, Kenya	M	Adult	M1, C, M2, M3
UM131	*Papio cynocephalus*	Loboi, Kenya	M	Adult	M1
UM169	*Papio cynocephalus*	Loboi, Kenya	F	Sub- adult	M1
UM122	*Papio cynocephalus*	Loboi, Kenya	F	Sub- adult	M1
UM167	*Papio cynocephalus*	Lobio, Kenya	M	Adult	M1
HP1	*Papio Anubis-hamadryas*	Awash National Park, Ethiopia	F	Adult	M1

Table 9: Identifying information for all seven baboons used in this study. None of these were known individuals. All individuals in this study, except "UM169" and "UM122", were classified as "adult" due to their M3s being fully formed. "UM" indicates an individual from the University of Michigan's non-human primate Osteology Collection, while "HP" refers to the hybrid *Papio* individual.

Table 10: Red-tailed monkey individuals in the comparative sample

ID #	Sex	Age category	Tooth used
ASC 9	F	Adult	M1
ASC 22	F	Adult	M1
ASC 45	M	Adult	M1
ASC 73	F	Adult	M1
ASC 78	M	Adult	M1
ASC 112	F	Adult	M1
ASC 207	M	Adult	M1
ASC 446	M	Adult	M1

Table 10: "ASC" stands for ascanius. "Adult" indicates that all teeth are fully formed and in occlusion.

Methods: Unanalyzed halves of previously sectioned teeth (Malone, Chapter 1) were used to create thin histological sections. These sections mirrored the structure and layout of a slide from the other half as closely as possible, by only lightly lapping and polishing the sectioned tooth surface before mounting it to the microscope slide. Once new thin sections were made and images taken to confirm periodic and accentuated variables from original sections from the other half of the tooth, the slides (left uncovered by coverslips) were then laser ablated.

Laser ablation inductively-coupled plasma mass spectrometry (LA ICP-MS) was used to obtain calcium- normalized barium ratios (Ba/Ca) and their distributions within the first molar thin sections, in order to detect and track the timing of dietary changes early in chimpanzee development. Laser ablation was conducted at Michigan State University's ICP-MS laboratory in

the Department of Earth and Environmental Sciences using a Photon-Machines Analyte G2 193nm excimer laser coupled with a Thermo Scientific ICAP Q quadrupole ICP-MS. Qtegra software was used to analyze Ba/Ca levels from 30-micron wide ablated tracks of enamel close to the enamel-dentine junction (EDJ). Standards used were NIST612 as well as an internal standard for enamel apatite calculated using the stoichiometric composition of a pure apatite. Once the Ba and Ca values were continuously collected and recorded as parts per million (ppm), those counts values were converted to concentrations, allowing a ratio to be created between the two elements. Ba/Ca values were charted using Excel (as in Figure 14), with the resulting values then being mapped onto the histological images of each tooth (as described below), which showed how the Ba/Ca ratios changed over developmental time within the ablated tracks in the enamel and dentine. Before each track was ablated, a round of pre-ablation took place, which removed ~1-2 microns (μm) of material from the section's surface along the planned track, cleaning it of contaminants within the area to be ablated.

Ba/Ca distribution mapping: For each individual track within each tooth a separate range of values was determined, with any obvious outliers removed from that range, since these can obscure true, often subtle, variation by creating a range in which the signal is lost within the noise (pers obsv). Since as many as 5000 values were collected from along a single ablated track, averages of every ten values were taken, and these averages (~200-500 colored points) were what made up the final range of values for each track.

Each final range of values was divided equally into ten parts, with each part being represented by a color from lowest (dark blue) to highest (deep red). Locations of the individual values were determined using the length of the track and the number of values collected from start to finish. Outlier values were determined by looking at their location within the track on the

thin section, and if there was damage or epoxy infill in that area, it could be confirmed that the variation was not biological but merely an artifact, and so it could be removed and a blank value (black for extremely low or white for extremely high) substituted in that space so that the value placement did not get thrown off. Once the individual values were laid down in the image of the ablated track on the tooth, the patterns of accentuated lines, already recorded in previous work, were overlain onto these maps to see how they corresponded with changing trace element values.

Method verification: In a prior project, (Malone, unpublished data), the M1s from a sample of yellow baboons (*Papio cynocephalus*) and red-tailed monkeys (*Cercopithecus ascanius*), were histologically prepared and analyzed, and then subjected to the trace element analysis described above. The sampling strategy was thus refined using the teeth of these two other taxa before analysis was conducted on the chimpanzee molars, since these two species, like other cercopithecoids, have been observed to complete their weaning process during M1 enamel formation, and were therefore likely to show trace elemental evidence of a completed weaning process that could be tracked within a single tooth crown.

Several questions guided the sampling design, based upon predictions from a previous study by the author and studies from the literature:

1) What factors will influence the distribution of Ba/Ca values in the enamel and dentine of these chimpanzees?

2) What factors will influence how these data appear in the output values resulting from the laser ablation process?

Prediction 1: Each chimpanzee individual will have a unique pattern of change in Ba/Ca intensity across developmental time, due to different levels in its mother's breast-milk (Austin et

al., 2013), first and foremost, but also due to different durations of exclusive breast-feeding, and sporadic bouts of increased nursing intensity (Smith et al., 2017).

Prediction 2: The values produced from the dentine will necessarily be higher than those in enamel, due to the greater amount of dentine material that will be ablated during each pass, since enamel is a much harder tissue. The patterns of change, however, should match up between areas of enamel and dentine that form simultaneously.

Prediction 3: It is likely that there will be areas of demineralization right along the EDJ that may affect the accuracy of values coming from that area, as this has been seen in other studies (Smith et al., 2018), and this can be expected in the teeth of these chimpanzees as well.

To determine whether this sampling procedure could produce consistent results, a number of tests were devised. First, elemental isotopes are present in different amounts in various tissues, and other studies that have used similar methods to obtain Ba/Ca values have done so using ^{138}Ba (e.g. Austin et al., 2013). Although it was found that the abundance of that particular isotope was quite low in some of these samples, the ^{137}Ba isotope was found to be present in similarly small amounts (see Figure 11). Consequently, despite these low levels, ^{138}Ba was used in this study in order to ensure comparability with the results from other studies.

Figure 11: ^{137}Ba/Ca (red) and ^{138}Ba/Ca (black) overlaid to show consistent values

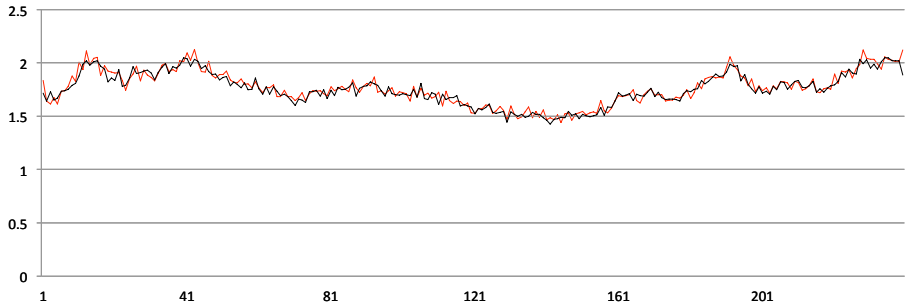

Figure 11: The x-axis shows how far along the yellow baboon's M1 enamel track the values are, and the y-axis shows ^{137}Ba/Ca and ^{138}Ba/Ca values.

As a further test of consistency, in one red-tailed monkey and two yellow baboons, two trials were conducted in the same tooth using different track widths, one at 65µm and one at 30µm, in order to test whether the same pattern of change could be seen in the smaller track and the wider track (Figure 12). This test provided insight into whether there was signal attenuation in the trace element values when moving further away from the enamel-dentine junction (EDJ).

Figure 12: M1 Ba/Ca patterns of change within 30 µm and 65 µm tracks of the same teeth of a red-tailed monkey and two yellow baboons

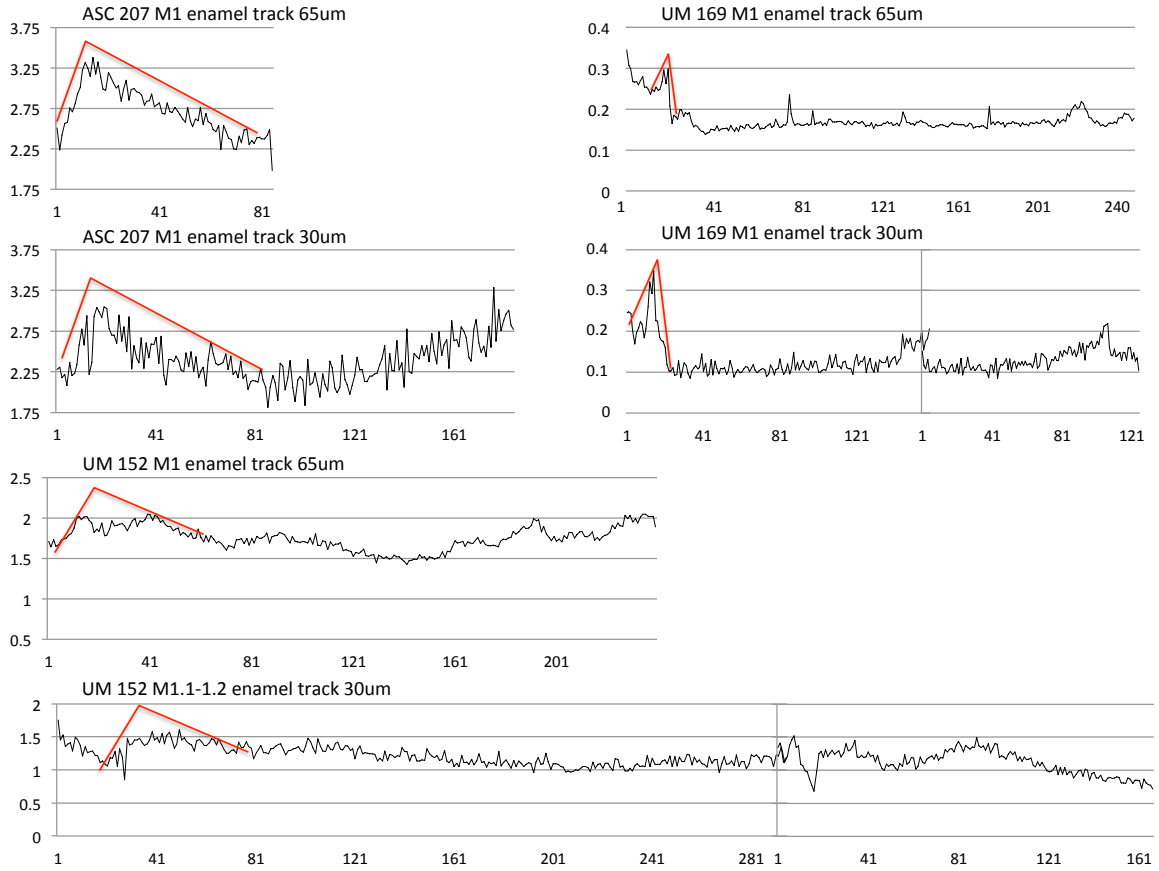

Figure 12: ASC207 is a red-tailed monkey, and UM152 and UM169 are female baboons in which 30µm and 65µm tracks were compared. The y-axis shows the Ba/Ca values and on the x-axis, from left to right, are the sampling points moving from the occlusal to cervical ends of the ablated tracks. Where the numbers on the x-axis start over, it indicates that one line ended and another picked up where it left off. The red lines highlight the increase in Ba/Ca intensity at the transition from pre- to postnatal regions of the enamel. Additional red-tailed monkey M1 Ba/Ca charts can be found in the Appendix.

The results of this test showed that the 65µm and the 30µm tracks revealed the same pattern of an increase in Ba/Ca followed by a decline soon after. The time periods over which this change occurred were different in each individual, but patterns of change between the 30µm and 65µm trials for the same individual were consistent. This meant that there was no significant decrease in the fidelity of the signal being obtained by ablating a narrower track.

As a final test, developmentally overlapping teeth of the same baboon were ablated along the inner enamel, permitting the sampling of areas of enamel forming simultaneously between these teeth. The ablated values from these overlapping teeth would be expected to show similar changes in Ba/Ca intensity if the path of the sampling track from one section was mirrored in the other.

Figure 13: Ba/Ca overlap between the M1, C, M2, and M3 in male baboon UM112

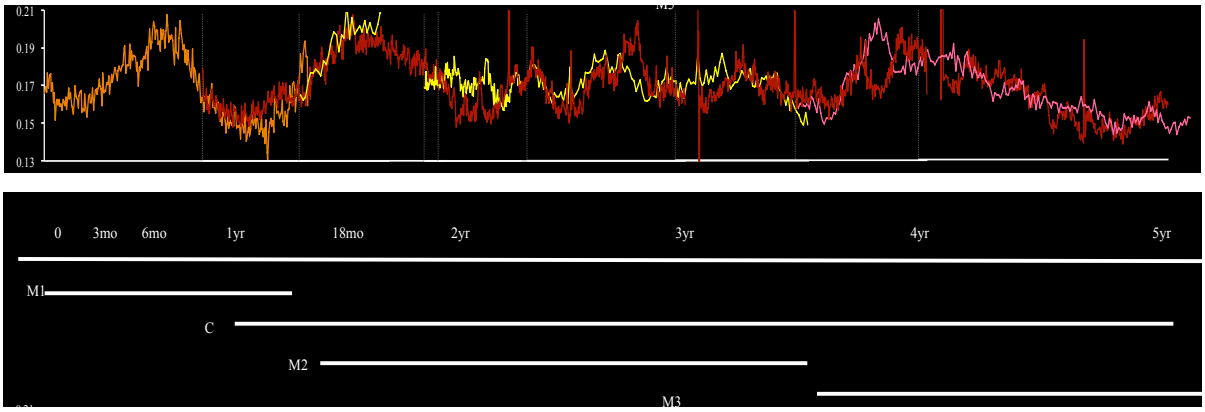

Figure 13: Enamel Ba/Ca values in the top part of the chart are from the male baboon UM 112 M1 (orange), C (red), M2 (yellow), and M3 (pink). On the y-axis are Ba/Ca values and on the x-axis, from left to right, are the sampling points moving from the occlusal to cervical ends of the ablated track. Below that is a chart of the amount of crown formation overlap (and the actual ages of that overlap) between the four teeth as indicated by the overlap in Ba/Ca values. Actual overlap is slightly greater, since the ablated tracks did not run all the way to utmost cervical end of the crowns.

The resulting chart of overlapping Ba/C values is seen in Figure 13, and the overlap in actual values between these simultaneously forming teeth shows the M1 (orange values) overlapping with the canine (red) but not with the M2 (yellow), which only overlapped with the canine. This

is followed by the canine's overlap with the M3 (pink). The timeline below the chart shows the ages of overlapping crown formation, inferred from the overlap in Ba/Ca values, and this begins before birth and goes up til slightly after age five. This test demonstrated the consistency of the values themselves between overlapping crowns, supporting the use of this method in the chimpanzee sample, while also confirming the amount of crown formation overlap between the teeth (Figure 13).

Results/Discussion: These results consist of numerous types of data. Charts of the general patterns of change in Ba/Ca values across M1 development are shown for all seven chimpanzees (Figure 14) . Ba/Ca intensity distribution maps for tracks in the enamel and dentine are given for five of the seven individuals, with accentuated lines overlaid (Figures 16-19) . For the seven individuals (Figure 21), charts of the overlap in the Ba/Ca values between consecutively forming teeth are shown (M1 and either M2 or P4), and for one of these individuals (NG012), a Ba/Ca intensity map for both teeth shows the location of the M1 root growth spurt in the second tooth's enamel (Figure 20). Ba/Ca distribution charts, from the M1s of the baboons used in the previous study, are also included here for comparison (Figure 15), along with Ba/Ca intensity maps obtained from these baboons (Figure 23). Because many of these types of results are interrelated, discussions of the relevance of the data, will be included in the results sections along the way.

Overall Ba/Ca variation: The changing Ba/Ca intensities from along the inner enamel tracks of six of the chimpanzee M1s are shown in Figure 14. The Ba/Ca concentrations varied considerably, ranging from 0.35 in parts of the Bwindi chimpanzee's M1 enamel to as high as 5.3 in the M1 of one of the Ngogo chimpanzee males (NG004).

Figure 14: Ba/Ca distributions in the M1s of four male and two female chimpanzees

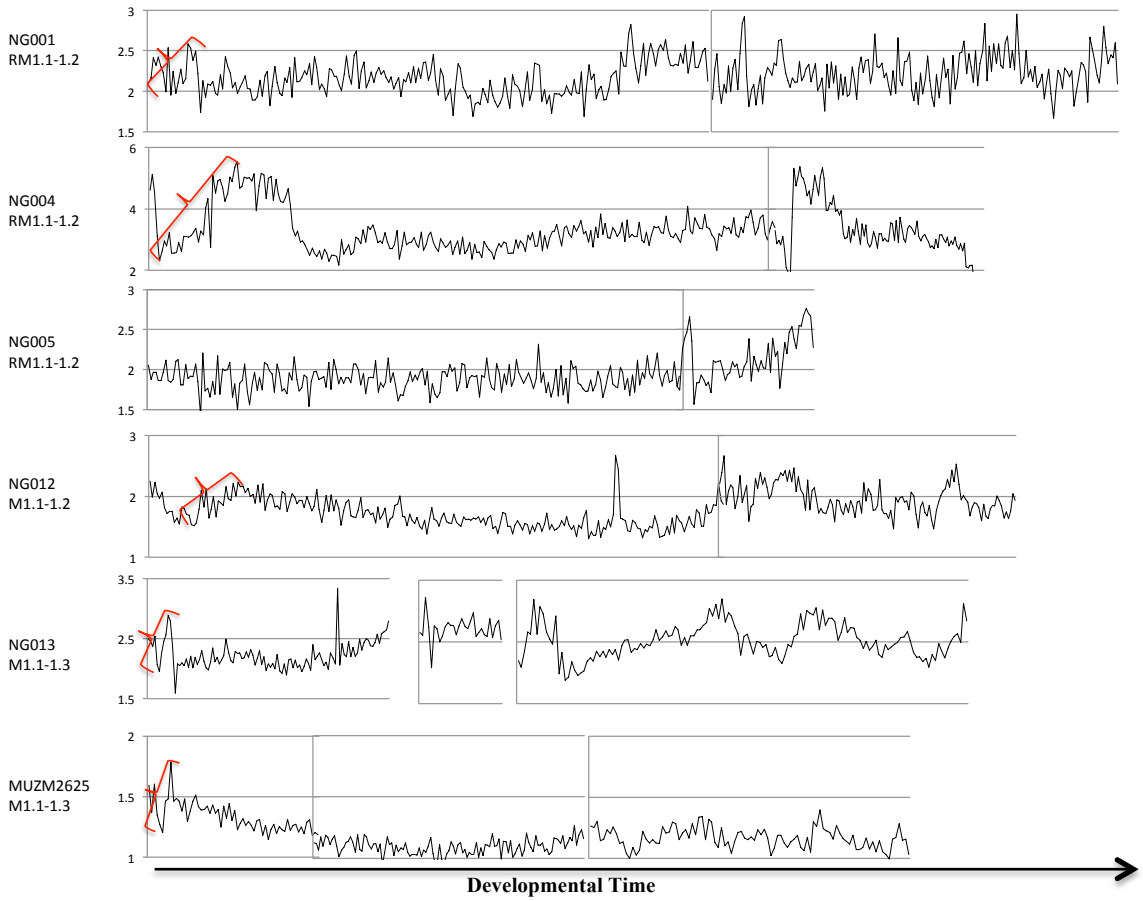

Figure 14: Individual IDs are listed next to each chart, along with the number of tracks ablated for that tooth. Ba/Ca values are on the y-axis. The x-axis, from left to right, depicts the sampling points moving from occlusal to cervical ends of the ablated tracks, representing Ba/Ca change over developmental time. Red brackets highlight increases in Ba/Ca values between birth and the inferred point when non-milk foods are introduced. Vertical lines within charts indicate the end of one track and the start of the next. Gaps indicate discontinuity in the track.

One of the M1s in the sample (NG002) did not contain any prenatal enamel, nor could the neonatal line be identified in the dentine due to cuspal wear, so it was not included here, since the aim was to identify this first signal of dietary transition from gestational diet to exclusive nursing. In NG005, no significant increase, like that seen in the others, could be detected in the earliest forming enamel. The implications of this are discussed below with the individual intensity maps. A prenatal-to-postnatal shift, presumed to reflect a dietary transition was detected in the other five chimpanzees in this sample.

Figure 15: Ba/Ca distribution in the M1s of seven baboons (6 *Papio cynocephalus &1 Papio hamadryas-anubis* hybrid*)*

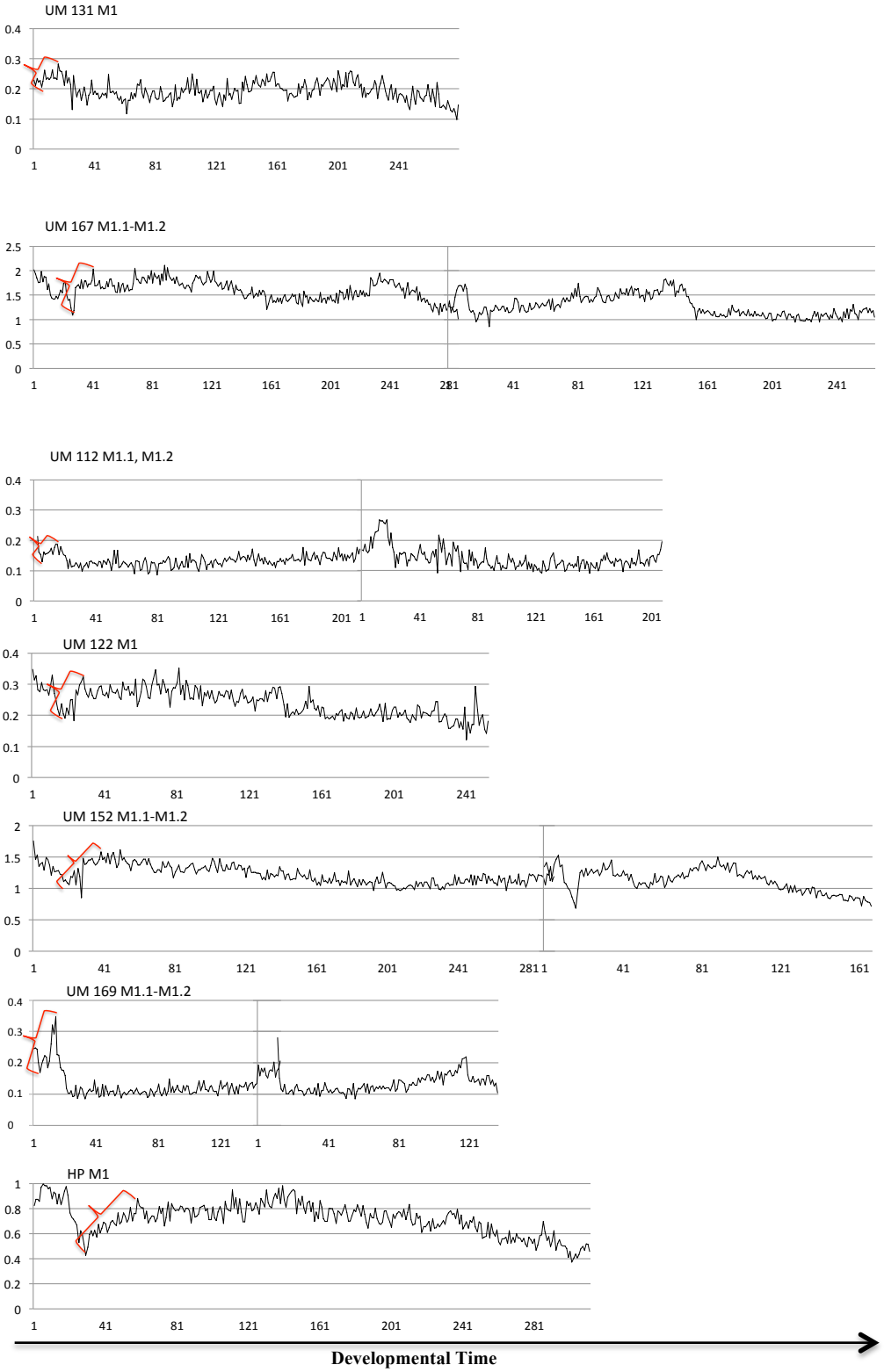

Figure 15: Parameters are the same as in Figure 6, but the top three are male and the next three are female yellow baboons and the final one (HP) is the female hybrid hamadryas baboon. (from Malone, unpublished data)

Case 1: NG001- Three sections were made from the M1 of individual NG001 (Figure 16), each one capturing the mesiobuccal cusp in a slightly different plane of section, and including the tip of the dentine horn with varying degrees of completeness. Section $LM_{1\text{-}1}$ is not in the ideal plane of section, as is slightly too thick for the optimal polarized microscopy view, but it was chosen for laser ablation.

Figure 16: Ba/Ca chart from M1 enamel (orange) and dentine (red) and a Ba/Ca intensity map from extra-group male chimpanzee "NG001"

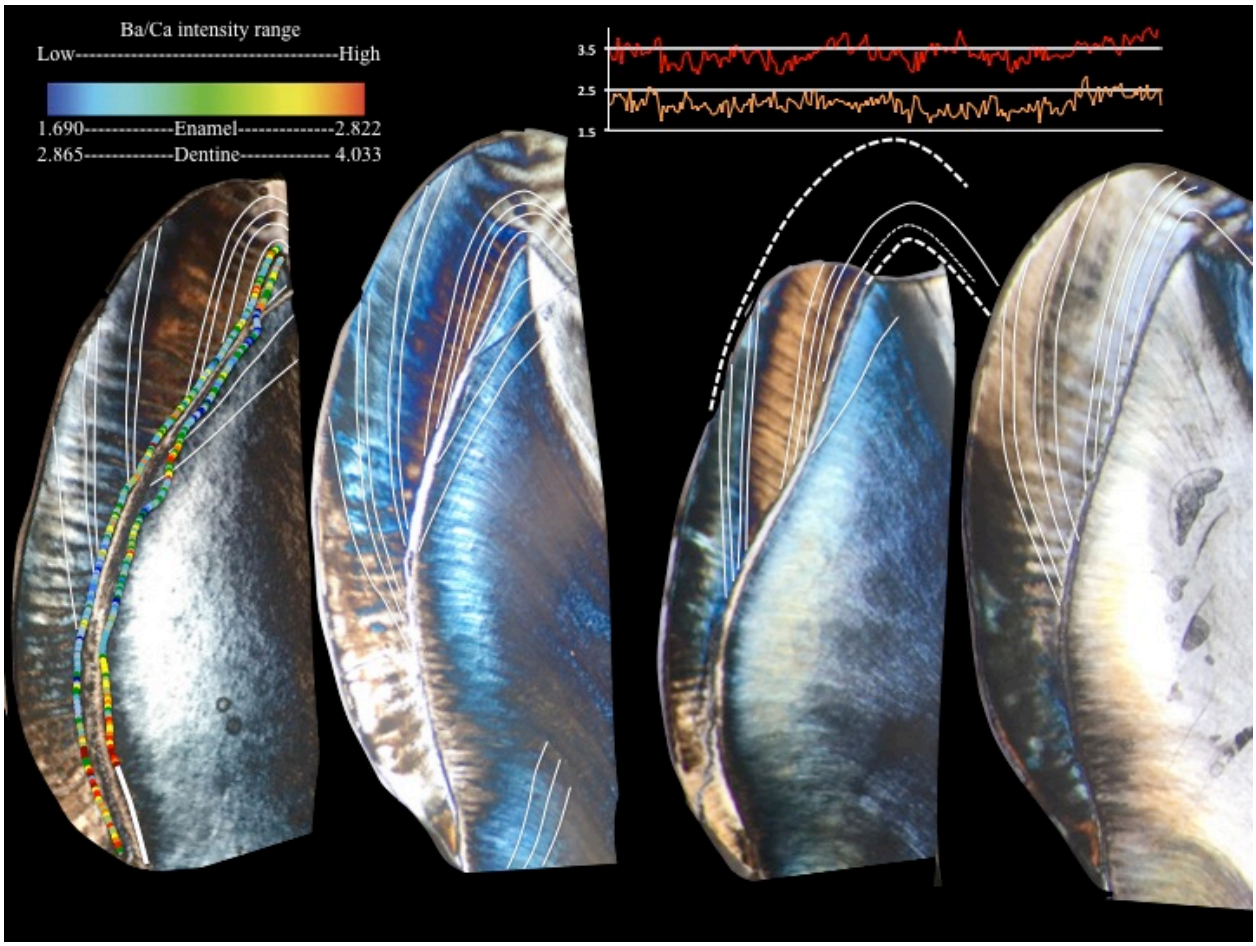

Figure 16: From left to right-$LM_{1.1}$, $LM_{1.3}$, $LM_{1.2}$ mb cusp, $LM_{1.2}$ ml cusp. Accentuated lines can be seen overlain in white. Ba/Ca from within the enamel and dentine tracks is visible in $LM_{1.1}$ In the third image, the missing area of the crown has been reconstructed to dhow the correspondence between the accentuated lines still visible and those complete ones in the other sections. The fourth image is the mesio-lingual cusp of the third section.

The chart above the histological images shows the changing Ba/Ca values from within the enamel (orange) and dentine (red) tracks. These values were mapped onto the tracks in $LM_{1.1}$ (left image) and the accentuated lines from the other three images were placed over the Ba/Ca values in order to age the changes along the tracks. In NG001, an extra-group male, the measured M_1 root growth spurt from the previous study was 2.65 years, making his estimated M_1 emergence age 2.15-2.45 years. This is the earliest estimated M_1 emergence age and root growth spurt from the sample.

Figure 17: Ba/Ca from the M1 enamel and dentine ablated tracks of male Ngogo chimpanzee "NG013"

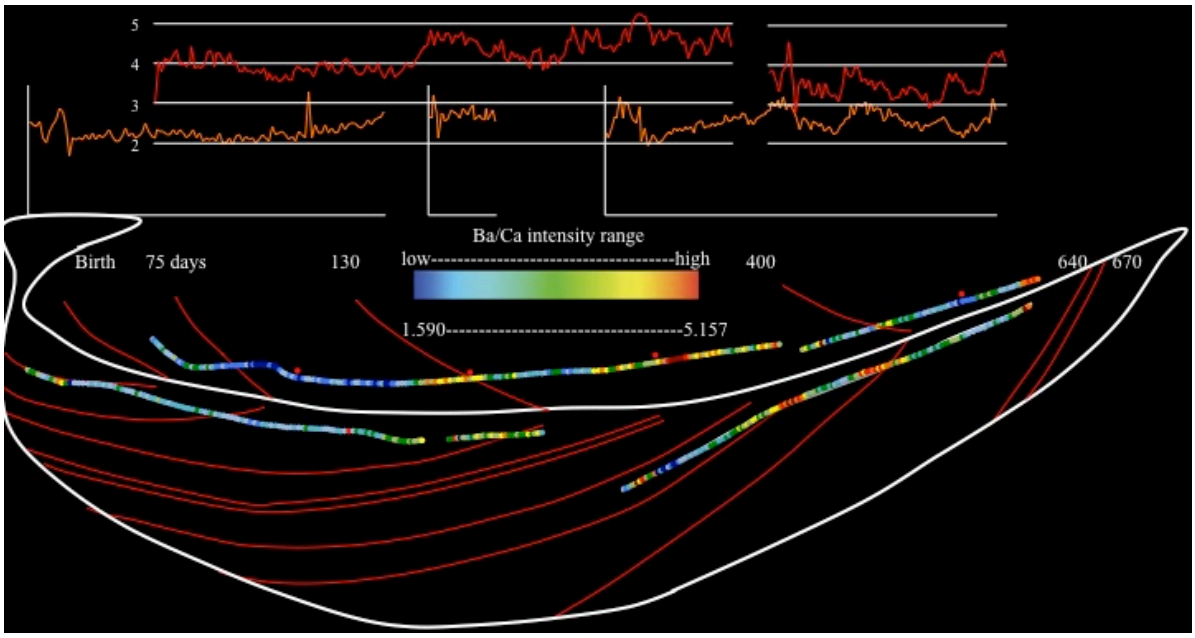

Figure 17: In the chart on top, are the changing Ba/Ca intensities from within the dentine (red) and enamel (orange). In the image on the bottom, the occlusal end is to the left and the cervical end is to the right. The tooth has been outlined in white, along with the dentine horn and the EDJ, and the histological image has been removed from beneath in order to better see the patterns of accentuated lines (red lines, some of which are arranged in "v"s showing the same lines in enamel (below) and dentine (above)). The Ba/Ca color intensity scale includes the enamel and dentine values. The gaps in the enamel track chart (orange) indicate that the track was discontinuous.

Case 2: NG013- The M_1 of this individual ("Webster") suffered some major cracks running through the crown, and this restricted the areas of the enamel and dentine that could be sampled (Figure 17). Instead of running the ablation track over the cracked area, the track was stopped at the border of the crack, and picked back up on the other side, where possible. In the case of the final line of the three in the enamel, the line had to begin further away from the EDJ than is ideal, so the values from the early part of that line are not taken as a signal with the same fidelity as the rest of the line that is close to the EDJ. The enamel (orange) and dentine (red) tracks in the chart at the top are aligned spatially to show where they correspond to the Ba/Ca map below, as well as where they correspond temporally to each other. Even with the gaps in the enamel values (and a few divergent areas where the track veers into later forming enamel) the patterns of change between the enamel and dentine are very similar.

Also included in this image are the ages of some of the major accentuated lines in enamel and Owen's lines in dentine. The prenatal-to-postnatal increase in Ba/Ca levels is visible in the enamel track but the dentine track did not begin in the earliest forming area of the crown. Webster's estimated M_1 emergence age was the latest in the entire chimpanzee sample, at 3.80-4.10 years. It should also be noted that NG013 shows the latest root growth spurt of any of the individuals in this study, yet the peak in line formation and Ba/Ca value fluctuations still occurs in tandem with the growth spurt, supporting the assertion that it is a true measure of this biological relationship, and not merely an artifact.

Figure 18: Ba/Ca from the M1 ablated dentine track of female Bwindi chimpanzee "MUZM2625"

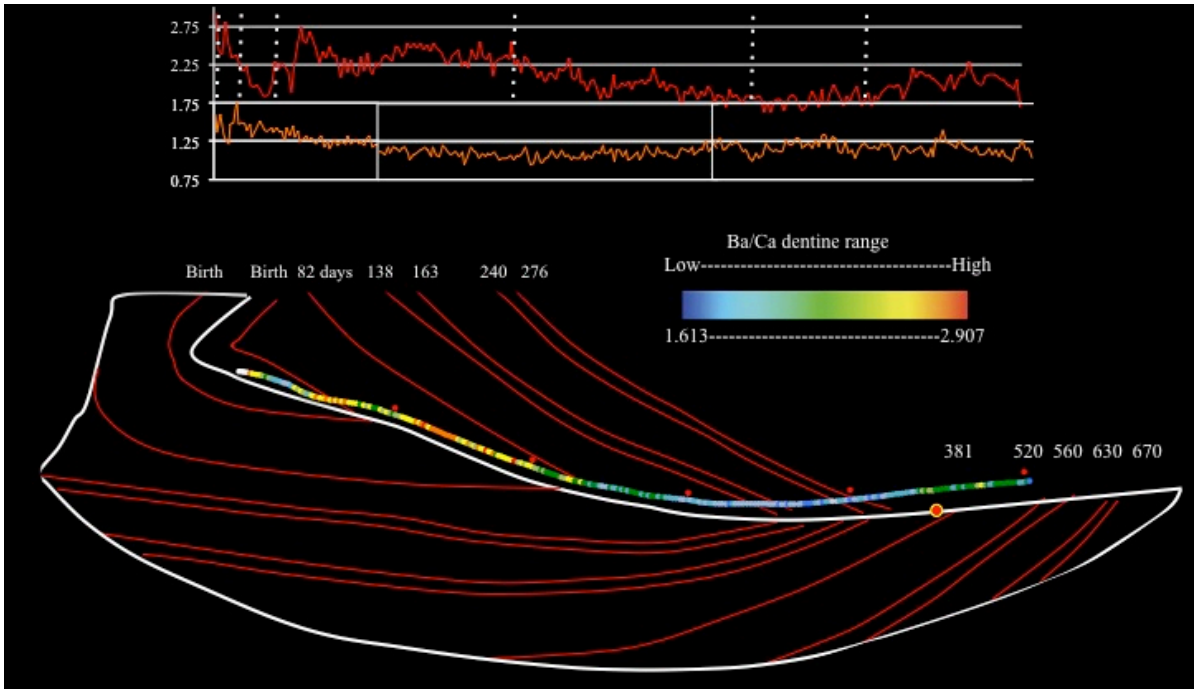

Figure 18: Parameters are the same as in Figure 17. The one-year mark is indicated by a red and yellow circle and in the charts above the map, white dotted lines indicate damage in prenatal enamel followed by major accentuated lines and their timing.

Case 3: MUZM2625- This individual is a female chimpanzee from the Bwindi Impenetrable National Park. Her M_1 emergence age was estimated to be between 3.19-3.49 years, which is in the middle of the Ngogo age range and on the very end of the Kanyawara range. This is also nearly a year later than the two extra-group Kibale males.

The Ba/Ca levels from within her dentine (Figure 18) conformed well with the predicted pattern of Ba/Ca change representing the amount and duration of variability surrounding dietary transitions. With the exception of several outlier values in the earliest prenatal dentine (indicated as white blanks on the map and a spike in the red dentine chart values), the Ba/Ca values rise at birth, remain high until about 82 days into growth, at which point the beginnings of mid-range values may be associated with reduction of milk in the diet due to an unknown

portion of nutrition coming from the incorporation of some adult foods. The Ba/Ca intensity stays at this level for about two months and then dips into the mid-low range for about 4.5 months only to rise again after she was one year old, suggesting another increase in nursing intensity lasting at least until the track ended, which was when she was about 1.42 years old.

Case 4: NG005- For this Ngogo male ("Tatum") (see Figure 19-top**)** an M_1 emergence age range of 2.95-3.25 years was previously estimated**,** which is on the early end of the Ngogo chimpanzee range. The charts of Ba/Ca variation in the dentine show a marked increase at the end of the enamel track (and this is even more pronounced in the dentine track), which resulted from the track running through an area of damaged enamel full of cracks. Those increased values are therefore very likely not the true biogenic signal from that developmental area, and may have increased the range of variability within those tracks too much to be able to pick up on the early life variation that we would expect to see in the area of enamel forming after the neonatal line, and during the period of exclusive nursing. In this individual, prenatal enamel was not captured, so the signal begins within the enamel and dentine formed just after birth. The dentine appears to pick up a bit of that higher Ba/Ca intensity, which then falls to much lower levels at 3-5 months. Ba/Ca intensities increase slightly several times in the enamel and dentine after that point (rising to light greens, yellows, and oranges in places), which may indicate periods of more intensive nursing In several areas, the track ventures too near to the EDJ, and runs into areas of demineralized enamel, causing the much lower values around the middle of that track.

Figure 19: Ba/Ca from the M1 enamel (orange) and dentine (red) of "NG005" (top) and "NG012" (bottom)

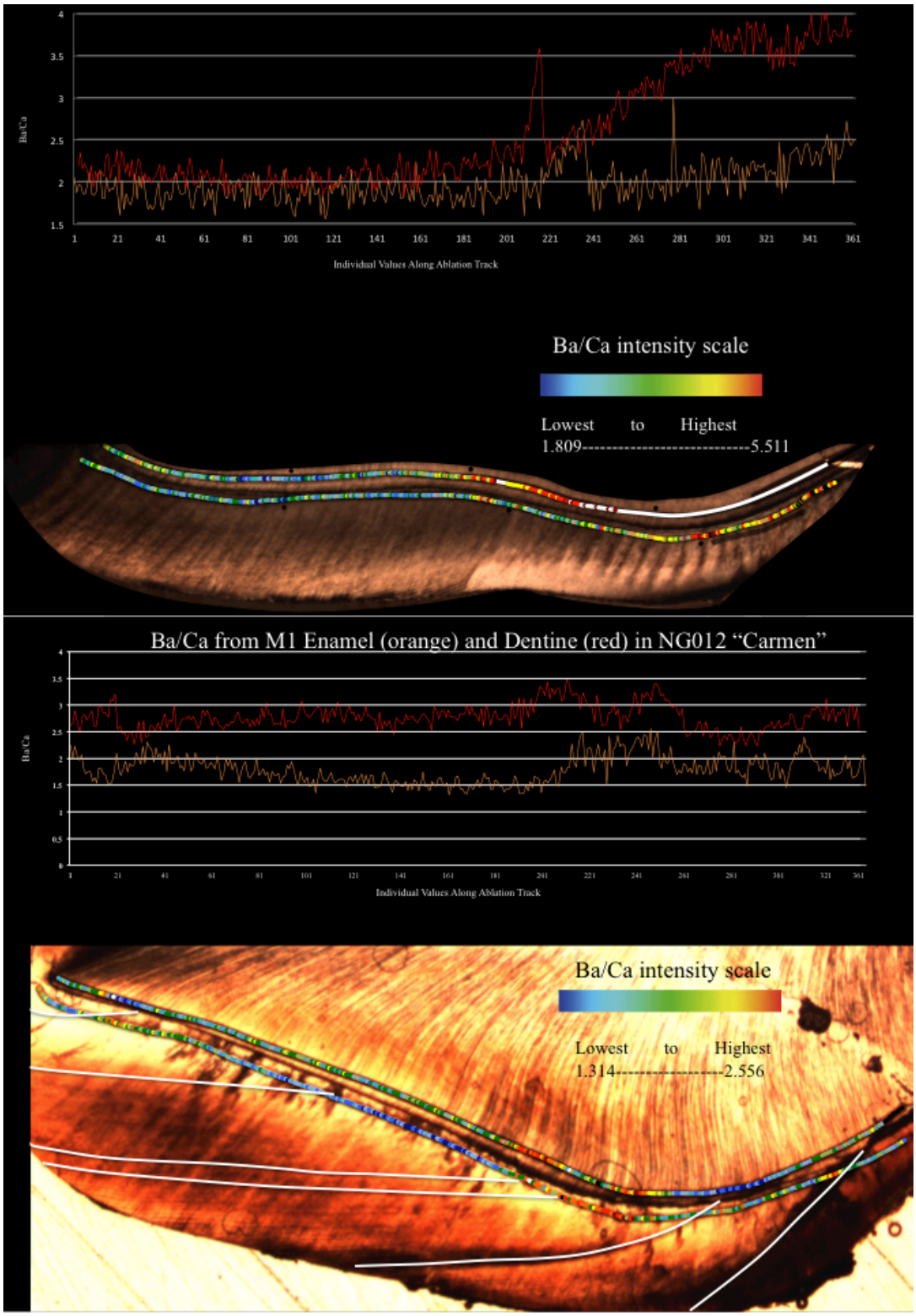

Figure 19: The two maps here include the histological section in the background for some context for the changing Ba/Ca values within the ablated tracks in enamel and dentine. The occlusal end is to the left and the cervical end is to the right.

Case 5: NG012- This individual, "Carmen", was the only female chimpanzee from the Ngogo sample. Her M_1 emergence age was estimated to be 3.43-3.73 years, with a root growth spurt age of 3.93 years, and this is on the late end of Ngogo range.

Her patterns of Ba/Ca variation (Figure 19-bottom) in the enamel have been affected by the track veering slightly into the more demineralized enamel next to the EDJ, but the track through her dentine tells a different story. Ba/Ca values (in red) and the values within the early part of the track (on the left of the image), show the tell-tale increase after the neonatal line, indicating the switch from a prenatal diet to one of exclusive nursing, and after this increase, and a short-lived decrease where the track runs over a crack, these values stay in the mid- to mid-high range (greens, light greens, and yellows) until around nine months, at which point there is a spike in in the Ba/Ca values (all oranges, reds, and dark reds). This spike coincides with the occurrence of two major accentuated lines about 20 days apart, and these may indicate an episode of increased suckling, or could suggest a short period of intensive illness or starvation, during which her skeletal calcium and barium stores would have been mobilized and incorporated into her forming teeth. After this point, there is another increase between ages 12-14 months, followed by a decrease as the track runs back into the demineralized dentine. Once the track remerges, the values stay within the mid-range (aqua, green, light green) with occasional spikes of yellow and orange, until the end of the track. This suggests that the relative contribution of milk has decreased, but that she was still nursing at a steady level through age 1.68 years (a minimum estimate from the enamel-based cusp-specific formation time (CFT)). This Ba/Ca information is continued in the M2 of NG012, seen in the overlap map in Figure 20.

Figure 20: Ba/Ca overlap between ablated tracks in M1-M2 in NG012 with the root growth spurt overlaid

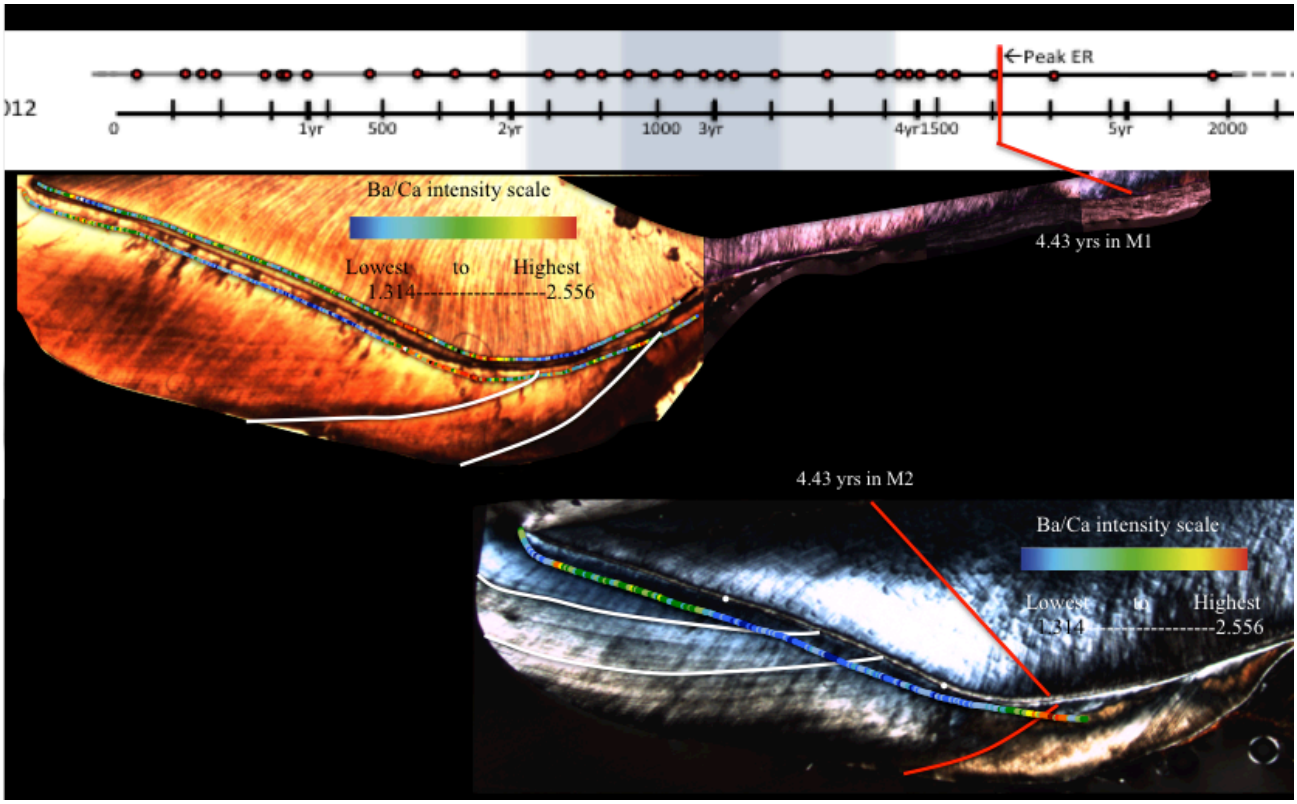

Figure 20: Accentuated lines used to cross match the M1 and M2 can be seen in white, and the root growth spurt age for the M_1 (top tooth) is indicated by a red line in the M_1 and in the M2 (bottom tooth). A chart of the distribution of accentuated lines (red circles) and their frequency before and after the M_1 root growth spurt is included on the top. The root growth spurt is where the peak extension rate occurs in the M_1.

In the NG012 M_1-M_2 overlap map (Figure 20), the M_1 root growth spurt age noted for this individual in a previous study (Malone, Chapter 1), is highlighted on the M_1 root with the same point registered within the crown of the M_2. This is in order to look for correlations between the accentuated lines, (indicating stress episodes) and the Ba/Ca values. In the example in Figure 11 (NG012 M_1-M_2), the root growth spurt age of 3.93 years is marked within the M_1 and M_2, and the pattern of accentuated lines in the M_1 crown and root dentine is shown at the top of the image (with red circles indicating accentuated line occurrences), in order to illustrate the surge and cluster of these lines leading up to the root growth spurt. That surge in structural markers of stress coincides with an area of heightened Ba/Ca intensity in

the enamel of M_2, which overlaps in time with the growth spurt in the root of M_1 (That area of the M_1 root was not ablated, so the simultaneously forming portion of M_2 crown was used as a substitute.) Similar, though less extreme, patterns of accentuated line frequency in the time just prior to the root growth spurt are recorded in the other M1s (Malone, Chapter 1).

Summary of Ba/Ca intensity maps: When the individual intensity maps of Ba/Ca distribution are considered for all five chimpanzee M1s, a subtle pattern begins to emerge. There is first a slight increase in the earliest forming enamel and dentine, coinciding with an inferred transition from prenatal enamel (before the neonatal line) to enamel formed while exclusively nursing. The Ba/Ca ratio then drops significantly with only occasional forays from low intensity (blues) to medium intensity (greens) until a major transition appears to occur around two-thirds of the way through M1 crown formation. At this point, often fluctuating greatly, the much higher values begin to appear (yellow-orange-red), coinciding with the occurrence of some of the most significant accentuated lines. This variation is more pronounced and visible within the dentine, but appears to occur at almost exactly the same time as the slightly more diffuse signal in the enamel, which supports the fidelity of the signal. From looking at the enamel and dentine values together (in the charts at the top of each map), it also becomes clear that the values produced by ablating the dentine are substantially higher in absolute terms than those created by ablating the enamel. However, these tracks do not extend into the M1 root dentine, and so any correspondence between Ba/Ca values and the root growth spurt must be sought in the next tooth to form, either the M2 or the P4 (see Figure 21).

Figure 21: Ba/Ca enamel overlap between M1&M2 (or P4) of the seven chimpanzees with M1s present

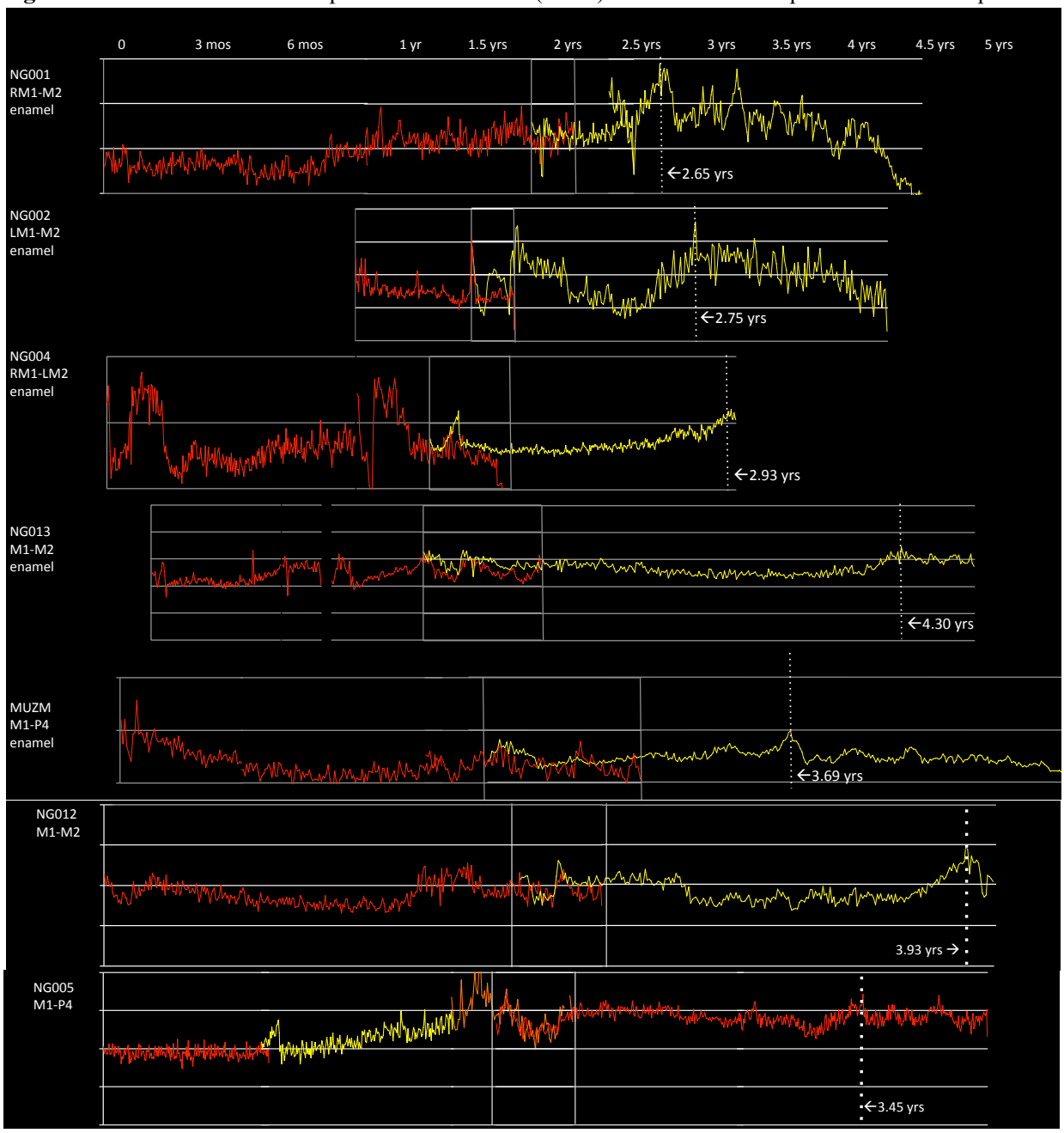

Figure 21. Developmental time is on the x-axis and Ba/Ca values are on the y-axis. In six out of seven of the individuals, there is one red line for the M1 and one yellow line for the M2 or P4. In NG005 (bottom) the M1 line is divided into three parts (red, yellow, & orange) due to the ablation line being interrupted, and part three (orange) overlaps with the P4 values (second red line). These sets of consecutively forming teeth overlap for between two and eleven months (higher amounts are between M1s and P4s, lower amounts are between M1s and M2s). Root growth spurts are overlaid as dashed white lines.

Table 11: M_1 root growth spurt ages for the seven chimpanzees in Figure 13

NG001	NG002	NG004	NG013	MUZM	NG012	NG005
2.65 years	2.75 years	2.93 years	4.30 years	3.69 years	3.93 years	3.45 years

Table 11: Root growth spurts are measured in M_1s or inferred in M^1s. (Modified from Malone, Chapter 1)

Multi-tooth Ba/Ca overlap charts: The charts in Figure 21 line up the areas of Ba/Ca pattern overlap for the laser ablation tracks in concurrently forming teeth for the seven chimpanzees. This was done using either the M1 and M2, or the M1 and P4, since both combinations show overlap in formation time for these individuals (Malone, Chapter 1) and the overlap in these teeth has been documented in other chimpanzee populations (e.g. Reid et al., 1998). Most significantly, the root growth spurts of the lower M1s in these individuals, are indicated in the M2 or P4 charts (Figure 21), and in each one, a spike in Ba/Ca values occurs in tandem with the root growth spurt, followed by a decrease in Ba/Ca throughout the rest of that track. This suggests that the pattern seen in the Ba/Ca overlap map (Figure 20) consistently occurs in each of the chimpanzee M1-M2 combinations, and demonstrates how this alignment between the structural and chemical indicators of the weaning process can be visualized.

Comparative yellow baboon Ba/Ca results: In addition to the data collected from the chimpanzee population, the amount of overlap in Ba/Ca values in the teeth of several yellow baboons (*Papio cynocephalus*) is also given (Figure 22). The amount of baboon Ba/Ca overlap is even more striking than that within the chimpanzees, and can be compared with histologically based overlap charts such as that from Dirks & Bowman (2007).

Figure 22: Ba/Ca enamel overlap between the M1, C, & M2 in a female baboon (top) and between the M1, C, M2 & M3 in a male baboon (bottom)

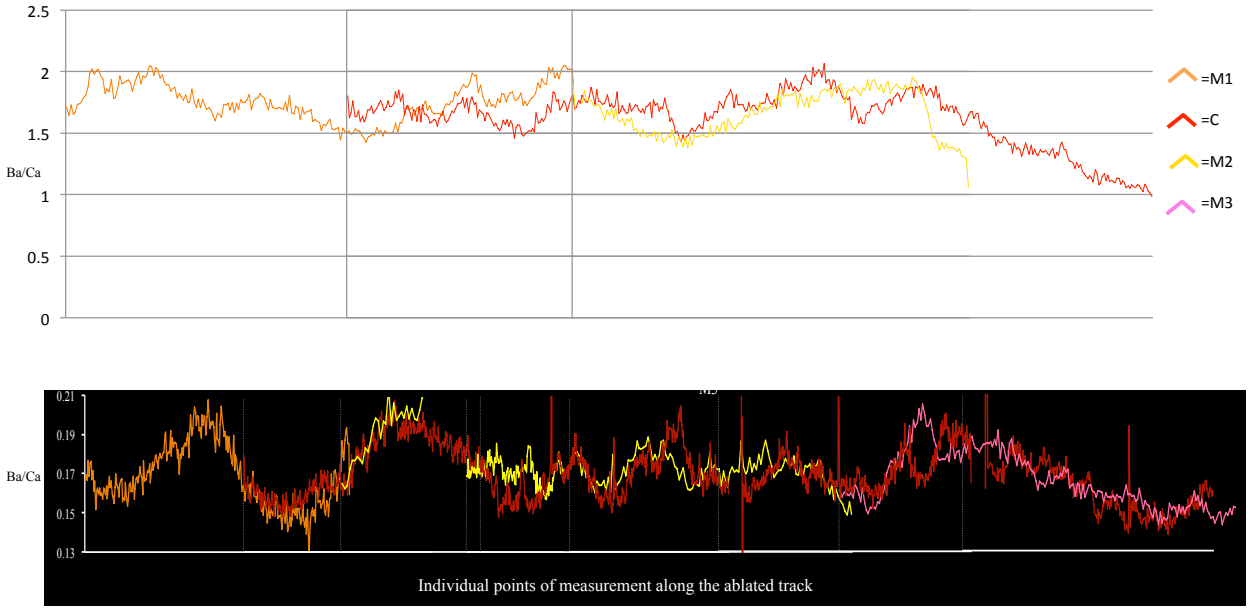

Figure 22: In both the female (top) and male (bottom) Ba/Ca overlap charts, the values from the M1s are in orange, those from the canines are in red, those from the M2s are in yellow, and in the male only, those from the M3 are in pink. Gray vertical lines indicate overlap between the tracks, and the spikes seen in the male canine values (red) are outliers.

In the yellow baboon study multiple tracks were ablated beginning with one close to the EDJ and subsequent ones ran parallel to that first track, but closer to the crown surface as seen in Figure 23 (Malone, unpublished data). In these teeth, the pattern of Ba/Ca change in the inner track changed fairly abruptly before and after the occurrence of particularly significant accentuated lines (red lines in Figure 23), while more diffuse changes were seen in tracks closer to the surface. It was determined, therefore, that the best way to obtain signal fidelity, if it were to be found anywhere in the tooth, would be right against the EDJ in the innermost enamel. Previous studies have explored the use of this inner layer (at least the first 10 μm or so) to obtain $\delta^{18}O$ values that most closely resemble the original water input values compared with any other area of the tooth, indicating that this area may mature soonest after it is formed, resulting in the least signal attenuation from sampling in that area (Passey & Cerling, 2013).

In the chimpanzee study, a 30-µm track was the narrowest that could be obtained using the equipment available for this study, but by keeping it close to the EDJ as much as possible, when there was not damage to the area, the signal obtained was at least able to be linked more closely with the original input signal than the wider tracks ablated closer to the crown surface in the previous study carried out using the baboons.

Figure 23: Ba/Ca distribution in the M1s of a male (left) and female (right) yellow baboon

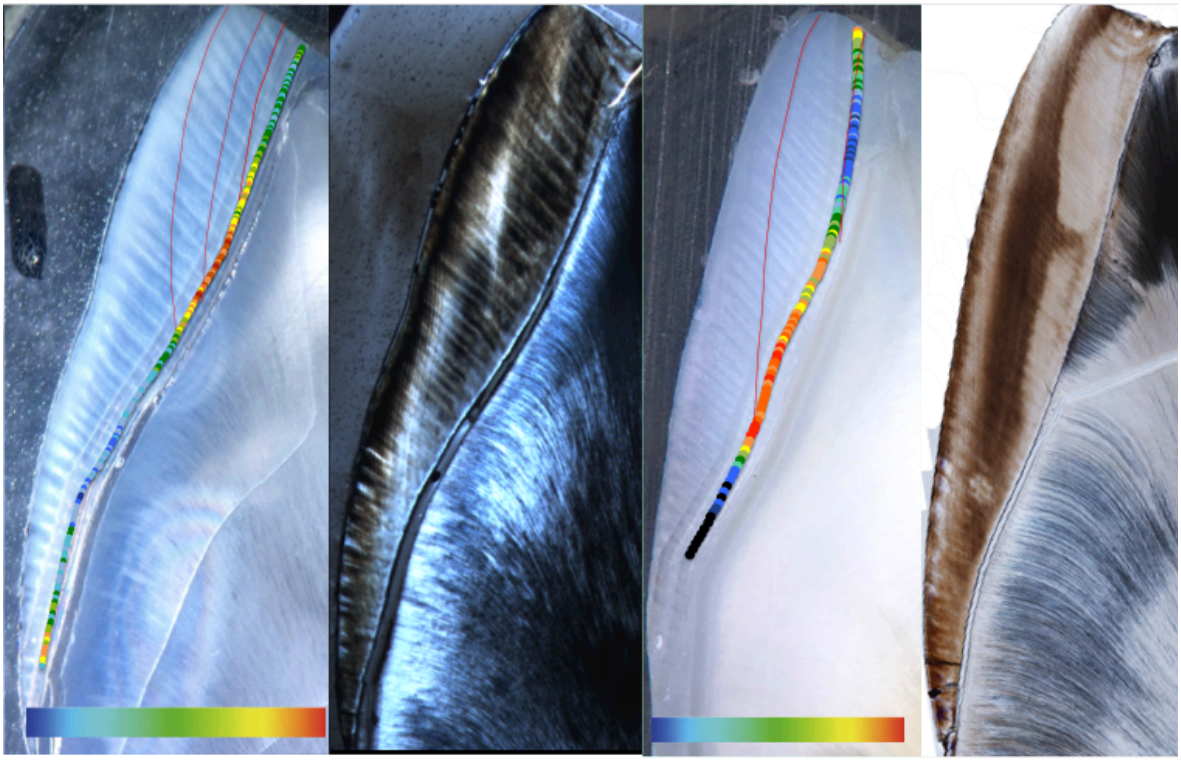

Figure 23: Images from left t right-Reflected light 4x microscope image of 110-um thin section from the UM112 M1 mesiobuccal cusp with two 65-um tracks ablated into the enamel adjacent to the EDJ. Ba/Ca intensities are overlaid on the inner track running form the occlusal edge (top) to the cervical margin (bottom). Early accentuated lines, including the neonatal line, are overlaid in red. Image 2 is of the same section of the same tooth before ablation, seen through polarized transmitted light to visualize internal structures. Image 3 is the M1 of a female baboon, and it is taken on a thicker section, so the reflected light doesn't pass through it as well. An 80 um-track was used in this tooth, and image 4, while of the same tooth, is of the opposing face of that section. Values from the lowest part of the Ba/Ca intensity range are dark blue and medium blue, moderately low are light blue and aqua, neutral/mid-range intensities are green and light green, medium high intensities are seen in yellow and orange, and the highest intensities are bright red and dark red. The area in black at the end of the track in UM152 contained damaged, cracked enamel, making the values from that region and the rest of the way down the track extreme outliers.

Conclusions: This study found that the changes in Ba/Ca intensity (that presumably reflect dietary changes) do show the same general patterns of increase and decrease through developmental time in chimpanzees as in other primates for which this has been assessed. It was also found that the Ba/Ca values increase at the time of the M1 age at peak root growth velocity, followed by a decrease that continues thereafter, (except in cases of enamel damage), which supports the hypothesis that weaning completion occurs just after the M_1 root growth spurt in chimpanzees. Since the M1 root growth spurts of these individuals were found to align well with the inferred ages at nutritional independence in Ngogo chimpanzees as assessed in a fecal isotope study, this lends further support to this study's proposed connection between M_1 root growth spurt and weaning completion.

One of the implications of these findings is that age at weaning completion, an important life history variable, can potentially be directly measured in isolated M1s, no longer in the mandible, since the root growth spurt can be measured in the M1 root and changing Ba/Ca values can be obtained from the root dentine. (We used the M1s and M2s or P4s, but it may be possible, and much simpler, to do this with only the M1s.) These structural and chemical correspondences should be confirmed in other chimpanzee populations, as well as in other primate taxa to assess whether this association holds true.

Another potential outcome of this study is that this method of determining the age of the M1 root growth spurt could be applied to dental remains in the fossil record, including those of fossil hominins, though further study into the integrity of the trace elemental signals in fossil enamel is a necessary precursor to such studies. Since this study successfully tracked this structural and chemical proxy for weaning completion in the teeth of adult individuals, it may be possible to significantly increase the sample size for which we can infer weaning completion age

in fossil taxa, if we do not have to rely upon using juvenile remains to infer M_1 emergence age. This also eliminates the potential complication of using dental remains from deceased juveniles whose early deaths may not indicate "typical" developmental patterns, compared with individuals that survived through adulthood (see Smith and Boesch, 2011).

Works Cited

Altmann, J. 1980. Baboon Mothers and Infants. Cambridge, Harvard University Press.

Altmann, J., Altmann, S.A., Hausfater, G., McCuskey, S.A. 1977. Life history of yellow baboons: Physical development, reproductive parameters, and infant mortality. Primates, 18: 315–330.

Altmann, J., Altmann, S., Hausfater, G. 1981. Physical maturation and age estimates of yellow baboons, *Papio cynocephalus*, in Amboseli National Park, Kenya. American Journal of Primatolology 1: 389–399.

Ambrose, S.H., Norr, L. 1993. Experimental evidence for the relationship of the carbon isotope ratios of whole diet and dietary protein to those of bone collagen and carbonate. In: Lambert, J.B., Norr, L. (Eds.), Prehistoric Human Bone and Archaeology at the Molecular Level. Springer-Verlag, pp. 1-38.

Antoine, D., Hillson, S., Dean, M.C. 2009. The developmental clock of dental enamel: A test for the periodicity of prism cross-striations and an evaluation of the likely sources of error in histological studies of this kind. Journal of Anatomy, 214:45-55.

Austin, C., Smith, T. M., Bradman, A., Hinde, K., Joannes-Boyau, R., Bishop, D., Arora, M. 2013. Barium distributions in teeth reveal early-life dietary transitions in primates. Nature, 498(7453), 216–219. http://doi.org/10.1038/nature12169.

Bădescu, I., Katzenberg, M. A., Watts, D. P., and Sellen, D. W. 2017. A novel fecal stable isotope approach to determine the timing of age-related feeding transitions in wild infant chimpanzees. American Journal of Physical Anthropology, 162(2), 285–299. http://doi.org/10.1002/ajpa.23116.

Balasse, M. 2002 Reconstructing dietary and environmental history from enamel isotopic analysis: time resolution of intra-tooth sequential sampling. International Journal of Osteoarchaeology, 12, 155–165.

Beynon, A.D., Dean, M.C., Reid, D.J. 1991. Histological study on the chronology of the developing dentition in gorilla and orangutan. American Journal of Physical Anthropology, 86:189-203.

Beynon, A. D., Clayton, C. B., Ramirez Rozzi, F. V, and Reid, D. J. 1998. Radiographic and histological methodologies in estimating the chronology of crown development in modern humans and great apes: a review, with some applications for studies on juvenile hominids. Journal of Human Evolution, 35(4–5), 351–70. http://doi.org/10.1006/jhev.1998.0234.

Boesch, C. 1991. The effects of leopard predation on grouping patterns in forest chimpanzees. Behaviour, 117, 220-241.

Boesch, C., Boesch-Achermann, H. 2000. The Chimpanzees of the Taï Forest: Behavioural Ecology and Evolution. Oxford University Press, Oxford.

Bogin, B. 1990. The evolution of human childhood. BioScience, 40:16-25.

Boyde, A. 1963. Estimation of age at death of young human skeletal remains from incremental lines in the dental enamel. In: Third International Meeting in Forensic Immunology, Medicine, Pathology, and Toxicology, London, April 1963, pp. 16e24.

Boyde, A. 1990. Developmental interpretations of dental microstructure. In (C. J. DeRousseau, Ed.) Primate Life History and Evolution. Monographs in Primatology Vol. 14, pp. 229–267. New York: Wiley Liss.

Bryant, D., Froelich, P. 1995. A model of oxygen isotope fractionation in body water of large mammals. Geochimica et Cosmochimica Acta, 59, 4523–4537.

Burton, J.H., Price, T.D., Middleton, W.D. 1999. Correlation of bone Ba/Ca and Sr/Ca due to biological purification of calcium. Journal of Archaeological Science, 26, 609-616.

Carlson, B. A., and Crowley, B. E. 2016. Variation in carbon isotope values among chimpanzee foods at Ngogo, Kibale National Park and Bwindi Impenetrable National Park, Uganda. American Journal of Primatology, 78, 1031–1040.

Cerling, T. E., Hart, J. A., and Hart, T. B. 2004. Stable isotope ecology in the Ituri Forest. Oecologia, 138, 5–12. http://doi.org/10.1007/s00442-003-1375-4.

Cerling, T. E., Manthi, F. K., Mbua, E. N., Leakey, L. N., Leakey, M. G., Leakey, R. E., … Wood, B. a. 2013. Stable isotope-based diet reconstructions of Turkana Basin hominins. Proceedings of the National Academy of Sciences of the United States of America, 110(26), 10501–6. http://doi.org/10.1073/pnas.1222568110.

Charnov, E.L. 1991. Evolution of life history variation among female mammals. Procedings of the National Academy of Sciences of the Uniten States of America, 88:1134-37.

Cheney, D.L., Seyfarth, R.M., Fischer, J., Beehner, J., Bergman, T., Johnson, S.E., Kitchen, D.M., Palombit, R.A., Rendall, D., Silk, J.B. 2004. Factors affecting reproduction and mortality among baboons in the Okavango Delta, Botswana. International Journal of Primatology, 25: 401–428.

Christensen, G. J. and Kraus, B. S. 1965. Initial calcification of the human permanent first molar. Journal of Dental Research, 44, 1338–1342.

Comar, C.L., Russell, L., Wasserman, R.H. 1957. Strontium–calcium movement from soil to man. Science, 126, 485–496.

Comar, C.L. 1963. Some over-all aspects of strontium-calcium discrimination. In: Wasserman RH, editor. The transfer of Calcium and Strontium across biological membranes. New York: Academic press. p 405–417.

Crowley, B. E., Sharp, and Crowley, B. E. 2012. Stable Isotope Techniques and Applications for Primatologists. International Journal of Primatology, 33(3), 673–701. http://doi.org/10.1007/s10764-012-9582-7.

Crowley, B. E., Reitsema, L. J., Oelze, V. M., and Sponheimer, M. 2016. Advances in primate stable isotope ecology-Achievements and future prospects. American Journal of Primatology, 78, 995-1003. http://doi.org/10.1002/ajp.22510.

Dean, M.C., Beynon, A.D., Thackeray, J.F., Macho, G.A., 1993. Histological reconstruction of dental development and age at death of a juvenile *Paranthropus robustus* specimen, SK 63, from Swartkrans, South Africa. American Journal of Physical Anthropology, 91, 401-419.

Dean, M.C., 2000. Progress in understanding hominoid dental development. Journal of Anatomy, 197, 77-101.

Dean, M. C., and Kelley, J. 2012. Comparative dental development in *Hispanopithecus laietanus* and *Pan troglodytes*. Journal of Human Evolution, 62(1), 174–8. http://doi.org/10.1016/j.jhevol.2011.10.003.

Dean, M. C., and Cole, T. J. 2013. Human life history evolution explains dissociation between the timing of tooth eruption and peak rates of root growth. PLoS ONE, 8(1). http://doi.org/10.1371/journal.pone.0054534.

Dean, M. C., and Elamin, F. 2014. Parturition lines in modern human wisdom tooth roots : do they exist, can they be characterized and are they useful for retrospective determination of age at first reproduction and / or inter-birth intervals? Annals of Human Biology, 41(4): 358-367. http://doi.org/10.3109/03014460.2014.923047.

Dirks, W. 1998. Histological reconstruction of dental development and age of death in a juvenile gibbon (*Hylobates lar*). Journal of Human Evolution, 35, 411-425.

Dirks, W., Reid, D. J., Jolly, C. J., Phillips-Conroy, J. E., and Brett, F. L. 2002. Out of the mouths of baboons: stress, life history, and dental development in the Awash National Park hybrid zone, Ethiopia. American Journal of Physical Anthropology, 118(3), 239–52. http://doi.org/10.1002/ajpa.10089.

Dirks, W., Bowman, J.E. 2007. Life history theory and dental development in four species of catarrhine primates. Journal of Human Evolution, 53, 309-320.

Dirks, W., Humphrey, L. T., Dean, M. C., and Jeffries, T. E. 2010. The relationship of accentuated lines in enamel to weaning stress in juvenile baboons (*Papio hamadryas anubis*). Folia Primatologica; International Journal of Primatology, 81(4), 207–23. http://doi.org/10.1159/000321707.

Dolphin, A. E., Goodman, A. H., and Amarasiriwardena, D. D. 2005. Variation in elemental intensities among teeth and between pre- and postnatal regions of enamel. American Journal of Physical Anthropology, 128(4), 878–88. http://doi.org/10.1002/ajpa.20213.

Elias, R.W., Hirao, Y., Patterson, C.C. 1982. The circumvention of the natural biopurification of calcium along nutrient pathways by atmospheric inputs of industrial lead. Geochimica et Cosmochimica Acta, 46:2561–2580.

Eli, I., Sarnat, H., and Talmi, E. 1989 Effect of the birth process on the neonatal line in primary tooth enamel. Pediatric Dentistry, 11:220-223.

Froehle, A.W., Kellner, C.M., Schoeninger, M.J. 2010. Effect of diet and protein source on carbon stable isotope ratios in collagen: follow up to Warinner and Tuross. Journal of Archaeological Science, 37:2662–2670.

Froehle, A.W., Kellner, C.M., Schoeninger, M.J. 2012. Multivariate carbon and nitrogen stable isotope model for the reconstruction of prehistoric human diet. American Journal of Physical Anthropology, 147: 352–369.

Gleiser, I., and Hunt, E. E. 1955. The Permanent Mandibular First Molar: Its Calcification, Eruption, and Decay, American Journal of Physical Anthropology, 13:253-84.

Goodman, A. H., and Rose, J. C. 1990. Assessment of Systemic Physiological Perturbations From Dental Enamel Hypoplasias and Associated Histological Structures, Yearbook of Physical Anthropology, 33, 59–110.

Green, D. R., Smith, T. M., Green, G. M., Bidlack, F. B., Tafforeau, P., and Colman, A. S. 2018. Quantitative reconstruction of seasonality from stable isotopes in teeth. Geochimica et Cosmochimica Acta, 235, 483–504. http://doi.org/10.1016/j.gca.2018.06.013.

Gustavson, G., Gustavson, A.G. 1967. Microanatomy and Histochemistry of enamel. In: Miles, A.E.W. (Ed.), Structural and Chemical Organisation of Teeth. Academic press, New York, pp. 75–134.

Harvey, P. H., and Clutton-Brock, T. H. 1985. Life History Variation in Primates. Evolution, 39(3), 559–581. Retrieved from http://www.jstor.org.

Humphrey, L. T. 2007. An evaluation of changes in strontium / calcium ratios across the neonatal line in human deciduous teeth. In S. E. Bailey (Ed.), Dental perspectives on human evolution (pp. 303–319). Springer.

Humphrey, L. T., Dirks, W., Dean, M. C., and Jeffries, T. E. 2008. Tracking dietary transitions in weanling baboons (*Papio hamadryas anubis*) using strontium/calcium ratios in enamel. Folia Primatologica; International Journal of Primatology, 79(4), 197–212. http://doi.org/10.1159/000113457.

Humphrey, L. T. 2014. Isotopic and trace element evidence of dietary transitions in early life. Annals of Human Biology, 41(4), 348–57. http://doi.org/10.3109/03014460.2014.923939.

Köndgen, S., Kühl, H., N'Goran, P.K., Walsh, P.D., Schenk, S., Ernst, N., Biek, R., Formenty, P., Mätz-Rensing, K., Schweiger, B., Junglen, S., Ellerbrok, H., Nitsche, A., Briese, T., Lipkin,W.I., Pauli, G., Boesch, C., Leendert, F.H. 2008. Pandemic human viruses cause decline of endangered great apes. Current Biology, 18, 260-264.

Krachler, M., Rossipal, E., Micetic-Turk, D. 1999. Trace element transfer from the mother to the newborn – investigations on triplets of colostrum, maternal and umbilical cord sera. European Journal of Clinical Nutrition, 53: 486–494.

Krishna, B.A., Singh, M., Singh, M., Kaumanns, W. 2008. Infant development and weaning in *Macaca silenus* in the natural habitats of the Western Ghats, India. Current Science 94: 347–355.

Krueger, H.W., Sullivan, C.H. 1984. Models for carbon isotope fractionation between diet and bone. In: Thornland, J.R., Johnson, P.E., editors. Stable isotopes in nutrition. Washington: American Chemical Society. p 205–220.

Lee, P. C. 1996. The meanings of weaning: Growth, lactation, and life history. Evolutionary Anthropology: Issues, News, and Reviews, 5(3), 87–98.

Lee, P. C. 2010. Growth and Investment in Hominin Life History Evolution: Patterns, Processes, and Outcomes. International Journal of Primatology, 33(6), 1309–1331. http://doi.org/10.1007/s10764-011-9536-5.

Leendertz, F.H., Ellerbrok, H., Boesch, C., Couacy-Hymann, E., Mätz-Rensing, K., Hakenbeck, R., Bergmann, C., Abaza, P., Junglen, S., Moebius, Y., Vigilant, L., Formenty, P., Pauli, G. 2004. Anthrax kills wild chimpanzees in a tropical rainforest. Nature, 430, 451-452.

Lonsdorf, E.V., Murray, C.M., Lonsdorf, E.V., Travis, D.A., Gilby, I.C., Chosy, J., Goodall, J., Pusey, A.E. 2011. A retrospective analysis of factors ccorrelated to chimpanzee (*Pan troglodytes schweinfurthii*) respiratory health at Gombe National Park, Tanzania. EcoHealth 8, 26-35.

Lough, S.A., Rivera, J., Comar, C.L. 1963. Retention of strontium, calcium and phosphorus in human Infants. Procedings of the Society for Experimental Biology and Medicine, 112: 631–636.

Luz, B., Kolodny, Y., Horowitz, M., 1984. Fractionation of oxygen isotopes between mammalian bone phosphate and environmental drinking water. Geochimica et Cosmochimica Acta, 48, 1689-1693.

Luz, B., Kolodny, Y., 1985. Oxygen isotope variations in phosphate of biogenic apatites. IV. Mammal teeth and bones. Earth and Panetary Sciences Letters, 75, 29-36.

Luz, B., Kolodny, Y. 1989. Oxygen isotope variation in bone phosphate. Applied Geochemistry, 4:317–323.

Machanda, Z., Brazeau, N. F., Bernard, A. B., Donovan, R. M., Papakyrikos, A. M., Wrangham, R., and Smith, T. M. 2015. Dental eruption in East African wild chimpanzees. Journal of Human Evolution, 2–9. http://doi.org/10.1016/j.jhevol.2015.02.010.

McDade, T. W. 2003. Life history theory and the immune system: steps toward a human ecological immunology. American Journal of Physical Anthropology, Supplement 37, 100–25. http://doi.org/10.1002/ajpa.10398.

Molnar, S., and Ward, S. C. 1975. Mineral Metabolism and Microstructural Defects in Primate Teeth American Journal of Physical Anthropology, 43(1), 3-18.

Moorees, C. F. A., Fanning, E. A., and Hunt, E. E. 1963. Age variation of formation stages for ten permanent teeth, Journal of Dental Research, 42, 1490–502.

Negrey, L.D., Reddy, R.B., Scully, E.J., Phillips-Garciad, S., Owens, L.A., Langergraber, K.E., Mitani, J.C., Emery Thompson, M., Wrangham, R.W., Muller, M.N., Otali, E., Machanda, Z., Hyerobag, D., Grindle, K.A., Pappas, T.E., Palmenberg, A.C., Gerne, J.E., and Goldberg , T.L. 2019. Simultaneous outbreaks of respiratory disease in wild chimpanzees caused by distinct viruses of human origin. Emerging Microbes & Infections, VOL. 8 https://doi.org/10.1080/22221751.2018.1563456.

Nelson, S. V. 2013. Chimpanzee fauna isotopes provide new interpretations of fossil ape and hominin ecologies. Procedings of the Royal Society, 280(November).

Nishida, T., Corp, N., Hamai, M., Hasegawa, T., Hiraiwa-Hasegawa, M., Hosaka, K., Hunt, K.D., Itoh, N., Kawanaka, K., Matsumoto-Oda, A. 2003. Demography, female life history, and reproductive profiles among the chimpanzees of Mahale. American Journal of Primatology, 59, 99-121.

Noren, J.G. 1984 Microscopic study of enamel defects in deciduous teeth of infants of diabetic mothers. Acta Odontologica Scandanavia 42, 153-156.

Nowell, A.A., Fletcher, A.W. 2007. Development of Independence from the Mother in *Gorilla gorilla gorilla.* International Journal of Primatology, 28: 441–455.

Passey, B. H. and Cerling, T. E. 2002. Tooth enamel mineralization in ungulates: Implications for recovering a primary isotopic time-series. Geochimica et Cosmochimica Acta, 66, 3225–3234.

Passey, B., and Cerling, T. 2006. In situ stable isotope analysis (δ13C, δ18O) of very small teeth using laser ablation GC/IRMS. Chemical Geology, 235(3–4), 238–249. http://doi.org/10.1016/j.chemgeo.2006.07.002.

Potts, K. B., Watts, D. P., and Wrangham, R. W. 2011. Comparative Feeding Ecology of Two Communities of Chimpanzees (*Pan troglodytes*) in Kibale National Park, Uganda. International Journal of Primatology, 32(3), 669–690. http://doi.org/10.1007/s10764-

Pusey, A.E., Wilson, M.L., Collins, D.A. 2008. Human impacts, disease risk, and population dynamics in the chimpanzees of Gombe National Park, Tanzania. American Journal of Primatology, 70, 738-744.

Reid, D.J., Schwartz, G.T., Dean, C., Chandrasekera, M.S., 1998. A histological reconstruction of dental development in the common chimpanzee, *Pan troglodytes*. Journal of Human Evolution, 35, 427-448.

Reid, D. J., Beynon, D., and Ramirez Rozzi, F. V. 1998. Histological reconstruction of dental development in four individuals from a medieval site in Picardie, France. Journal of Human Evolution, 35(4–5), 463–77. http://doi.org/10.1006/jhev.1998.0233.

Risnes, S., 1998. Growth tracks in dental enamel. Journal of Human Evolution, 35, 331-350.

Robbins, M.M., Nkurunungi, J.B., McNeilage, A., 2006. Variability of the feeding ecology of eastern gorillas. In: Hohmann, G., Robbins, M.M., Boesch, C. (Eds.), Feeding Ecology of Apes and Other Primates. Cambridge University Press, Cambridge, pp 25-47.

Robson, S. L., Wood, B., Shea, B. T., Arnold, C., … Soligo, C. 2008. Hominin life history: reconstruction and evolution. Journal of Anatomy, 212(4), 394–425. http://doi.org/10.1111/j.1469- 7580.2008.00867.

Rose, J.C. 1977 Defective enamel histology of prehistoric teeth from Illinois. American Journal of Physical Anthropology, 46, 439-446.

Rose, J.C. 1979 Morphological variations of enamel prisms within abnormal striae of Retzius. Human Biology, 51, 139-151.

Rose, J. C., Armelagos, G. J., and Lallo, J. W. 1978. Histological enamel indicator of childhood stress in prehistoric skeletal samples. American Journal of Physical Anthropology, 49:511–516.

Rossipal, E., Krachler, M., Li, F., Micetic-Turk, D. 2000. Investigation of the transport of trace elements across barriers in humans: studies of placental and mammary transfer. Acta Paediatrica, 89:1190–1195.

Rushton, M.A., 1933. On the fine contour lines of the enamel of milk teeth. Dental Records, 53, 170-171.

Schour, I., 1936. The neonatal line in the enamel and dentin of human deciduous teeth and first permanent molar. Journal of the American Dental Association, 23, 1946-1955.

Schwartz, G. T. 2012. Growth, Development, and Life History throughout the Evolution of *Homo*. Current Anthropology, 53(S6), S395–S408. http://doi.org/10.1086/667591.

Schwartz, G.T., Reid, D.J., Dean, M.C., Zihlman, A.L., 2006. A faithful record of stressful life events preserved in the dental developmental record of a juvenile gorilla. International Journal of Primatology, 22, 837-860.

Shellis, R.P. 1998. Utilization of periodic markings in enamel to obtain information on tooth growth. Journal of Human Evolution, 35, 387-400.

Sillen, A., Kavanagh, M. 1982. Strontium and paleodietary research: a review. Yearbook of Physical Anthropology, 25:67–90.

Skinner, M.F., and Anderson, G.S. 1991 Individualization and enamel histology: a case report in forensic anthropology. Journal of Forensic Sciences, 36:939-948.

Smith, C. C., Morgan, M. E., and Pilbeam, D. 2010. Isotopic ecology and dietary profiles of Liberian chimpanzees. Journal of Human Evolution, 58(1), 43–55. http://doi.org/10.1016/j.jhevol.2009.08.001.

Smith, B. H. 1989. Dental development as a measure of life history in primates. Evolution 43:683-88.

Smith, B. H. 1991. Dental development and the evolution of life history in Hominidae. American Journal of Physical Anthropology, 86(2), 157–174. http://doi.org/10.1002/ajpa.1330860206.

Smith, C. E. (1998). During Enamel Maturation. Critical Reviews in Oral Biology & Medicine, 9(2), 128–161.

Smith, B.H., Tompkins, R.L., 1995. Toward a life history of the Hominidae. Annual Review in Anthropology, 24, 257-279.

Smith, T.M. 2004. Incremental development of primate dental enamel. Ph.D. Dissertation. StonyBrook University.

Smith, T. M. 2008. Incremental dental development : Methods and applications in hominoid evolutionary studies. Journal of Human Evolution, 54(2), 205–224. http://doi.org/10.1016/j.jhevol.2007.09.020.

Smith, T. M., Reid, D. J., Dean, M.C., Olejniczak, A.J., Ferrell, R.J., Martin, L.B. 2007. New perspectives on chimpanzee and human molar crown development. In S. E. & H. Bailey (Ed.), Dental perspectives on human evolution (pp. 177–192). Springer.

Smith, B. H., and Boesch, C. 2011. Mortality and the magnitude of the "wild effect" in chimpanzee tooth emergence. Journal of Human Evolution, 60(1), 34–46. http://doi.org/10.1016/j.jhevol.2010.08.006.

Smith, T. M., Machanda, Z., Bernard, A. B., Donovan, R. M., Papakyrikos, A. M., Muller, M. N., and Wrangham, R. 2013. First molar eruption, weaning, and life history in living wild chimpanzees. Proceedings of the National Academy of Sciences of the United States of America, 110(8) 2787-2791. http://doi.org/10.1073/pnas.1218746110.

Smith, T. M., Austin, C., Hinde, K., Vogel, E. R., and Arora, M. 2017. Cyclical nursing patterns in wild orangutans. Science Advances, (May), 3, 1–9.

Smith, T. M., Austin, C., Green, D. R., Joannes-boyau, R., Bailey, S., Dumitriu, D., … Arora, M. 2018. Wintertime stress, nursing, and lead exposure in Neanderthal children. Science Advances, 4:eaau9483.

Stanford, C. B., and Nkurununngi, J. B. 2003. Behavioral Ecology of Sympatric Chimpanzees and Gorillas In Bwindi Impenetrable National Park, Uganda : Diet International Journal of Primatology, 24(4) 901-918.

Struhsaker, T. T. 1997. Ecology of an African rainforest. Gainesville: University Press of Florida.

Suga, S. 1982 Progressive mineralization pattern of developing enamel during the maturation stage. Journal of Dental Research, 61, 1532–1542.

Teivens, A., Mornstad, H., Noren, J.G., Gidlund, E. 1996. Enamel incremental lines as recorders for disease in infancy and their relation to the diagnosis of SIDS. Forensic Science International, 81:17–183

Tieszen, L.L., Fagre, T., 1993. Effect of diet quality and composition on the isotopic composition of respiratory CO2, bone collagen, bioapatite, and soft tissues. In: Lambert, J.B., Norr, L. (Eds.), Prehistoric Human Bone and Archaeology at the Molecular Level. Springer-Verlag, pp. 121-155.

Thomas, R.F., 2003. Enamel defects, well-being and mortality in a medieval Danish village. Ph.D. Dissertation, Pennsylvania State University.

Trayler, R. B., and Kohn, M. J. 2017. Tooth enamel maturation re-equilibrates oxygen isotope compositions and supports simple sampling methods. Geochimica et Cosmochimica Acta, 198, 32–47. http://doi.org/10.1016/j.gca.2016.10.023.

Tsukahara, T. 1993. Lions eat chimpanzees: the first evidence of predation by lions on wild chimpanzees. American Journal of Primatology, 29, 1-11.

Tsutaya, T., and Yoneda, M. 2014. Reconstruction of breastfeeding and weaning practices using stable isotope and trace element analyses: A review. American Journal of Physical Anthropology, 00 (October 2014), 2–21. http://doi.org/10.1002/ajpa.22657.

Watts, D. P. 1991. Mountain gorilla reproduction and sexual behaviour. American Journal of Primatology, 24:211-226.

Watts, D. P., Muller, M. N., Amsler, S. J., Mbabazi, G., and Mitani, J. C. 2006. Lethal Intergroup Aggression by Chimpanzees in Kibale National Park , Uganda, American Journal of Primatology, 180 (February 2005), 161–180. http://doi.org/10.1002/ajpa.

Watts, D.P., Potts, K.B., Lwanga, J.S., Mitani, J.C. 2012. Diet of chimpanzees (*Pan troglodytes schweinfurthii*) at Ngogo, Kibale National Park, Uganda, 1. Diet composition and diversity. American Journal of Primatology, 74, 114-129.

Williams, J., Lonsdorf, E., Wilson, M., Schumacher-Stankey, J., Goodall, J., Pusey, A., 2008. Causes of death in the Kasekela chimpanzees of Gombe National Park, Tanzania. American Journal of Primatology, 70, 766-777.

Wood, B. M., Watts, D. P., Mitani, J. C., and Langergraber, K. E. 2017. Favorable ecological circumstances promote life expectancy in chimpanzees similar to that of human hunter-gatherers. Journal of Human Evolution, 105, 41-56. http://doi.org/10.1016/j.jhevol.2017.01.003.

Chapter 4: Isotopic Variability Within the Tissues of *Pan troglodytes schweinfurthii* Informs Efforts at Fossil Hominin Dietary Reconstruction and Underscores the Need for Habitat-specific Plant Isotope Studies

Abstract: The importance of the role of diet, and changes in diet, in hominin evolution, cannot be overemphasized. One of the main sources of information about diet in the fossil record is the biogenic isotopic signal in the bioapatite of tooth enamel, preserved in specimens millions of years old due to the resistance of enamel to diagenetic alteration. The stable carbon and oxygen isotope ($\delta^{13}C$ and $\delta^{18}O$) values of the enamel of extant taxa, and knowledge of their diets, are used as a comparative guide for interpreting the isotopic signature and diet of a fossil organism.

This study attempts to address how sources of variation in diet, and the complex ways that dietary items are incorporated into the tissues of the body in living taxa, complicate direct attempts to use stable isotopic analysis of enamel apatite to characterize the diets of fossil taxa, including hominins. Isotopic analyses of various tissues from a sample of Ugandan chimpanzees (*Pan troglodytes schweinfurthii*), from several *Pan* communities within Kibale National Park as well as one from Bwindi Impenetrable National Park. Tissue included in this study are: (1) bone collagen, (2) bone apatite, (3) hair keratin, (4) enamel apatite, and (5) dentine. Baseline levels of isotopic variation are established for each tissue type, and bulk isotopic offsets between tissues of the same individual, and among all individuals from the sample, are determined and compared with the $\delta^{13}C$, $\delta^{18}O$, and $\delta^{15}N$ values of chimpanzee tissues from previous studies. Serial sampling of enamel apatite reveals intra-tooth $\delta^{13}C$ and $\delta^{18}O$ variability, potentially reflecting sub-annual dietary and environmental variation. Dentine inter-tooth sampling reveals $\delta^{13}C$ and

$\delta^{15}N$ differences of up to 4‰, possibly related to changes in diet or climate during dentine development. "Total dietary" $\delta^{13}C$ and $\delta^{15}N$ input values are proposed based on published plant isotopic data, and novel *Pan*-specific diet-to-tissue offsets are calculated, resulting in a proposed diet-to-enamel $\delta^{13}C_{apatite}$ value of 12.3‰ for the Ngogo chimpanzees. Implications for the application of these data to studies of fossil hominin dietary reconstruction are considered, as well as their relevance to studies of weaning and overall life history evolution. Diet-to-tissue offset values are calculated for the other available tissues, as well, and while these cannot be used directly in studies of fossil dietary reconstruction, their relevance for increasing sample sizes of comparative isotopic data from extant taxa, is discussed.

Introduction: The diet of a primate has important implications for nearly all aspects of its life. The items in an organism's diet are products of the local habitat and ecological conditions, and it is to these conditions that the organism must adapt in terms of its locomotion, its reproductive behavior, its territory use, its social structure, its life history, its relationships with sympatric taxa, and its place within an ever-changing environment. Such considerations are central to studies of hominin evolution, and while changing and variable environments may be drivers of evolution, it is the studies of diet, dietary changes, and the diverse ways that dietary components are incorporated into tissues of the body, that provide a window onto the many selective pressures that have shaped our lineage and that ultimately shape all life.

Before interpreting the diets of fossil taxa, it is necessary to develop an understanding of how the isotopic signatures of dietary items are altered by the processes of ingestion, digestion, metabolism, and eventual routing to, and incorporation into, different body tissues. Unfortunately these processes are not uniform or universal across organisms, resulting in biased

uptake of different isotopes (fractionation), which complicate reconstructions of dietary inputs based on the isotopic signature of specific tissues. This study attempts to quantify the nature of these fractionation processes so we can reconstruct the dietary patterns and environments for fossil taxa using isotopic analyses.

Background: The three elements for which isotopes are most commonly used in studies of paleodiet and paleoclimate are carbon, nitrogen, and oxygen. Relative isotopic abundances of these elements can inform us about an organism's total dietary content (Kellner and Schoeninger, 2010), their protein intake (Krueger and Sullivan, 1984; Ambrose and Norr, 1993; Tieszen and Fagre, 1993; Froehle et al., 2012), and their sources of water, respectively (Luz et al., 1984; Luz and Kolodny, 1989; Bryant and Froelich, 1995). The relationship between the amount of the heavier isotope to the amount of the lighter one is expressed as $\delta^{13}C$, $\delta^{15}N$, and $\delta^{18}O$. While $\delta^{15}N$ can be obtained from sources like bone collagen, dentine, and hair (Crowley, 2008), these substrates do not preserve well in the fossil record. We must look to the enamel apatite of fossil teeth for isotopic signatures that do not significantly alter once they have been incorporated into the tissue, and can thus be retrieved even millions of years after an organism's death. From enamel apatite we can obtain $\delta^{13}C$ and $\delta^{18}O$ signatures, and these isotopes have been sampled from numerous fossil taxa in attempts to reconstruct paleodiets and paleoclimates. The enamel of extant taxa has also been extensively sampled, and given what we know and can observe about a living organism's diet and local habitat, this allows for the development of a modern template for interpreting the fossil record.

Carbon: Carbon isotopes used in dietary reconstruction are ^{12}C and ^{13}C and are found in

different proportions in the plants that incorporate them into their tissues during photosynthesis. ^{12}C makes up the bulk of the carbon found in all plants, since they preferentially incorporate this lighter and more abundant isotope from atmospheric CO_2 (O'Leary, 1988). Almost all dicots (which include most fruits, trees, shrubs, and temperate grasses) use the Calvin-Benson (C_3) photosynthetic pathway, a process which discriminates against the heavy isotope ^{13}C, resulting plant tissue enriched in ^{12}C. C_4 plants (many monocots, like tropical grasses and sedges), however, use the Hatch-Slack photosynthetic pathway (Ehleringer & Monson, 1993), which discriminates less against the heavier isotope during photosynthesis, resulting in a significantly higher amount of ^{13}C in their tissues relative to C_3 plants. There are also succulents that use the CAM photosynthetic pathway, or Crassulacean Acid Metabolism, and the $\delta^{13}C$ of these plants tends to fall in between those of C_3 and C_4 plants. The $\delta^{13}C$ of C_3 plants ranges from -22‰ to -35‰, C_4 pants range from -9‰ to -14‰, and CAM plant $\delta^{13}C$ values falling in the intermediate range, or slightly closer to the C_4 range. Most primates live in tropical forests where C_3 vegetation predominates (Carlson and Kingston, 2014), and so it is important to characterize variation in the $\delta^{13}C$ values of C_3 plants in these biomes.

Nitrogen: The nitrogen values in plants reflect plant physiology, nutrient availability, and also interactions with specific bacteria (Handley et al. 1999; Marshall et al. 2007; Werner and Schmidt 2002). Plants generally obtain their nitrogen directly from soil nitrate, and in these cases, the $\delta^{15}N$ values are greater than 0‰, although some plant $\delta^{15}N$ values can be <0‰ if they grow in particularly moist forests (Handley et al. 1999). Certain legumes also contain N-fixing bacteria that fix nitrogen directly from the atmosphere, making the $\delta^{15}N$ of such plants close to 0‰, though not all plants that have these bacteria fix nitrogen in such a way (Codron et al. 2005; Muzuka 1999). CAM plants can be higher in $\delta^{15}N$ values than sympatric C_3 and C_4 plants

(Codron et al. 2006; Crowley et al. 2011), but also different plant parts can vary in their $\delta^{15}N$ values (Werner and Schmidt, 2002). As an example, $\delta^{15}N$ values of a preferred chimpanzee dietary item at Ngogo, *Pterygota mildbraedii*, range from 1.8 ± 0.9‰ in the flowers and cambium to 3.6 ± 1.1‰ in the seeds. There is an even greater difference of 2.1‰ between the $\delta^{15}N$ values of the fruit and the flowers of the *Cordia millenii* plant from Ngogo (Carlson, 2011).

Oxygen: A plant's water sources is mirrored in its $\delta^{18}O$ values, and such sources can be groudwater or a mix of surface water and the precipitation available in the area. Most parts of a plant tend not to be enriched in $\delta^{18}O$ relative to the water they take in, but evapotranspiration can result in the leaf $\delta^{18}O$ values being somewhat more enriched in ^{18}O in more arid climates (Barbour, 2007). $\delta^{18}O$ values of an animal's tissues reflect the water that it drinks and the water in the foods it eats, as well as the oxygen released metabolically (Bryant and Frölich 1995; Fricke and O'Neil 1996; Luz and Kolodny 1985).

Dietary information accessible through different tissues*:*

Enamel: Hydroxyapatite, $[Ca_{10}(PO_4, CO_3)_6)(OH, CO_3)_2]$ is the main component of tooth enamel, and its highly inorganic, non-porous composition is what allows it to retain an accurate signal of dietary ($\delta^{13}C$) and water source ($\delta^{18}O$) inputs once it is formed (Kohn and Cerling 2002; Lee-Thorp and van der Merwe 1991). Carbon isotope values of enamel carbonate reflects that of blood biocarbonate, which is an integrated signal of the total dietary carbon (Passey et al. 2005). It is possible to obtain information about gestational diet and in-vitro water sources from the $\delta^{18}O$ signature of enamel that forms in deciduous teeth, or during the earliest part of permanent M1 formation (Fricke and O'Neil 1996) Signals from enamel forming during the exclusive nursing period or through the weaning process can also be detected using enamel apatite.

Dentine: Dentine is also made up of hydroxyapatite within a collagen fiber matrix, but it is much less mineralized than enamel. Once primary dentine is formed, it does not remodel during life, and so retains a fairly reliable record of early diet (Beaumont et al., 2013). Secondary dentine does form on the inner wall of the dentine that surrounds the pulp cavity, and tertiary dentine forms in areas of damage to the crown, or in response to caries (Nanci, 2003). However, sampling of both of these areas of dentine can be avoided or removed before a tooth is sampled, allowing the early dietary information from the primary dentine to be accessed.

Dentine sampling has been used to access a number of types of information. Seasonal dietary variations have been accessed in a several taxa through incremental sampling of dentine that follows the pattern of formation, and this type of sampling can produce fairly high-resolution records of changes in diet and metabolism (Balasse et al. 2001; Kirsanow et al. 2008; Wiedemann-Bidlack et al. 2008). Dentine is also often used to investigate dietary changes related to the weaning process, due to trophic level differences detectible in the $\delta^{15}N$ values between dentine formed while an infant is breastfeeding and that formed later in life (Fahy, et al., 2014). Trophic level differences between infants' forming tissues and mothers' breastmilk can also be noted in the $\delta^{13}C$ from dentine, although this isotopic difference is smaller than that of $\delta^{15}N$ (Wright and Schwarcz, 1999).

Bone collagen: As in dentine and hair keratin, the carbon isotope values ($\delta^{13}C$) in bone collagen are related to many parts of the diet, though they do reflect the protein component more heavily than carbon isotopes from other sources. (Froehle et al. 2010; Hedges and van Klinken 2000; Jim et al. 2004). The nitrogen values $\delta^{15}N$ also reflect protein in the diet primarily. Collagen experiences turnover during an organism's life (Gannes et al. 1998), so at any given time, the bone collagen content is likely to reflect many years of dietary signal.

Bone apatite: The carbon isotopic values from bone apatite reflect the isotopic signatures of lipids, carbohydrates, and proteins in the diet (Jim et al. 2004), while the oxygen isotopes reflect more of the signal of the imbibed water (Koch, 2007). Bone apatite also experiences turnover throughout life, so it will reflect a version of the adult dietary signal, unlike the early signal reflected in tooth enamel and dentine.

Hair keratin: Much like bone collagen, keratin $\delta^{13}C$ values reflect the whole diet, while keratin $\delta^{15}N$ values predominantly reflect protein (Gannes et al. 1998; Hedges and van Klinken 2000; Martínez del Rio et al. 2009). Keratin is like enamel in that once it is formed, the isotopic values are maintained, and it doesn't reform or turnover within the strand (Martínez del Rio et al. 2009). Also like enamel, keratin exibits a time-delay in terms of the dietary shifts it records, due to isotopic inertia, which may mask short-term shifts in diet (Sponheimer et al. 2003). Seasonal dietary shifts should be discernible, nevertheless (Dammhahn and Kappeler 2010; O'Brien and Wooller 2007). In addition, the collection and analyses of hair is non-invasive relative to teeth and bone.

Stable isotope use in extant ape dietary reconstruction

Studies that have analyzed various isotopes from different tissues in chimpanzees, are listed below. The isotope values are included also, and entries have been grouped by tissue type so that values may be more easily compared.

Table 12: Isotopic values for *Pan troglodytes* tissues compared between this study and other studies

Taxo/ site collected	**Tissue**	**$\delta^{13}C$ ‰ (average)**	**$\delta^{15}N$ ‰ (average)**	**$\delta^{18}O$ ‰ (average)**	**Study**
Pan troglodytes schweinfurthii/ Bwindi	Hair keratin	-24.8 (n = 10)	5.8	N/A	Oelze et al., 2016
Pan troglodytes schweinfurthii/ Ngogo/Wantabu	Hair keratin	-23.4 (n = 2)	7.67	N/A	This study
Pan troglodytes verus/ Taï	Hair keratin	-24.3 (n = 30)	7.4	N/A	Oelze et al., 2016
Pan troglodytes schweinfurthii/ Bwindi	Bone apatite	-17.31 (n = 1)	N/A	0.28	This study
Pan troglodytes schweinfurthii/ Kibale	Bone apatite	-14.5 (n = 7)	N/A	-1.1	This study
Pan troglodytes verus/ Taï	Bone apatite	-16.9 ± 0.4 (corrected*) (n = 18)	N/A	-6.5	Fahy et al., 2015
Pan troglodytes schweinfurthii/ Bwind*i*	Enamel apatite	-15.49 (n = 1)	N/A	0.37	This study
Pan troglodytes verus/ Ganta	Enamel apatite M1, M3	-17.8 ± 0.4 (n = 33), -17.3 ± 0.9 (n = 30) (corrected‡)	N/A	-2.4 ± 0.6 (n = 33), -2.6 ±0.4	Smith et al., 2010
Pan troglodytes verus/ Taï	Enamel apatite	-16.1 ± 0.4 (corrected*) (n = 14)	N/A	-3.2 ± 1.4	Fahy et al., 2015
Pan troglodytes schweinfurthii/ Kibale	Enamel apatite	-14.5 (n = 13)	N/A	0.7 ± 0.4	Nelson, 2013
Pan troglodytes/ Ituri	Enamel apatite	-14.5 (n = 1)	N/A	-1.1	Cerling at al., 2004
Pan troglodytes/ Itombwe	Enamel apatite	-13.5 (n = 1)	N/A	-3.1	Cerling et al., 2013
Pan troglodytes verus/ Taï	Bone collagen	-21.6 (corrected*) (n = 22)	8.0 (n = 22)	N/A	Fahy et al., 2015
Pan troglodytes verus/ Ganta	Bone collagen	-22.6 ± 0.5 (corrected‡) (n = 36)	7.1 ± 0.7 (n = 21)	N/A	Smith et al., 2010

Table 12: (*corrected for modern atmospheric CO_2 using +1.5‰ after Trudinger et al., 1999) (‡corrected for modern atmospheric CO_2 using -1.1‰ after Hoppe et al., 2006)

Stable isotope use in fossil taxa dietary reconstruction

The enamel apatite of numerous fossil hominins has been sampled and subjected to isotopic analysis, with some of their $\delta^{13}C$ values listed in Table 13.

Table 13: $\delta^{13}C_{enamel\ apatite}$ values determined by other studies for 12 hominin taxa

Taxon	**$\delta^{13}C$**	**Study**
Paranthropus boisei	-1.2 ± 1.1‰	Cerling et al., 2011b; Cerling et al., 2013; van der Merwe et al., 2008
Australopithecus bahrelghazali	-2.6 ± 1.8‰	Lee-Thorp et al., 2012
Paranthropus aethiopicus	-3.7 ± 2.2‰	Cerling et al., 2013
Homo sapiens	-4.8 ± 2.3‰	Cerling et al., 2013
Kenyanthropus platyops	-6.2 ± 2.7‰	Cerling et al., 2013
Homo spp	-6.3 ± 1.9‰	Cerling et al., 2013; Lee-Thorp et al., 2000; van der Merwe et al., 2008
Australopithecus africanus	-7.1 ± 1.8‰	Lee-Thorp et al., 2010; Sponheimer and Lee-Thorp, 1999; Sponheimer et al., 2005; Sponheimer et al., 2013; van der Merwe et al., 2003
Paranthropus robustus	-7.5 ± 1.2‰	Lee-Thorp et al., 1994; Lee-Thorp et al., 2000; Sponheimer et al., 2005; Sponheimer et al., 2006a
Australopithecus afarensis	-7.5 ± 2.6‰	Wynn et al., 2013
Ardipithecus ramidus	-10.3 ± 0.9‰	White et al., 2009
Australopithecus anamensis	-10.9 ±0.8‰	Cerling et al., 2013
Australopithecus sediba	-11.7 ± 0.1‰	Henry et al., 2012

These enamel $\delta^{13}C$ values have led researchers to reconstruct the isotopic paleodiets of these hominin taxa as ranging from about -26‰ for *Au. sediba* to -15‰ in *P. boisei.* These interpretations have traditionally used a diet-to-apatite enrichment factor of 14‰, and dietary values are calculated by adding -14‰ to the $\delta^{13}C_{enamel}$ values, which represent the ratio of possible C_3/C_4 resources in their diets (Cerling and Harris, 1999). A potential problem with this approach is that the 14‰ enrichment factor derives from controlled studies of large-bodied ruminating herbivores (Passey et al., 2005). This enamel-to-diet offset is, to a large extent, a function of gut fermentation and it has been suggested that primates with generally higher quality diets may have diet-enamel offsets as low as 10‰ (Smith et al., 2010). Controlled feeding

experiments to obtain such an enrichment factor in primates, however, are not feasible given the time frame required. Studies of detailed chimpanzee plant food composition and isotopic values (e.g. Carlson and Kingston, 2014; Crowley and Carlson, 2016) have attempted to establish isotopic baseline values for a potential chimpanzee dietary input, and these studies set the stage for determining a true diet-to-enamel apatite enrichment factor for chimpanzees (which also is likely to vary by the types of dietary plants, elevation, canopy architecture, and climatic patterns at the sites (Carlson and Kingston, 2014)).

Sources of variability

Interpreting intra-tissue variability: In order to know the period of time in an organism's life that is being sampled and analyzed, it is imperative to know about the age, timing, and duration of tissue formation, as well as turnover rates, where applicable. It is useful to consider how variable $\delta^{13}C$ and $\delta^{18}O$ values may be from serial enamel samples of the same chimpanzee tooth. Once this is assessed it can address whether such variability is conflated when just analyzing bulk samples that average the isotopic composition of the whole tooth.

Intra-individual variability: Variation between similar tissues of different teeth of the same individual (i.e. the enamel of one individual's M2 and M3) will be obscured if only one tooth type is sampled, or if multiple teeth forming at the same time are sampled (i.e. a deciduous tooth and the M1, or the P4 and the M2 in some taxa). If this source of variability isn't taken into account, the overall inferred isotopic signal for that individual, or population, or taxon based on a single tooth may not be representative of the average adult diet.

Inter-individual variability: It is important to consider how variable the isotopic signature of a given tissue is between as many members of a population as possible. If we can establish ranges

of intra-population variability in $\delta^{13}C$ and $\delta^{18}O$ in a specific chimpanzee tissue (i.e. an M3), we can better develop inferences about the paleodiets of fossil hominin based upon a single tooth or a single tooth type.

Inter-tissue isotopic routing: There are numerous tissue sources for the each of the isotopes (i.e. $\delta^{15}N$ in hair, dentine, bone collagen, and feces, $\delta^{13}C$ in bone collagen, bone apatite, enamel apatite, dentine, and hair, and $\delta^{18}O$ in bone apatite and enamel apatite) and they usually cannot all be obtained from study subjects at different sites. Therefore, it is useful to be able to compare the general patterns of isotopic enrichment or depletions of one element between the tissues to assess variation in offsets. The consistency with which isotopes are routed to different tissues, however, is not well established, and may vary extensively between sites.

Diet-to-tissue fractionation variability: Instead of assuming a 14‰ $\delta^{13}C$ fractionation factor between diet and enamel apatite, as has been determined for ungulates (Cerling and Harris, 1999; Passey and Cerling, 2002), it is necessary to assess how the isotopic variability in different plant parts of different dietary items (at different elevations, from different levels in the canopy, in different proportions), affect a "total dietary input" isotopic measure and how this manifests in different tissues. Based on the variability of these factors in the chimpanzees in this sample, and output values in the different tissues of these individuals, we need to explore ways to estimate a reasonable diet-to-enamel apatite fractionation factor for *Pan*. Once this is accomplished, it is worth noting how this empirically determined fractionation factor may affect interpretations of fossil hominin diets based on $\delta^{13}C_{enamel}$ values that assume a 14‰ fractionation factor.

Inter-population dietary variability: This can be fully assessed only if the isotopic contents of the various plant food items (and ideally, the non-plant items, too) and their % feeding time can be

recorded for other populations. Without the diet information, comparisons can still be made between tissue outputs for members of different populations. However, as Carlson and Crowley (2016) demonstrated, some of the same plant types that grow within the chimpanzee site of Ngogo also grow at Bwindi, but their isotopic compositions are different due to the different environmental contexts represented by the two sites. Feeding time spent on each plant item is likely to be different too, so it becomes increasingly difficult to identify fractionation levels between diets and tissues of chimpanzees from different populations without a comprehensive characterization of the local isotopic baseline(s).

Materials: Samples of several body tissues of one infant and eight adult chimpanzees (*Pan troglodytes schweinfurthii)* were analyzed in this study (Table 14). Eight of the chimpanzees (seven adults and one infant) were from Kibale National Park, Uganda, and one adult was from Bwindi Impenetrable National Park, Uganda. The remains of all individuals are housed at Makerere University's Zoology Museum (MUZM) in Kampala, Uganda, with the exception of the infant chimpanzee (NG0-57), which is housed in the University of Michigan's Department of Anthropology in Ann Arbor, Michigan.

Identifying data for the chimpanzees in this study are as follows: Approximate dates of death are known for seven of the nine chimpanzees. Dates of birth have been estimated for the five Ngogo chimpanzees using genetic data, which provides geneological information regarding individual relationships, combined with observations of the behavior and physical condition of animals when first observed (Wood et al., 2017). Six of the eight adult individuals are male, while one Ngogo chimpanzee and the single individual from Bwindi are female. The sex of the infant is unkown. All of the individuals died between 2002 and 2014. NG001 and NG002 are

unnamed extragroup males killed by the Ngogo males during episodes of intergroup aggression (Watts et al., 2006). Another male "Grappelli" (NG003), died as a result of a within-group coalitionary attack (Watts, 2004). "Stravinsky" (NG004) was an Ngogo male who was a victim of intergroup aggression, and he was the maternal brother of "Tatum" (NG005), whose cause of death is unknown (Ngogo Chimpanzee Project unpublished data). "Webster" (NG013) may have died from respiratory disease (Wood et al., 2017). Causes of death for the Bwindi female (MUZM2625) and the single Ngogo female "Carmen" (NG012) are not known.

Rib bone samples approximately two centimeters in length were obtained from five of the adult individuals. For those chimpanzees for which ribs were unavailable, samples were taken from available bone sources. For the Bwindi specimen (MUZM) the bone came from the mandibular ramus, for NG004 it came from an unidentified bone fragment, and for NG057, it came from the occipital bone. For the NG004 sample, the bone had been too degraded and diagenetically altered to produce results (NG004). Finally, for individual NG003, no bone was available and only teeth were sampled. Bone samples were processed and partitioned for apatite and collagen isotopic analysis protocols.

In a previous study (Malone, Chapter 2) the extraction of three teeth from each of the eight adult chimpanzees was described. In this study, the M2s and M3s (and in a few cases the P4s) were selected for bulk enamel and dentine sampling as well as for serial enamel sampling. (In two cases of dentine sampling, the M1 was used intead of the M2 or P4 if it was all that was available.) Enamel and dentine preparation and sampling are described below. Hair samples were also obtained for two of the adult chimpanzees in our sample (NG002 and NG012) and these represent an extra-group male and an Ngogo female.

Table 14: Chimpanzees included and tissues sampled in this study

ID #	Bone collagen	Bone apatite	Enamel apatite	Dentine	Hair keratin (bulk)	Enamel serial samples	Dentine multi-tooth samples	Hair serial samples
NG001	X	X	X	X	—	X	—	—
NG002	X	X	X	X	X	X	X	—
NG003	—	—	X	X	—	X	X	—
NG004	—	—	X	X	—	X	X	—
NG005	X	X	X	X	—	X	X	—
NG012	X	X	X	X	X	X	X	X
NG013	X	X	X	X	—	X	—	—
NG057*	X	X	X	—	—	—	—	—
MUZM	X	X	X	X	—	X	X	—

Table 14: ID # is the Accession number of the individual chimpanzees ("NG" refers to an Ngogo community member or an extra-group male killed by Ngogo chimpanzees, MUZM refers to Makerere University Zoology Museum) X refers to a tissue being present and — refers to absent tissues. * infant Ngogo chimpanzee

Methods

Bone sample preparation: The ~ 2cm bone samples were all ultrasonicated in distilled H_20 for 10 minutes, removed and gently cleaned with a soft brush to get rid of surface debris. Samples were then ultrasonicated a second time to remove any additional contaminating surface particles, and then allowed to air dry in a covered container overnight. They were then placed in an oven at 50°C for eight hours. They were weighed and they were then divided into four subsamples in order to have enough mass to run bone collagen analysis, bone apatite analysis, and to have sufficient sample to archive. Final dried weights of the bone apatite samples varied from 6-15mg, and each of the bone collagen samples weighed at least 30mg, in order to ensure sufficient collagen could be extracted from each sample.

Bone apatite extraction: The bone apatite samples were carefully crushed with a mortar and pestle, and samples were reweighed to assess any loss due to the powdering process. Each sample still weighted at least 5mg. Bone carbonate powdered samples were treated with 50% NaOCl (bleach) for 16 hours. Samples were rinsed to neutral with dH_2O four times, and fresh

NaOCl added each each rinse to neutral. Then 0.2 M Ca-buffered acetic acid was added to the samples and let sit for six hours. Samples were rinsed to neutral again, and the final round of dH_2O was pipetted out and the samples were placed into a freeze-dryer for two days, after which time they were removed and shipped to the University of Florida's Stable Isotope Laboratory, as were all other samples described below.

Bone collagen extraction: Approximately 15-18 ml of 1.0 M HCl was added to the intact (unpowdered) bone sample in a 20ml vial and agitated thoroughly. The lid was left slightly open to let out the gas produced by the demineralization reaction. After 18 hours, the acid was pipetted out and replaced with fresh HCl. These steps were repeated until the bone fraction within the vial was spongy. Spongy samples were then transferred into 2 mL tubes and rinsed to neutral with dH_2O. Tubes were then centrifuged for 10 minutes, the dH_2O was pipetted out, and fresh dH_2O was added to the tubes. This step was repeated 3~ 4 times, checking with pH strips to make sure neutral was achieved.

Approximately 2 ml 0.125 NaOH was added to the tube with the neutralized collagen solution and agitated thoroughly. The samples were let sit for 16 hours. The solution was then rinsed to neutral with dH_2O as described above. Samples were then transferred to glass vials and put in the oven on 95°C for 4~5 hours. Several more drops of 1M HCl were added to the vial to completely dissolve the collagen and the samples were returned to the oven for another 4~5 hours. Contents were transferred back to the clean tubes, which were centrifuged for ~15-20 minutes with the caps loosened as the pressure build-up from the warm solution may cause the tube to explode.

For each sample, only the solution was then transferred from the tube back to its vial using a pipette. Vials, without lids on, were then placed in the drying oven on 65°C. After samples had condensed to ~2ml, the vials were removed from the oven, let cool, and lids put back on. They were then placed into the freezer. After samples were completely frozen, lids were loosened slightly and vials were placed in a freeze dryer for ~ 2 days until the contents of the vial appeared as dried bubbles. Vials were removed from the freeze dryer, and shipped for analysis.

Enamel sample preparation: As described in a previous study (Malone, Chapter 1), the M2s (or P4s) and M3s of the eight adult chimpanzees were embedded in epoxy, sectioned through the mesial cusps, and then a thin section was made from one half of the sectioned block. The preparation of these thin sections has been described elsewhere, but they were ultimately imaged and measured to create grids dividing up the cut surface into temporally distinct regions that were also aged within each tooth. A second slightly thicker section was made from the opposing face of the block, using minimal lapping and polishing before creating the slide, so as to lose as little additional surface as possible. This was so that the image created form the thinner section would reflect the same time period as that of the thicker section, as much as possible. The dicing grid was then superimposed onto a reflected light image of the thicker section (transmitted light would not pass through the section thickness), and measurements were made of the angles of the grind and the dimensions of the individual diced units to be extracted. The periodic and accentuated structures were used as a guide to divide the crown into temporally distinct units, and the grid was used to program an ADT 7100 dicing saw to mechanically separate these individual blocks of enamel and permit them to be individually extracted and aged. Individual units were far smaller than the minimum weight threshold for conducting GC-IRMS, so several

adjacent units were combined to form this minimum weight, while making sure the temporal distinction between samples was maintained. Diced units from each of the two samples from each of the two teeth from each of the eight chimpanzees) were crushed into powder using a marble rolling pin with the diced enamel units placed between two sheets of sampling paper, in order to minimize loss of powder. Weights of the diced units before crushing and weights of the powdered samples after they were crushed, resulted in very little loss.

Powdered samples were then subjected to 30% hydrogen peroxide pretreatment. The hydrogen peroxide was decanted and the powder was rinsed twice with deionized water. After rinsing, the powders were treated with a 1.0 M Ca-acetate – acetic acid buffer overnight to remove labile carbonates. After pretreatment the powders were rinsed three times with deionized water, centrifuging and decanting between rinses, and dried in an oven at 40 °C. Samples were then removed and shipped for analysis.

Dentine sample preparation: The protocol for extracting the collagen portion of the dentine was modified from that of Beaumont et al. (2013). The powdered dentine samples were demineralized in 0.5M hydrochloric acid at about 4°C. The samples demineralized quickly, within ~5 days. The demineralized samples were then rinsed with deionized water and placed in sealed microtubes with a pH 3 hydrochloric acid solution at 70°C for 24 h to denature the collagen. The samples were frozen and then freeze-dried for 2 days before the samples were removed and shipped for analysis.

Hair sample preparation: The two bulk hair samples were rinsed with dH_2O and then treated with chloroform to remove lipids and any external contaminants before being placed in vials to be sampled. The hair used for serial sampling was treated in the same way, but then also

carefully cut up into five approximately equal pieces (~1.5 cm each) and put into labeled vials according to their order of growth (sample 1 was the oldest, from the hair tip, and sample 5 was the newest, from the bulb end.)

Instrumentation: The organics were analyzed using a Thermo Electron DeltaV Advantage isotope ratio mass spectrometer, coupled with a ConFlo II interface, linked to a Carlo Erba NA 1500 CNHS Elemental Analyzer at the University of Florida Geosciences Stable Isotopic Lab. 600-800 micrograms of sample were loaded into tin capsules and placed in a 50-position automated Zero Blank sample carousel on a Carlo Erba NA1500 CNS elemental analyzer. After combustion in a quartz column at 1020 C in an oxygen-rich atmosphere, the sample gas was transported in a He carrier stream and passed through a hot reduction column (650 oC) consisting of elemental copper to remove oxygen. The effluent stream then passed through a chemical (magnesium perchlorate) trap to remove water followed by a 0.7 meter GC column at 120 C to separate N2 from CO2. The sample gas next passed into a ConFlo II interface and into the inlet of a Thermo Electron Delta V Advantage isotope ratio mass spectrometer running in continuous flow mode where the sample gas was measured relative to laboratory reference N2 and CO2 gases. All carbon isotopic results are expressed in standard delta notation relative to VPDB. All nitrogen isotopic results are expressed in standard delta notation relative to AIR.

The carbonates were processed using a Finnigan-MAT 252 isotope ratio mass spectrometer coupled with a Kiel III carbonate preparation device. (Protocol from Jason Curtis, pers. comm.)

Results

The isotopic results are grouped here in the discussion to highlight the numerous sources of potential variability based on tissues type in the same chimpanzee individuals, variation within the tissue itself, the isotope in question, the sampling methods used, and the unknown actual dietary contributions. The results for the chimpanzee samples are divided into subsamples, since Kibale Forest is where the Ngogo chimpanzees and the extragroup males derive, and the Bwindi individual is from a different forest located nearby. One subsample is therefore called "Kibale + Bwindi", and the Kibale chimpanzees are further divided into "Ngogo chimpanzees", and "Ngogo adult chimpanzees".

The small number of individuals being sampled here allows only for general trends to be observed along with some measures of central tendency and dispersion (i.e., means, ranges, and standard deviations). Results are divided into: (1) ***intra-tissue isotopic variation***, in which serial sampling methods for several tissue types reveal subtle variation within the same tissue, either tooth enamel or hair; (2) ***intra-individual isotopic variation***, in which dentine samples from two teeth of the same individuals are compared; 3) ***inter-tissue isotopic variation*** in which bulk isotopic offset values between different tissues are presented; 4) ***variation due to unknown diet-to-tissue isotopic fractionation factors***, in which this issue is explored using known isotopic values from 35 of the most commonly-eaten Ngogo chimpanzee food items and observed times spent feeding on each, to attempt to model "total diet" $\delta^{13}C$ and $\delta^{15}N$ input values; and (5) ***inter-individual differences in bulk tissue values.***

Intra-tissue (serial) isotopic variation

Hair: The individual that was serially sampled (NG002) was divided into five samples of approximately 1.5 cm each, and each weighing between 200 and 280 micrograms. These samples revealed a difference of 0.46‰ between the highest and lowest $\delta^{15}N$ values, though the calculated bulk value for the serially sampled hair (8.31‰) differed from the bulk value from another hair from that same individual (7.46‰) by 0.85‰ (Table 17). For these same hair samples the $\delta^{13}C$ values differed by 0.91‰, and the serial samples of NG002 differed by 0.45‰, while the calculated bulk value for the serial samples, and that for the bulk sample for a different hair from the same individual, differed by 0.41‰ (Table 17).

Enamel variation: The enamel of nine chimpanzees were sampled (Table 15/Figure 24). For individual "NG005", six enamel apatite samples were obtained, three each from the P4 and M3, but for most of the other chimpanzees only four samples couple be taken, and these were either from the M2 and M3 or from the P4 and the M3. For three of the individuals, "NG012", "NG013", and "MUZM", only three samples could be obtained, two from one tooth and one from the other, and in the infant chimpanzee, only one sample could be obtained, and it was from the deciduous first molar (dm1) (Table 15).

The enamel apatite $\delta^{13}C$ values range throughout this sample from -14.3‰ to -17.0‰, a difference of 2.7‰. The $\delta^{18}O$ values ranged from -2.0 to 1.2‰, a difference of 3.1‰. However, this range is primarily a result of the different values for the infant chimpanzee (see Discussion). For the adults only, the overall $\delta^{13}C$ range in slightly less, at -14.3 to -16.0‰, a difference of 1.7‰, and the adult $\delta^{18}O$ range is 1.2 to -1.4‰, a range of 2.5‰. The greatest difference in $\delta^{13}C$

Table 15: Serial $\delta^{13}C$ and $\delta^{18}O$ values from enamel apatite of nine chimpanzees

Individual/tooth.sample#	Enamel apatite $\delta^{13}C$ (‰)	Enamel apatite $\delta^{18}O$ (‰)
NG001 M2.1	**-15.8**	**-0.2**
NG001 M2.2	-15.8	0.3
NG001 M3.1	-15.5	-0.3
NG001 M3.2	-15.7	0.1
NG002 M2.1	**-14.3**	**-1.1**
NG002 M2.2	-14.4	-1.4
NG002 M3.1	-14.5	-1.3
NG002 M3.2	-14.9	0.4
NG003 M2.1	**-14.6**	**-0.3**
NG003 M2.2	-15.1	-0.6
NG003 M3.1	-14.7	0.1
NG003 M3.2	-15.9	-1.1
NG004 M2.1	**-15.6**	**-1.2**
NG004 M2.2	-14.9	0.1
NG004 M3.1	-15.2	-0.9
NG004 M3.2	-14.7	-0.1
NG005 P4.1	**-16.0**	**0.9**
NG005 P4.2	-15.3	0.5
NG005 P4.3	-15.3	0.9
NG005 M3.1	-15.4	1.2
NG005 M3.2	-15.7	0.9
NG005 M3.3	-15.2	0.7
NG012 M2.1	**-15.0**	**0.5**
NG012 M3.1	-15.3	1.0
NG012 M3.2	-15.7	0.7
NG013 M2.1	**-15.6**	**-0.1**
NG013 M3.1	-15.0	-0.9
NG013 M3.2	-14.8	-0.1
MUZM P4.2	**-16.0**	**0.0**
MUZM M3.1	-15.3	0.3
MUZM M3.2	-15.1	0.8
NG0-57 dm1.1	**-17.0**	**-2.0**

The first sample from each new individual is listed in bold

values in an individual tooth is seen in NG003's M3 and these were -14.7 and -15.9, a difference of 1.1‰. For the $\delta^{18}O$ values, the greatest intra-tooth difference was in NG002's M3 values of -1.3 and 0.4‰, a difference of 1.7‰. Between two teeth of the same individual, the greatest $\delta^{13}C$ difference was between the M2 and M3 of NG012, with values of -15.0 and -15.7‰, a difference of 0.7‰. With respect to $\delta^{18}O$, the greatest difference between two teeth of the same individual was in the M2 and M3 of NG002, with values of -1.4 and 0.4‰, a 1.8‰ difference.

Intra-individual variation

Table 16: Intra-individual and inter-individual $\delta^{13}C_{dentine}$ and $\delta^{15}N_{dentine}$ variation of eight chimpanzees

Individual/tooth	$\delta^{15}N_{dentine}$ (‰)	$\delta^{13}C_{dentine}$ (‰)
NG001 M2	8.0	-23.1
NG002 M1	9.4	-21.9
NG002 M3	6.0	-26.0
NG003 M2	7.6	-25.0
NG003 M3	7.7	-23.2
NG004 M1	7.6	-24.1
NG004 M2	8.8	-22.5
NG005 P4	7.9	-22.2
NG005 M3	5.2	-26.2
NG012 M2	8.5	-23.5
NG012 M3	7.8	-25.3
NG013 M2	8.7	-24.7
MUZM P4	7.9	-24.5
MUZM M3	8.9	-24.2

Dentine variation: For the eight chimpanzees from which dentine could be sampled (Table 16), different combinations of teeth were sampled for each individual, depending upon availability. In the two M1s from which dentine was sampled, the $\delta^{15}N$ ranged from 7.6‰ to 9.4‰, a 1.8‰ difference. The $\delta^{15}N$ in the five M2s that were sampled ranged from 7.6‰ to 8.8‰, a 1.3‰ difference. The five M3s ranged in their dentine $\delta^{15}N$ values from 5.2‰ to 8.9‰, which is a 3.7‰ difference. The two P4s that were sampled were identical in their dentine $\delta^{15}N$ values of 7.9‰ and 7.9‰. It is also worth noting that, in chimpanzees, the formation ages of the P4 and M2 crowns overlap almost entirely, which means that the isotopic values for crown dentine from these teeth should overlap within the same individual. They did not come from the same individuals in this case, however, which is why we have not directly compared them. The overall range of dentine $\delta^{15}N$ values in all the teeth sampled was from 5.2‰ to 9.4‰, which is a difference of 4.2‰.

Figure 24 : Inter-tooth $\delta^{13}C$ and $\delta^{15}N$ variation from the dentine of eight chimpanzees (top) and $\delta^{13}C$ and $\delta^{18}O$ intra-tooth variation from the enamel of nine chimpanzees (bottom)

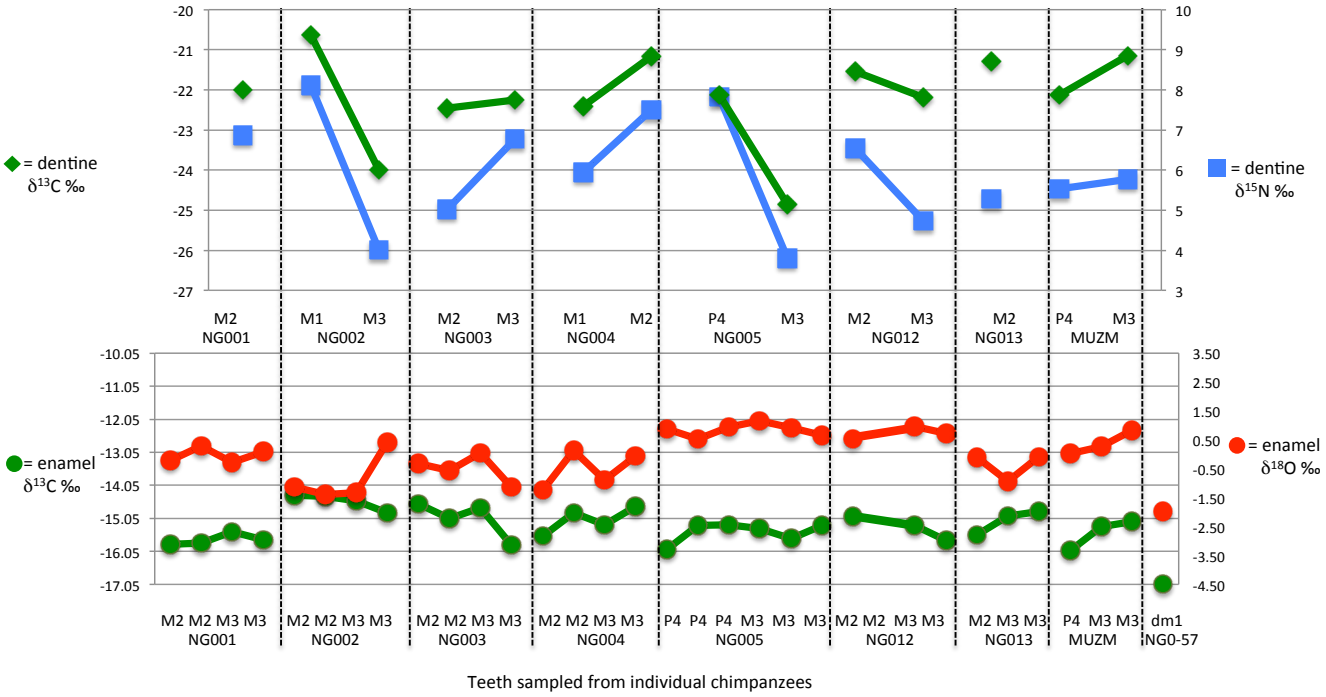

For those same teeth of the eight chimpanzees, the overall dentine (Table 16) $\delta^{13}C$ values ranged from -21.9‰ to -26.2‰, a difference of 4.3‰. The difference between the two M1 values was 2.2‰, while the M2 values ranged from -22.5‰ to -25.0‰, a difference of 2.5‰. The P4s ranged from -22.2 to -24.5‰, a difference of 2.3‰. The M3s ranged from -23.2‰ to -26.2‰, a difference of 3.0‰. The range of differences between the same teeth of different individuals was again highest in the M3s. (Figure 24-top) It is also worth noting that the individual with the lowest (most depleted) values in both $\delta^{13}C$ and $\delta^{15}N$ was the M3 of NG005 and that with the most enriched values in both isotopes was the M1 of NG002.

Inter-tissue isotopic variation

Bone collagen: For all the chimpanzees in this study (Table 17), the mean bone collagen $\delta^{13}C$

value was -22.6‰ (S.D. ±0.8). When the Ngogo chimpanzees were considered without the Bwindi chimpanzee or the extra-group males, that mean was nearly identical, with a value of -22.7‰ (S.D. ±0.9). When the infant chimpanzee was removed from that sample, however, the adult Ngogo chimpanzee mean was -23.0‰ (S.D. ±0.7). When all subsamples were considered, the means varied by 0.4‰, and most of that difference came from the inclusion of the infant chimpanzee. The highest and lowest Ngogo adult values were NG002 at -21.8 and NG013 at 22.9‰, respectively, a range of 1.0‰.

The mean bone collagen $\delta^{15}N$ value for the whole sample was 7.3‰ (S.D. ±1.6), with that value changing to 7.2‰ (S.D. ±2.0) when only the Ngogo chimpanzees were included, and becoming even less enriched with a value of 6.6‰ (S.D. ±1.9) when the infant chimpanzee was removed. The means for these subsamples varied by as much as 0.7‰, and again, most of this difference was driven by the inclusion of the infant chimpanzee, and not the individual from Bwindi. The individuals with the highest and lowest Ngogo adult $\delta^{15}N$ values were not the same as those with the highest and lowest $\delta^{13}C$ values. Instead these chimpanzees, NG002 at 8.1 and NG012 at 7.2‰, had a range of 0.9‰.

Bone apatite: The mean bone apatite $\delta^{13}C$ value for all the chimpanzee samples (Table 17) was 15.4‰ (S.D. ±1.7) with that value becoming the slightly more negative -15.5‰ (S.D. ±1.7) when only the Ngogo chimpanzees were included, and becoming less negative -14.7‰ (S.D. ±0.8) when the infant chimpanzee was removed. The highest and lowest adult Ngogo $\delta^{13}C$ values were -13.2 and -15.3‰ from NG001 and NG012, which is a difference of 2.1‰.

The mean $\delta^{18}O$ value in the bone apatite for the full chimpanzee sample (Table 17) was -0.7‰ (±0.7), and when the Ngogo chimpanzees were considered without the Bwindi individual or the extra-group males, that values changed to -0.8‰ (±0.7). That value changes to -1.1‰

(±0.5) when the infant chimpanzee is excluded, making the final difference in means between the various subsamples 0.3‰, with three times as much of that difference coming from the inclusion of the Ngogo infant as the inclusion of the Bwindi individual. The lowest and highest adult Ngogo values were -1.4 and -0.6‰ from NG012 and NG013, respectively, a range of 2.0‰.

Hair: There were only hairs available for two of the chimpanzees in this sample (Table 17), and the hair $\delta^{15}N$ values were 7.9‰ and 7.5‰ differing by 0.4‰, and the $\delta^{13}C$ values were -22.9‰ and -23.8‰, with a difference of 0.9‰.

Enamel apatite: The mean of the bulk enamel $\delta^{13}C$ values for these chimpanzees (Table 18) was -15.3‰ (S.D. ±0.8), while the mean for the Ngogo samples only was essentially the same at -15.3‰ (S.D. ±1.0), rising to -15.0‰ (S.D. ±0.5) when the infant value was excluded. The means of these subsamples differed by up to 0.4‰. The highest (most $\delta^{13}C$ enriched) value was -14.1‰, and the lowest (most depleted) value was -17.0‰, but if only the adults are considered, the lowest was -15.7‰, giving the overall adult bulk enamel samples a range 1.6‰. For the $\delta^{18}O$ values, the mean bulk value for the whole chimpanzee sample was -0.3‰ (S.D. ±0.8), while that for the Ngogo individuals was -0.4‰ (S.D. ±1.0), which became the much less negative 0.0‰ (S.D. ±0.6) without the Ngogo infant. These subsample means differed by 0.3‰. The highest overall value was 0.8‰ and the lowest was -2.0‰, though only -0.9‰ when adults only were considered, making the adult range 1.7‰.

Dentine: The mean bulk $\delta^{13}C$ for the dentine from the chimpanzees in this sample (Table 18) was -24.0‰ (S.D. ±0.5), and when only the Ngogo individuals were considered, that mean became -24.1‰ (S.D. ±0.5). There was no dentine sample from the infant chimpanzee, so only adults were included. The lowest and highest values were -24.7‰ and -23.1‰, a range of 1.6‰.

Table 17: Bulk $\delta^{13}C$, $\delta^{18}O$, and $\delta^{15}N$ values for bone apatite and bone collagen of seven chimpanzees and bulk and serial $\delta^{13}C$ and $\delta^{15}N$ hair samples from two chimpanzees

ID #	Bone collagen $\delta^{15}N$ ‰	ID #	Bone collagen $\delta^{13}C$ ‰	ID #	Bone apatite $\delta^{18}O$‰	ID #	Bone apatite $\delta^{13}C$‰	ID #	Hair $\delta^{15}N$ ‰	ID #	Hair $\delta^{13}C$ ‰
NG001	7.6	NG001	-22.5	NG001	-1.1	NG001	-13.2	NG002	7.9	NG002	-22.9
NG002	8.1	NG002	-21.8	NG002	-1.0	NG002	-15.3	NG012	7.5	NG012	-23.8
NG005	7.7	NG005	-22.3	NG005	-1.4	NG005	-13.8	NG002 1.1	8.4	NG002 1.1	-23.6
NG012	7.2	NG012	-22.8	NG012	-1.5	NG012	-15.3	NG002 1.2	8.3	NG002 1.2	-23.3
NG013	7.8	NG013	-22.9	NG013	-0.6	NG013	-14.9	NG002 1.3	8.3	NG002 1.3	-23.2
NG057	9.3	0-57	-21.6	NG057	0.0	0-57	-17.8	NG002 1.4	8.0	NG002 1.4	-23.3
MUZM	6.9	MUZM	-23.0	MUZM	0.3	MUZM	-17.3	NG002 1.5	8.5	NG002 1.5	-23.2
Mean (SD)	7.3 (±1.6)	Mean (SD)	-22.6 (±0.8)	Mean (SD)	-0.7 (±0.7)	Mean (SD)	-15.4 (±1.7)	Mean	7.7	Mean	-23.4
Ngogo mean (SD)	7.2 (±2.0)	Ngogo mean (SD)	-22.7 (±0.9)	Ngogo mean (SD)	-0.8 (±0.7)	Ngogo mean (SD)	-15.5 (±1.7)	Serial "bulk" mean	8.3	Serial "bulk" mean	-23.3
Ngogo adult mean (SD)	6.6 (±1.9)	Ngogo adult mean (SD)	-23.0 (±0.7)	Ngogo adult mean (SD)	-1.1 (±0.5)	Ngogo adult mean (SD)	-14.7 (±0.8)	NG002 mean	8.1	NG002 mean	-23.1

Table 18: Averaged $\delta^{13}C$, $\delta^{18}O$, and $\delta^{15}N$ values for enamel apatite and dentine of nine chimpanzees

ID #	Enamel apatite $\delta^{13}C$ ‰	ID #	Enamel apatite $\delta^{18}O$ ‰	ID #	Dentine $\delta^{13}C$ ‰	ID #	Dentine $\delta^{15}N$ ‰
NG001	-15.7	NG001	-0.0	NG001	-23.1	NG001	8.0
NG002	-14.5	NG002	-0.9	NG002	-23.9	NG002	7.7
NG003	-15.1	NG003	-0.5	NG003	-24.1	NG003	7.7
NG004	-15.1	NG004	-0.5	NG004	-23.3	NG004	8.2
NG005	-15.5	NG005	0.8	NG005	-24.2	NG005	6.5
NG012	-14.1	NG012	0.4	NG012	-24.4	NG012	8.1
NG013	-15.1	NG013	-0.4	NG013	-24.7	NG013	8.7
NG057	-17.0	NG057	-2.0	NG057	N/A	NG057	N/A
MUZM	-15.5	MUZM	0.4	MUZM	-24.3	MUZM	8.4
Mean (SD)	-15.3 (±0.8)	Mean (SD)	-0.3 (±0.8)	Mean (SD)	-24.0 (±0.5)	Mean (SD)	7.9 (±0.7)
Ngogo mean (SD)	-15.3 (±1.0)	Ngogo mean (SD)	-0.4 (±1.0)	Ngogo mean (SD)	N/A	Ngogo mean (SD)	N/A
Ngogo adult mean (SD)	-15.0 (±0.5)	Ngogo adult mean (SD)	-0.0 (±0.6)	Ngogo adult mean (SD)	-24.1 (±0.5)	Ngogo adult mean (SD)	7.8 (±0.8)

N/A indicates no value for this parameter

For the dentine $\delta^{15}N$ values, the total sample mean was 7.9‰ (S.D. ±0.7), changing only slightly to 7.8‰ (S.D. ±0.8) when the Ngogo individuals were considered alone. The lowest value was 6.5‰ and the highest was 8.7‰, a range of 2.2‰.

Variation from unknown diet-tissue fractionation factors

Research by Carlson (2011), Carlson et al. (2013), Carlson and Kingston (2014), and Carlson and Crowley (2016), provided a framework for the next phase of this analysis. These studies meticulously documented the $\delta^{13}C$ and $\delta^{15}N$ contents of 60 of the most commonly eaten chimpanzee food items from Ngogo, as well as $\delta^{13}C$ values from 51 chimpanzee foods from Bwindi. Isotopic values of 35 plants that Ngogo chimpanzees spent the most time feeding on are listed in Table 19, along with the percentages of total feeding time they spend eating each one (Watts, 2014). Isotopic values are reported for each plant type, as well as for their leaves, fruit, and seeds, since each plant part yields different isotopic values, and contributes differentially to the overall diets of these chimpanzees. Added together, these 35 items comprise 89.29% of the total Ngogo chimpanzee feeding time. The percentages were normalized to 100% to provide a rough estimate of the overall contribution of each item to the total diet (Table 20). Using the $\delta^{13}C$ and $\delta^{15}N$ contents of each plant, and the converted percentage of total time spent feeding on each plant, the proportional amount of each isotope from that plant relative to the total dietary input was calculated, creating a "total dietary input" value for both $\delta^{13}C$ and $\delta^{15}N$. For $\delta^{13}C$ the total dietary isotopic input is -27.4‰ and for $\delta^{15}N$ this is 4.2‰. This same calculation was not possible for the single Bwindi chimpanzee as there is no information on percentages of time spent feeding on each of the known dietary items.

Table 19: $\delta^{13}C$ and $\delta^{15}N$ proportional input values, per plant part, from observed % feeding time, and feeding time converted to 100% for chimpanzees at Ngogo

	Species/food type (top 35 w/$\delta^{13}C$ and $\delta^{15}N$ values)	% of feeding time	89.29% converted	Plant part-specific mean $\delta^{13}C$ (±S.D.)	Plant part-specific mean $\delta^{15}N$ (±S.D.)	Proportional -$\delta^{13}C$ contribution	Proportional -$\delta^{15}N$ contribution
1	*Ficus mucuso fruit*	18.0	20.1	-26.9 ± 0.3	4.1 ± 0.3	5.4	0.8
2	*Uvariopsis congensis fruit*	10.0	11.2	-27.4 ± 0.6	4.3 ± 1.3	3.1	0.5
3	*Pterygota mildbraedii leaves*	8.5	9.5	-30.9 ± 1.0	3.0 ± 0.9	2.9	0.3
4	*Pseudospondias microcarpa fruit*	4.9	5.5	-27.3 ± 0.6	3.0 ± 1.2	1.5	0.2
5	*Cordia millenii fruit*	4.8	5.4	-26.4 ± 1.5	4.9 ± 1.0	1.4	0.3
6	*Monodora myristica fruit*	4.6	5.2	-28.4 ± 2.5	5.7 ± 1.5	1.5	0.3
7	*Pterygota mildbraedii seeds*	3.6	4.0	-27.5 ±1.3	3.6 ± 1.1	1.1	0.1
8	*Morus lactea fruit*	3.3	3.7	-25.4 ± 0.5	4.3 ± 0.8	0.9	0.2
9	*Ficus exasperata leaves*	3.2	3.6	-28.0 ± 1.7	5.9 ± 1.8	1.0	0.2
10	*Celtis africana leaves*	3.1	3.6	-29.1 ± 1.6	3.8 ± 1.1	1.0	0.1
11	*Aningeria altissima fruit*	3.0	3.3	-25.7 ± 1.5	4.8 ± 0.3	0.9	0.2
12	*Mimusops bagshawei fruit*	2.8	3.1	-26.7 ± 0.9	3.7 ± 0.9	0.8	0.1
13	*Treculia africana fruit*	2.6	2.9	-26.0 ± 1.4	3.8 ± 1.0	0.8	0.1
14	*Ficus dawei fruit*	2.5	2.7	-26.0 ± 0.9	4.0 ± 0.8	0.8	0.1
15	*Chrysophyllum albidum fruit*	2.3	2.6	-27.3 ± 1.0	4.7 ± 1.7	0.7	0.1
16	*Ficus natalensis fruit*	2.3	2.5	-26.9 ± 0.8	3.8 ± 0.7	0.7	0.1
17	*Celtis durandii fruit*	1.6	1.8	-26.2 ± 0.8	6.9 ± 0.8	0.5	0.1
18	*Ficus brachylepis fruit*	1.6	1.7	-28.3 ± 1.6	4.3 ± 1.4	0.5	0.1
19	*Morus lactea flowers*	0.9	1.0	-24.5 ± 0.8	5.9 ± 0.9	0.3	0.1
20	*Celtis mildbraedii leaves*	0.8	0.8	-30.2 ± 0.7	6.1 ± 1.2	0.3	0.1
21	*Afromomum mildbraedii pith*	0.7	0.8	-29.5 ± 1.8	3.9 ± 1.7	0.2	0.03
22	*Acanthus pubescens pith*	0.6	0.7	-29.4 ± 2.3	1.4 ± 2.3	0.2	0.01
23	*Morus lactea leaves*	0.6	0.6	-25.0 ± 0.7	5.0 ± 0.4	0.2	0.03
24	*Chaetacme aristata leaves*	0.5	0.6	-28.9 ± 1.8	6.1 ± 2.0	0.2	0.03
25	*Warburgia*	0.5	0.5	-24.6 ± 2.2	4.0 ± 1.0	0.1	0.02

	ugandensis fruit						
26	*Cyperus papyrus*	0.4	0.5	-10.6 ± 0.5	1.5 ± 0.4	0.05	0.01
27	*Ficus exasperata figs*	0.4	0.4	-26.3 ± 1.4	4.9 ± 1.0	0.1	0.02
28	*Pterygota mildbraedii flowers*	0.4	0.4	-24.4 ± 1.0	1.8 ± 0.9	0.1	0.01
29	*Neoboutonia macrocalyx roots*	0.4	0.4	-26.3 ± 1.3	3.0 ± 1.0	0.1	0.01
30	*Piper capense pith*	0.2	0.3	-31.3 ± 1.4	4.5 ± 1.3	0.1	0.01
31	*Pterygota mildbraedii cambium*	0.2	0.3	-25.8 ± 1.0	1.8 ± 0.9	0.1	0.005
32	*Cordia millenii flowers*	0.2	0.2	-25.8 ± 1.1	2.8 ±0.5	0.04	0.005
33	*Marantachloa sp.*	0.1	0.1	-32.3 ± 1.7	5.5 ± 1.6	0.04	0.006
34	*Monodora myristica sapling leaves*	0.02	0.02	-32.1 ± 1.4	4.0 ±1.3	0.01	0.001
35	*Chaetacme aristata cambium*	0.003	0.0003	-27.1 ± 0.7	6.7 ± 1.5	0.0001	0.00002
Total		**89.293**	**100.0003**			**-27.4**	**4.2**

$\delta^{13}C$ and $\delta^{15}N$ data from Carlson, (2011), % feeding time from Watts et al. (2012)

The most ^{13}C depleted plant item was *Marantachloa sp.*with a $\delta^{13}C$ value of -32.3 ± 1.7‰ and the most ^{13}C enriched plant item was *Cyperus papyrus,* the only C^4 plant found at Ngogo, with a value of -10.6 ± 0.5‰. The most ^{15}N depleted plant item was the *Acanthus pubescens* pith at $\delta^{15}N$ value of 1.4 ± 2.3‰, and the most enriched was the fruit of the *Celtis durandii* at 6.9 ± 0.8‰. (Table 19)

As noted earlier, different plant parts from the same taxon revealed as much as a 2.1‰ difference in $\delta^{15}N$ values, and a difference of as much as 6.5‰ in their $\delta^{13}C$ values.

Table 20: Diet-tissue fractionation levels for all tissues from the Kibale chimpanzees in this sample, given $\delta^{13}C$ and $\delta^{15}N$ "total dietary input" values adjusted from 89.29% of total diet

Individual	Tissue type	Tissue value - $\delta^{13}C$	89.29% of total dietary input -$\delta^{13}C$	Diet-tissue $\delta^{13}C$ fractionation (input value)	Tissue value $\delta^{15}N$	89.29% of total dietary input $\delta^{15}N$	Diet-tissue $\delta^{15}N$ fractionation (input value)
NG001	Bone collagen	22.5	27.4	4.8	7.6	4.2	3.4
NG001	Bone apatite	13.3	27.4	14.1	N/A	4.2	N/A
NG001	Enamel apatite	15.7	27.4	11.7	N/A	4.2	N/A
NG001	Dentine	23.1	27.4	4.2	8	4.2	3.8
NG002	Bone collagen	21.8	27.4	5.6	8.1	4.2	3.9
NG002	Bone apatite	15.3	27.4	12.1	N/A	4.2	N/A
NG002	Enamel apatite	14.5	27.4	12.8	N/A	4.2	N/A
NG002	Hair	22.9	27.4	4.5	7.9	4.2	3.7
NG002	Dentine	23.9	27.4	3.4	7.7	4.2	3.5
NG003	Enamel apatite	15.1	27.4	12.3	N/A	4.2	N/A
NG003	Dentine	24.1	27.4	3.3	7.7	4.2	3.5
NG004	Bone collagen	24.0	27.4	3.4	3.8	4.2	-0.4
NG004	Enamel apatite	15.1	27.4	12.3	N/A	4.2	N/A
NG004	Dentine	23.3	27.4	4.1	8.2	4.2	4.0
NG005	Bone collagen	22.3	27.4	5.1	7.7	4.2	3.5
NG005	Bone apatite	13.8	27.4	13.6	N/A	4.2	N/A
NG005	Enamel apatite	15.5	27.4	11.9	N/A	4.2	N/A
NG005	Dentine	24.2	27.4	3.2	6.5	4.2	2.3
NG012	Bone collagen	22.8	27.4	4.6	7.2	4.2	3.0
NG012	Bone apatite	15.3	27.4	12.1	N/A	4.2	N/A
NG012	Enamel apatite	14.1	27.4	13.3	N/A	4.2	N/A
NG012	Hair	23.8	27.4	3.5	7.5	4.2	3.3
NG012	Dentine	24.4	27.4	3.0	8.1	4.2	3.9
NG013	Bone collagen	22.9	27.4	4.5	7.8	4.2	3.6
NG013	Bone apatite	14.9	27.4	12.5	N/A	4.2	N/A
NG013	Enamel apatite	15.1	27.4	12.2	N/A	4.2	N/A
NG013	Dentine	24.7	27.4	2.7	8.7	4.2	4.5
NG0-57	Bone collagen	21.6	27.4	5.8	9.3	4.2	5.1
NG0-57	Bone apatite	17.3	27.4	10.1	N/A	4.2	N/A
NG0-57	Enamel apatite	15.5	27.4	11.9	N/A	4.2	N/A

Table 21: Provisional diet-to-tissue fractionation factors by subsample

Input of -27.4 for total diet $\delta^{13}C$ and 4.2 for total diet $\delta^{15}N$	
Mean Ngogo Bone collagen-diet C fractionation	4.7
Mean Ngogo Bone apatite-diet C fractionation	12.0
Mean Ngogo Enamel apatite-diet C fractionation	12.3
Mean Ngogo Hair-diet C fractionation	4.0
Mean Ngogo Dentine-diet C fractionation	3.3
Mean Ngogo Bone collagen-diet N fractionation	3.8
Mean Ngogo Hair-diet N fractionation	3.5
Mean Ngogo Bone Dentine-diet N fractionation	3.7

Mean Kibale Bone collagen-diet C fractionation	4.8
Mean Kibale Bone apatite-diet C fractionation	12.4
Mean Kibale Enamel apatite-diet C fractionation	12.3
Mean Kibale Hair-diet C fractionation	4.0
Mean Kibale Dentine-diet C fractionation	3.4
Mean Kibale Bone collagen-diet N fractionation	3.7
Mean Kibale Hair-diet N fractionation	3.5
Mean Kibale Bone Dentine-diet N fractionation	3.7

Kibale + Bwindi Bone collagen-diet C fractionation	4.8
Kibale + Bwindi Bone apatite-diet C fractionation	12.1
Kibale + Bwindi Enamel apatite-diet C fractionation	12.3
Kibale + Bwindi Hair-diet C fractionation	No change
Kibale + Bwindi Dentine-diet C fractionation	3.4
Kibale + Bwindi Bone collagen-diet N fractionation	3.6
Kibale + Bwindi Hair-diet N fractionation	No change
Kibale + Bwindi Dentine-diet N fractionation	3.7

The modeled "total dietary input" values for $\delta^{13}C$ and $\delta^{15}N$ were then compared with the resulting isotope values from each tissue from each chimpanzee to determine the diet-to-tissue fractionation factor assuming the input value was truly representative of the whole diet (Table 20). The resulting fractionation factors are listed in Table 21, where they are grouped according

to tissue type, but also within separate subsamples. (In the case of the sample that includes the Bwindi individual, the $\delta^{13}C$ and $\delta^{15}N$ values do not actually apply, as they spend different amounts of time feeding on a few of the same foods as the chipanzees from Kibale, but mostly different ones.) In all three subsamples, this fractionation factor is 12.3‰. Figure 25 depicts the relationship between these tissue-specific fractionation factors in different subsamples of chimpanzees from this study.

Figure 25: Fractionation values by tissue and isotope for three subsamples in this chimpanzee sample

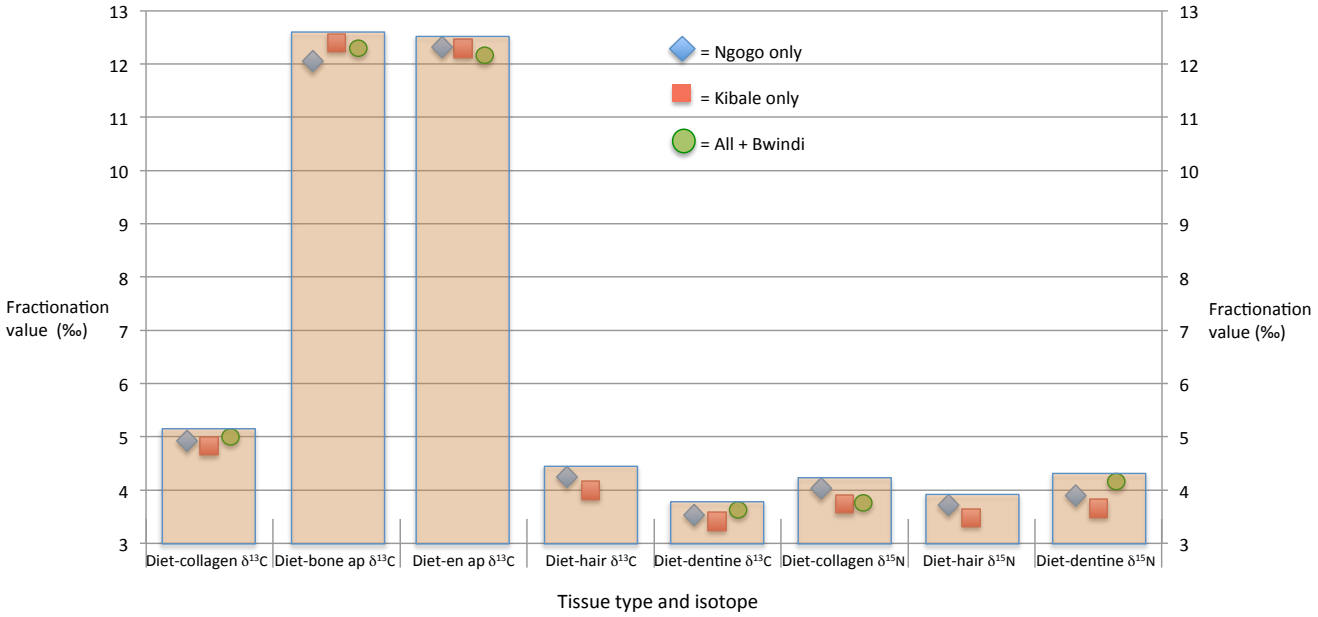

Discussion

Intra-tissue variability: Variability of $\delta^{13}C$, $\delta^{18}O$, and $\delta^{15}N$ values within tissues that could be serially sampled (enamel and hair) was documented (Figure 24/Tables 15 and 16), based on the ages and rates at which the tissue(s) formed as well as their rates or lack of turnover. Tooth

enamel and dentine begin forming in-utero in all deciduous teeth and the first permanent molar (M1) and culminates with the mineralization of the M3 at around age 13 for chimpanzees. This means that these teeth record the diet from the earliest part of life through to subadult/adulthood. Sampling different areas of enamel within a single tooth can can document short term variation in diet and environment, producing variable $\delta^{13}C$ and $\delta^{18}O$ values. Documenting this variation is contingent on: (1) the length and thickness of the crown, (2) the area of the crown the sample is taken from, (3) the internal geometry of the tooth, and (4) the sampling orientation. As depicted in Figure 26, traditional drilled sampling methods might permit four time-transgressive drilled samples to be taken from the length of a molar crown of a baboon (pictured) or a chimpanzee, but the initial mineralization age of the enamel.

Figure 26: Illustration of temporal overlap between adjacent drilled enamel samples in a baboon M1 cusp

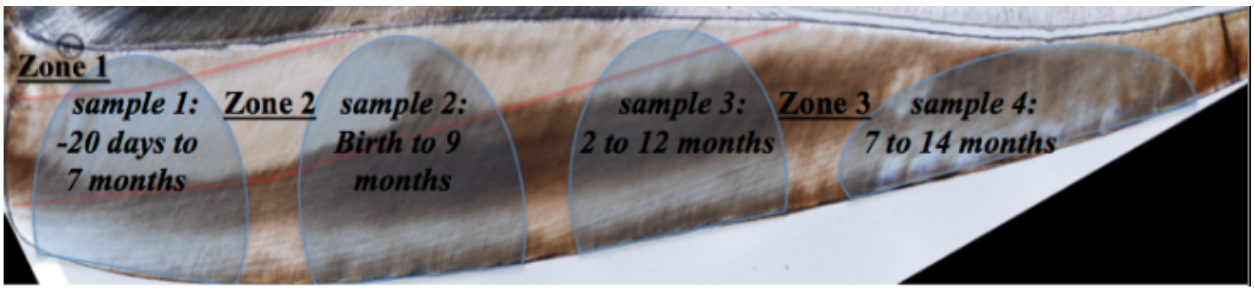

Figure 26: This is the mesiobuccal cusp of an M_1 from female yellow baboon "UM 152". Zone 1 is all prenatal enamel, Zone 2 is between the neonatal line (first highlighted in red) and 3 months, Zone 3 is from the accentuated line that formed at 3 months (second line highlighted in red) through the end of M1 formation at ~14months. The blue areas represent areas that were drilled into the side of the enamel crown to each produce ≥600 μg of enamel powder.

areas that would be intermixed in each sample would obscure the potential higher resolution variation within that tooth. To minimize the intermixture seen in Figure 26 only two samples were taken from each molar crown, and these were from an area equivalent spatially to what is

seen in “sample 1” and a second consisting of enamel from an area equivalent to “sample 4” below.This sampling strategy, while it cannot separate a prenatal diet from an exclusive nursing diet from fully adult diet, it can separate the samples by the ages during which the enamel initially mineralized. Drilling, per sé, was not used, but instead a modified method of thin section micro-dicing (Daniel Green, pers com) was employed to mechanically isolate enamel from these temporally distinct areas, using the accentuated and periodic structures as guides (Malone, unpublished data). While this only allowed two minimum sized samples for isotopic analyses (≥ 600 μg) to be obtained from each tooth, the time periods during which they each initially mineralized were known, which is a distinct advantage. These samples were taken from M2s and M3s, so the actual ages of the zones in Figure 26 (from an M1) do not apply directly to the diced samples. It must be noted that the second stage of enamel formation, known as maturation, also attenuates the dietary signal, since a large proportion of the final inorganic makeup of enamel enters into the already mineralized tissue matrix somewhat later than the periodic structures are laid down. This means that the final mineral content of a given area of the crown may contain dietary signals from a point in time up to several months or even a year later than the microstructures indicate, causing inferences of earlier dietary change than what actually occurred. This complicates sampling strategies that try to obtain temporally distinct signal of diet from within a single tooth. In a previous study we developed sampling methods using laser ablation inductively coupled plasma-mass spectrometry (LA ICP-MS) to samples trace elements from along the inner enamel, which is the area thought to mature soonest after initial mineralization, and if so, it contains the least attenuated signal of diet of any area of enamel.

The results of the serial enamel sampling of the two teeth from each of the eight adult chimpanzees (and one from the infant chimpanzee) indicate that there is some variation in $\delta^{13}C$

and $\delta^{18}O$ values between the two teeth of many of these individuals (Figure 24), as well as a great amount of variation among samples taken from the same teeth (Table 15). Within the M3 of one individual (NG003) $\delta^{13}C$ values varied by 1.1‰, and the $\delta^{18}O$ values by 1.7‰. With the most depleted $\delta^{13}C$ value of -15.9‰ and the corresponding $\delta^{18}O$ value of -1.1, the NG003 M3 isotopic values place that individual outside the range of chimpanzee enamel apatite values from Kibale (Nelson, 2013 p.2). Instead, the NG003 M3 value situates this individual in the reported range for olive baboons in Kibale (Nelson, 2013). A number of the additional serial sample isotopic signatures from enamel of chimpanzees in this study are situated within the red-tailed monkey range (Nelson, 2013) and again, outside the chimpanzee range for both isotopes. This suggests that, if the tooth being sampled or even the area of the tooth being sampled, is not specified, interpretations of dietary ecology have the potential to be variable and inconsistent.

Intra-individual isotopic variation: Between two teeth of the same individual (Table 15), enamel $\delta^{13}C$ values varied by as much as 0.7‰, and the $\delta^{18}O$ values varied by as much as 1.8‰. This indicates that the amount of the $\delta^{18}O$ variation between two samples from the same tooth can be as great as the variation between bulk values from two consecutively forming teeth, even if the $\delta^{13}C$ values aren't as variable in the two teeth. All of this should be considered when designing enamel-sampling strategies, as well as when interpreting isotopic values that result from the chosen sampling strategy.

Figure 27: M2 and M3 serial enamel apatite $\delta^{13}C$ and $\delta^{18}O$ values separated by chimpanzee community

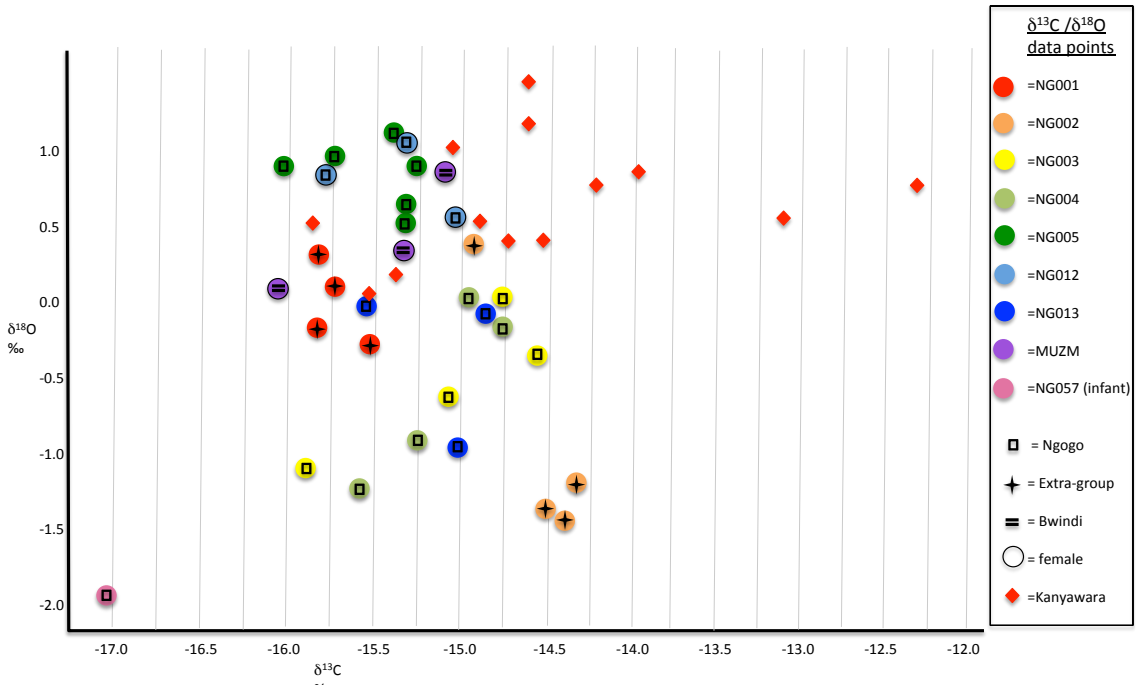

Between two teeth of the same chimpanzee, the dentine $\delta^{13}C$ values varied as much as 4.1‰ and the $\delta^{15}N$ values varied as much as 3.4‰ (Table 16). These differences were between the M1 and the M3 of individual NG002. The amount of variation in dentine $\delta^{15}N$ and $\delta^{13}C$ values between these teeth may reflect the fact that the dentine in these teeth comes from areas that start forming before birth in the M1 up to age 12-13 in the M3 root dentine. (Although, samples were not taken from dentine located more than ~2mm apical to the CEJ, so the latest forming samples came from dentine forming up until age eight in these chimpanzees.) Samples containing dentine that formed prenatally, and those that formed long after the age when weaning is thought to be complete in these chimps, should therefore contain quite isotopically distinct signals. Careful sampling of primary dentine only, either by abrading away areas of tertiary dentine, or by stopping short of sampling secondary dentine from the pulp cavity wall, can avoid mixing later forming dentine into samples that aim to assess early life diets.

Inter-individual isotopic variation: The range of 3.7‰ for the $\delta^{15}N$ values from the dentine of the same tooth type (M3) of different individuals, was considerable, as was the 3.0‰ difference between the corresponding $\delta^{13}C$ values. This indicates that studies that use bulk dentine sampling within the same tooth type need to anticipate this level of possible variability among individuals, or risk interpreting such disparate values as indicators of a trophic-level difference between members of population. This difference could also be linked with differences in baseline levels of local plant isotopic ecology at different sites, and not necessarily differences in the types of food items being eaten (Oelze et al., 2016). In fact, the mean $\delta^{13}C$ value from the same plant part (fruit) of the same plant type (*Ficus natalensis*) growing at Ngogo and growing at Bwindi can vary as much as 1.3‰ and (*Chrysophyllum albidum*) can vary as much as 2.0‰ between these two sites. (Carlson and Crowley, 2016 pp. 1036-1037). Chimpanzees from the two sites eating the same fruit from the same type of tree could, therefore, easily be interpreted as having very different diets based upon this amount of difference

Inter-tissue isotopic routing: This section explores how variable the $\delta^{13}C$, $\delta^{18}O$, and $\delta^{15}N$ values are between the different tissues into which they are metabolically routed. Bulk sampling of bone collagen, bone apatite, enamel apatite, dentine, and hair produces $\delta^{13}C$ which presumable reflect different metabolic pathways that differentially biopurify the carbon input from dietary items. Mean values for each isotope within each tissue are given in Tables 17-18.

In order to ultimately be able to compare/contrast the diet and/or environmental conditions based on the $\delta^{13}C$, $\delta^{18}O$, and $\delta^{15}N$ values from different tissues between primate populations, it is imperative to know how variable these values are within the population (Tables 17-18/Figures 28-29). For example, in our population, the intra-individual differences between

$\delta^{13}C$ values in bone collagen and bone apatite are quite variable - the lowest offset is 3.7‰ and the highest is 9.3‰. To compare populations in which different tissues were analyzed – i.e $\delta^{13}C_{\text{bone collagen}}$ values in one population and $\delta^{13}C_{\text{bone apatite}}$ values in another, it is critical to 'convert' $\delta^{13}C_{\text{bone collagen}}$ values to $\delta^{13}C_{\text{bone apatite}}$ values using the offset values in Table 21. Having such a large range of these offset values in our population, however, makes this conversion problematic, and imprecise at best. Minimal differences in the $\delta^{15}N$ offsets between any of the tissue combinations ($\delta^{15}N_{\text{bone collagen-hair}}$=0.2‰, $\delta^{15}N_{\text{bone collagen-dentine}}$ =0.5-1.5‰, $\delta^{15}N_{\text{hair-dentine}}$ =0.2-0.7‰) suggest a more consistent conversion value to extrapolate the $\delta^{15}N$ of one unknown tissue in another population from a known one (e.g. we could infer the $\delta^{15}N_{\text{hair}}$ values for another population by adding 0.2-0.7‰ to their known $\delta^{15}N_{\text{dentine}}$ values). There is a slightly larger range of offset values between the $\delta^{13}C$ from bone apatite and that from enamel apatite, and the same is true of $\delta^{18}O$ offsets. ($\delta^{13}C_{\text{bone apatite-enamel apatite}}$ = 0.2-2.5‰ and $\delta^{18}O_{\text{bone apatite-enamel apatite}}$ = 0.1-2.2‰). This suggests that it may be easier and more feasible to infer some unknown tissue-specific isotope values from known ones, by using the offset values from other populations, than it may be for others. Studies that use such offsets from other populations to make inferences about unknown isotopes values from known ones should use caution in the application of conversion factors to compare diets and environmental conditions based on different tissues from different populations.

Table 22: Tissue-specific isotope offset ranges

$\delta^{15}N_{\text{collagen-hair}}$ = 0.23	$\delta^{15}N_{\text{hair-dentine}}$ = 0.19-0.67	$\delta^{15}N_{\text{collagen-dentine}}$ = 0.45-1.52	$\delta^{18}O_{\text{bone apatite-enamel apatite}}$ = 0.09-2.21	$\delta^{13}C_{\text{bone apatite-enamel apatite}}$ = 0.23-2.45	$\delta^{13}C_{\text{bone apatite-bone collagen}}$ = 3.71-9.29	$\delta^{13}C_{\text{bone apatite-hair}}$ = 7.66-8.51
$\delta^{13}C_{\text{bone apatite-dentine}}$ = 7.03-10.39	$\delta^{13}C_{\text{enamel apatite-collagen}}$ = 4.51-8.89	$\delta^{13}C_{\text{enamel apatite-hair}}$ = 8.39-9.73	$\delta^{13}C_{\text{enamel apatite/dentine}}$ = 7.44-10.26	$\delta^{13}C_{\text{bone collagen-hair}}$ = 1.08 -1.1	$\delta^{13}C_{\text{bone collagen-dentine}}$ = 0.6-2.12	$\delta^{13}C_{\text{hair-dentine}}$ = 0.53-1.02

Figure 28: $\delta^{15}N$ (top) and $\delta^{13}C$ (bottom) bulk value offsets between bone collagen, hair, and dentine of chimpanzees from four Ugandan communities

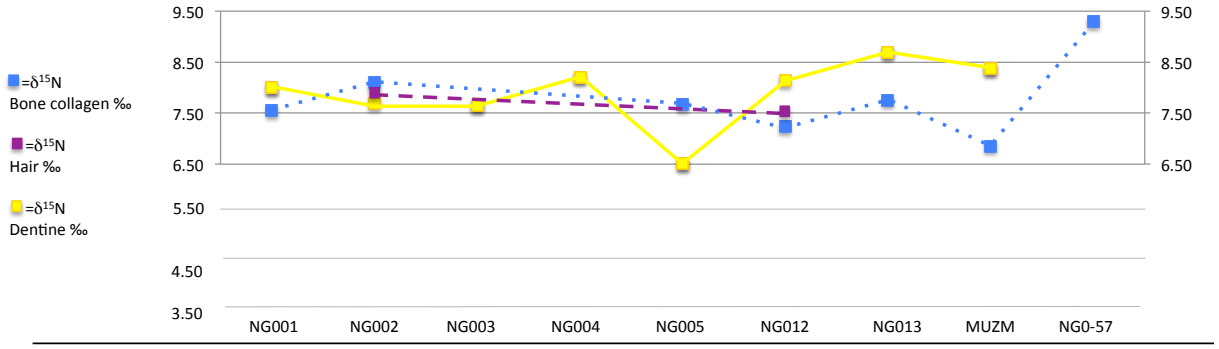

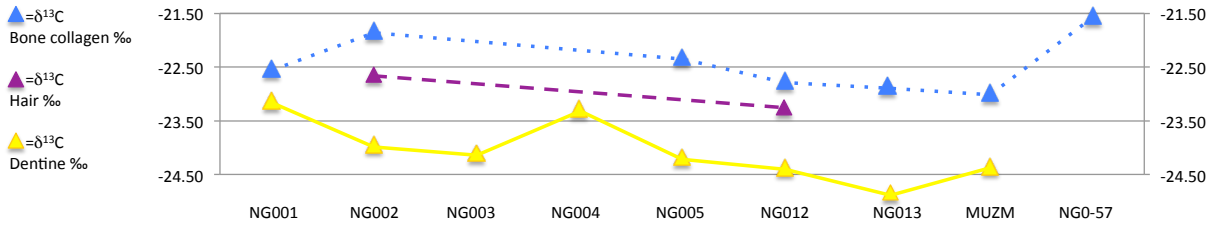

Offset Ranges ‰

$\delta^{15}N$	$\delta^{13}C$
-bone collagen/hair = 0.23	-bone collagen/hair = 1.08 -1.1
-hair/dentine = 0.19-0.67	-bone collagen/dentine = 0.6-2.12
-bone collagen/dentine = 0.45-1.52	-hair/dentine = 0.53-1.02

Figure 29: Offsets in $\delta^{18}O$ (top) and $\delta^{13}C$ (bottom) from bone apatite and enamel apatite of chimpanzees from four Ugandan communities

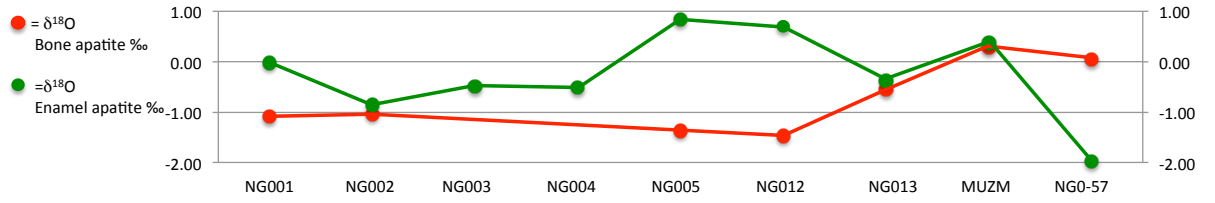

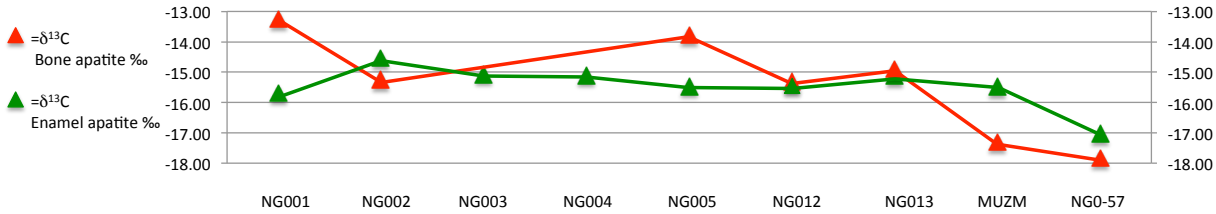

Offset ranges ‰

-bone apatite/enamel apatite = 0.09-2.21	-bone apatite/enamel apatite = 0.23-2.45

Hair: There were only two individuals with hair that could be sampled (NG002 and NG012), and one of them NG012 had hairs too short for serial sampling. The bulk $\delta^{13}C_{hair}$ value from NG002 is -22.9‰ and but the calculated "bulk" value using the combined serial sample values (N=5) from another hair was -23.3‰ (The average of these two values, 23.1‰, is used below.) In a studiy on rodents (DeNiro and Epstein (1981) determined that hair keratin is consistently +2.0‰ higher (more enriched) than that of bone collagen, and this offset has been utilized in numerous studies requiring conversions (Fahy et al., 2013; Fahy et al., 2014). Our results, however, support a more modest offset between $\delta^{13}C_{hair}$ and $\delta^{13}C_{collagen}$. The bone collagen $\delta^{13}C$ from these same two individuals were -21.8‰ (NG002) and -22.8‰ (NG012), while their respective hair keratin $\delta^{13}C$ values were -23.1‰ and -23.8‰, an enrichment from the bone collagen values of only +1.3 and +1.1‰ relative to hair keratin. With more numerous hair samples, it will be possible to better establish the pattern offset values in our chimpanzee sample, but these two offset values are incongruent with reported values.

In one study (Fahy et al., 2013) hair keratin $\delta^{13}C$ values are converted to bone collagen values, using this +2‰ enrichment factor, and they point out that there is no difference in $\delta^{15}N_{hair}$ and $\delta^{15}N_{bone\ collagen}$, which is supported by the data from this study's chimpanzees, as well (offset by only 0.2 and 0.0‰ in our two samples). However, in a subsequent study (Fahy et al., 2014), the $\delta^{15}N_{bone\ collagen}$ values from the 2013 study were utilized as though they were equivalent to $\delta^{15}N_{dentine}$ values, a conversion which is not supported by the data in the current study (Figure 28/Table 22. Our $\delta^{15}N_{dentine\text{-}bone}$ collagen offsets range from 0.5 to 1.5‰, and in this parameter our sample size is a bit larger (n=6) than the bone collagen-hair comparison (n=2).

On the other hand, if such an offset could be established for $\delta^{13}C_{enamel\ apatite\text{-}hair}$, and it was one that was consistent between different taxa at different sites, it would allow direct

comparisons to be made between $\delta^{13}C$ values of fossil taxa from their teeth, and living apes for whom we can collect hair samples. This is would be extremely useful, given the fact that hair samples are readily available for collection from museum specimens and from living primates while teeth and bone can only be sampled from deceased individuals

Inter-population variability: Some comparisons can be made here between the $\delta^{13}C_{enamel\ apatite}$ and $\delta^{18}O_{enamel\ apatite}$ values from the chimpanzees of this study and those of several other studies. The greatest difference in $\delta^{13}C$ values within any single adult tooth from the current study was 1.13‰, and this was within the M3 of "NG003". It is worth noting that M1s were not sampled as they would almost certainly have increased this level of overall variation greatly, given that M1s contain both prenatal enamel and enamel that formed during the period of exclusive nursing.

Another study (Fahy et al., 2015) looked at enamel apatite variation using samples from 15 M1s, and one premolar, from adult chimpanzees from the Taï Forest, Cote d'Ivoire. Their results yielded an overall $\delta^{13}C$ range of -17.0 to -18.3‰, compared with the range of -14.3 to -17.0‰ for the chimpanzees in our study, and a much larger $\delta^{18}O$ range of 0.3 to -5.8‰, compared with the 1.2 to -2.0‰ range seen here. They also point out the differences between their mean $\delta^{13}C_{enamel\ apatite}$ values (-17.0‰ ± 0.4) and those from Ituri (-14.5‰) and Itombwe (-13.5‰), two sites in the DRC (Cerling et al., 2004, 2013), as well as those from Kibale (-14.5 ± 1.0‰) (Nelson, 2013). They note that their $\delta^{13}C$ values are significantly more depleted than those from all the other sites, but the fact that they used only M1s may have a great deal to do with that. Had they included M2s and M3s as well, their overall values might not have been so depleted, since, as we have seen, M1s and other teeth that contain prenatal and nursing enamel will skew the overall $\delta^{13}C$ values to more negative. It is telling that the only $\delta^{13}C$ value from our

data set that falls into the range from the study of the Taï chimpanzee M1s is the one deciduous tooth. Unfortunately, we can't directly compare the values from their teeth to those used in the study of the Kibale chimpanzees (Nelson, 2013), since the tooth types were not listed in that study, apart from describing them as "premolars and molars" (Nelson, 2013-p.3). There is no indication, however, of how many of which teeth they are, or even how many chimpanzee individuals are represented. Detailed information on specific teth sampled would aid in identifying the sources of such variation between studies and inform interpretations of isotopic differences as dietary content-driven or site-specific ecology-driven (Oelze et al., 2016).

Smith et al. (2010) also present $\delta^{13}C_{\text{enamel apatite}}$ and $\delta^{18}O_{\text{enamel apatite}}$ values for the Ganta chimpanzees from Liberia (*Pan troglodytes verus*), and their comparison of values from M1s and M3s shows consistent enrichment from the earlier to later forming tooth (bulk M1 $\delta^{13}C_{\text{enamel apatite}}$ = -16.7 ±0.6‰, range = 2.6‰ and bulk M3 $\delta^{13}C_{\text{enamel apatite}}$ = -16.2 ± 0.9‰, range = 4.2‰). This further supports the current study's assertion that, in order to access the adult diet, sampling should not be limited to the M1s, since samples from that tooth will reflect dietary isotopic signal(s) from before weaning was complete.

Conclusions: This study's results suggest that there may be a habitat-specific difference in $\delta^{13}C_{\text{bone collagen-hair keratin}}$ offsets, since these values, limited though they are, show a lower offset than has been recorded for other sites (DeNiro and Epstein, 1981). The overall adult $\delta^{13}C_{\text{enamel apatite}}$ range for the chimpanzees in this sample is -14.3 to -16.0‰ and the $\delta^{18}O_{\text{enamel apatite}}$ range is 1.2 to -1.4‰. Based upon the tissue-specific isotope values of all of these chimpanzees, and the isotopic contents of their food items and percent of time spent feeding on each, we have calculated "total dietary input" values of $\delta^{13}C$ -27.4‰ and $\delta^{15}N$ 4.2‰. These values are used to

generate numerous diet-to-tissue fractionation factors, but the most relevant one for fossil hominin dietary reconstructions is the $\delta^{13}C_{\text{diet-enamel apatite}}$ fractionation factor for the Ngogo chimpanzees, which is estimated as +12.3‰.

Study limitations/Future directions: This study's "total dietary input" values do not include $\delta^{15}N$ from meat eating. For males, hunting would especially influence this in the bone collagen, and hair keratin values, though not as much in the dentine since it forms early in life, before hunting would begin. Juveniles may eat small amounts of meat, but observations at Taï show that meat consumption is heavily biased toward adult males (Fahy et al., 2013). Meat consumption is based upon merit (hunt participation) and not nepotism, with adult males consuming 7x more meat than females. At Ngogo, the risk-taking involved with hunting may play in important role in male-male bonds in allowing them to assess one another's reliability, providing a foundation for cooperation (Mitani and Watts, 2001). Also excluded from the calculated $\delta^{13}C$ and $\delta^{15}N$ total dietary input values are contributions from other non-plant foods like termites. The $\delta^{15}N$ values, especially, are likely to be affected by this omission from our dataset. Honey also accounts for 0.15% of the feeding time of Ngogo chimpanzees (Potts et al., 2011), and this has also not been included in this study's calculation of a "total dietary input" value. Such matters ought to be considered in future studies of this kind.

Additionally, similar tissues are available for study from the red-tailed monkeys whose teeth were used in a previous study (Malone, Chapter 3), and since these monkeys inhabited the same area as the chimpanzees in this study (Kibale National Park), and much is known about their preferred dietary items (Lambert, 1997; Bryer et al., 2013), a similar set of diet-to-tissue fractionation factors could potentially be constructed for these sympatric primates. Doing so

would augment the previously published enamel $\delta^{18}O$ and $\delta^{13}C$ data from these same red-tailed monkey individuals (Nelson, 2013), and demonstrate how sympatric taxa ingesting many of the same plant items from the same forest might differentially incorporate those dietary contents into their tissues.

Works Cited

Ambrose, S.H., Norr, L. 1993. Experimental evidence for the relationship of the carbon isotope ratios of whole diet and dietary protein to those of bone collagen and carbonate. In: Lambert, J.B., Norr, L. (Eds.), Prehistoric Human Bone and Archaeology at the Molecular Level. Springer-Verlag,1-38.

Barbour, M. G. 2007. Stable oxygen isotope composition of plant tissue: a review. Functional Plant Biology, 34, 83–94.

Beaumont, J., Gledhill, a., Lee-Thorp, J., and Montgomery, J. 2013. Childhood Diet: a Closer Examination of the Evidence From Dental Tissues Using Stable Isotope Analysis of Incremental Human Dentine*. Archaeometry, 55(2), 277–295. http://doi.org/10.1111/j.1475-4754.2012.00682.x

Bryant, D., Froelich, P. 1995. A model of oxygen isotope fractionation in body water of large mammals. Geochimica et Cosmochimica Acta, 59:4523–4537.

Bryer, M. A. H., Chapman, C. A., and Rothman, J. M. 2013. Diet and polyspecific associations affect spatial patterns among redtail monkeys (*Cercopithecus ascanius*). Behaviour, 150, 277–293. http://doi.org/10.1163/1568539X-00003049

Carlson, B. A. 2011. Reconstructing diet from the ground up: Isotopic Dietary Ecology of Chimpanzees at Ngogo, Kibale National Park, Uganda. PhD. Dissertation, Emory University.

Carlson, B. A., Rothman, J. M., and Mitani, J. C. 2013. Diurnal Variation in Nutrients and Chimpanzee Foraging Behavior. American Journal of Primatology, 75, 342–349. http://doi.org/10.1002/ajp.22112

Carlson, B. A., and Kingston, J. D. 2014. Chimpanzee isotopic ecology: A closed canopy C3 template for hominin dietary reconstruction. Journal of Human Evolution, 76(C), 107–115. http://doi.org/10.1016/j.jhevol.2014.06.001

Carlson, B. A., and Crowley, B. E. 2016. Variation in carbon isotope values among chimpanzee foods at Ngogo, Kibale National Park and Bwindi Impenetrable National Park, Uganda. American Journal of Primatology, 78, 1031–1040.

Cerling, T., Harris, J. 1999. Carbon isotope fractionation between diet and bioapatite in ungulate mammals and implications for ecological and paleoecological studies. Oecologia, 120, 347–363.

Cerling, T.E., Hart, J.A., Hart, T.B., 2004. Stable isotope ecology in the forest. Oecologia 138, 5-12.

Cerling, T.E., Mbua, E., Kirera, F.M., Manthi, F.K., Grine, F.E., Leakey, M.G., Sponheimer, M., Uno, K.T. 2011. Diet of *Paranthropus boisei* in the early Pleistocene of East Africa. Procedings of the National Academy of Sciences, 108 (23), 9337-9341.

Cerling, T.E., Manthi, F.K., Mbua, E.N., Leakey, L.N., Leakey, M.G., Leakey, R.E., Wood, B.A., 2013. Stable isotope-based diet reconstructions of Turkana Basin hominins. Procedings of the National Academy of Sciences, 110 (26), 10501-10506.

Codron, J., Codron, D., Lee-Thorp, J. A., Sponheimer, M., Bond, W. J., de Ruiter, D. 2005. Taxonomic, anatomical, and spatio-temporal variations in the stable carbon and nitrogen isotopic compositions of plants from an African savanna. Journal of Archaeological Science, 32, 1757–1772.

Codron, D., Lee-Thorp, J. A., Sponheimer, M., de Ruiter, D., and Codron, J. 2006. Inter-and intrahabitat dietary variability of Chacma baboons (*Papio ursinus*) in South African savannas based on fecal $\delta^{13}C$, $\delta^{15}N$, and %N. American Journal of Physical Anthropology, 129, 204–214.

Crowley, B. E., Thorén, S., Rasoazanabary, E., Vogel, E. R., Barrett, M. A., Zohdy, S. 2011. Explaining geographical variation in the isotope composition of mouse lemurs (*Microcebus*). Journal of Biogeography, 38, 2106–2121

Crowley, B. E., Sharp, and Crowley, B. E. 2012. Stable Isotope Techniques and Applications for Primatologists. International Journal of Primatology, 33(3), 673–701. http://doi.org/10.1007/s10764-012-9582-7

Dammhahn, M., Kappeler, P.M. 2014. Stable isotope analyses reveal dense trophic species packing and clear niche differentiation in a Malagasy primate community. American Journal of Physical Anthropology 153:249–259.

DeNiro, M.J., Epstein, S. 1981. Influence of diet on the distribution of nitrogen isotopes in animals. Geochimica et Cosmochimica Acta, 45:341–351.

Ehleringer, J. R., Monson, R. K. 1993. Evolutionary and ecological aspects of photosynthetic pathway variation. Annual Review of Ecology and Systematics, 24:411–439.

Fahy, G.E., Richards, M., Riedel, J., Hublin, J-J., Boesch, C. 2013. Stable isotope evidence of meat eating and hunting specialization in adult male chimpanzees. Proceedings of the National Academy of Sciences of the United States of America, 110:5829–5833.

Fahy, G. E. 2014. Stable Nitrogen Isotope Analysis of Dentine Serial Sections Elucidate Sex Differences in Weaning Patterns of Wild Chimpanzees (*Pan troglodytes*). American Journal of Physical Anthropology, 153, 635-642.

Fahy, G. E., Boesch, C., Hublin, J., and Richards, M. P. 2015. The effectiveness of using carbonate isotope measurements of body tissues to infer diet in human evolution : Evidence from wild western chimpanzees (*Pan troglodytes verus*) *. Journal of Human Evolution, 88, 70–78. http://doi.org/10.1016/j.jhevol.2015.09.002

Fricke, H. C., and O'Neil, J. R. 1996. Inter- and intra-tooth variation in the oxygen isotope composition of mammalian tooth enamel phosphate: implications for palaeoclimatological and palaeobiological research. Palaeogeography, Palaeoclimatology, Paleoecology, 126(1–2), 91–99.

Froehle, A.W., Kellner, C.M., Schoeninger, M.J. 2010. Effect of diet and protein source on carbon stable isotope ratios in collagen: follow up to Warinner and Tuross. Journal of Archaeological Science, 37:2662–2670.

Froehle, A.W., Kellner, C.M., Schoeninger, M.J. 2012. Multivariate carbon and nitrogen stable isotope model for the reconstruction of prehistoric human diet. American Journal of Physical Anthropology, 147: 352–369.

Gannes, L. Z., Martinez Del Rio, C. and Koch, P. 1998. Natural abundance variation in stable isotopes and their uses in animal physiological ecology. Comparative Biochemistry and Physiology, 119A, 725–737.

Handley, L. L., Austin, A. T., Robinson, D., Scrimgeour, C. M., Raven, J. A., Heaton, T. H. E. 1999. The N-15 natural abundance (δ15N) of ecosystem samples reflects measures of water availability. Australian Journal of Plant Physiology, 26, 185–199.

Hedges, R. E. M., and Van Klinken, G. J. 2000. "Consider a Spherical Cow..."—on Modeling and Diet. See Ambrose and Katzenberg 2000, pp. 211–31

Henry, A.G., Ungar, P.S., Passey, B.H., Sponheimer, M., Rossouw, L. 2012. The diet of *Australopithecus sediba*. Nature, 487:90–93.

Hoppe, K.A., Paytan, A., Chamberlain, P., 2006. Reconstructing grassland vegetation and paleotemperatures using carbon isotope ratios of bison tooth enamel. Geology, 34, 649–652.

Jim, S., Ambrose, S.H., Evershed, R.P., 2004. Stable carbon isotopic evidence for differences in the dietary origin of bone cholesterol, collagen and apatite: implications for their use in palaeodietary reconstruction. Geochimica et Cosmochimica Acta, 68, 61–72.

Kirsanow, K., Makarewicz, C., Tuross, N., 2008. Stable oxygen ($\delta^{18}O$) and hydrogen (δD) isotopes in ovicaprid dentinal collagen record seasonal variation. J. Archaeol. Sci. 35, 3159e3167.

Koch, P. L. 2007 Isotopic study of the biology of modern and fossil vertebrates. In Stable Isotopes in Ecology and Environmental Science (eds. R. Michener and K. Lajtha). Blackwell Publishing, pp. 99–154.

Kohn, M. J., and Cerling, T. E. 2002. Stable isotope compositions of of biological apatite. Review of Mineral Geochemistry, 48, 455–488.

Krueger, H.W., Sullivan, C.H. 1984. Models for carbon isotope fractionation between diet and bone. In: Turnland JR, Johnson PE (eds) Stable isotopes in nutrition, vol 258, American Chemical SocietyWashington, DC, pp 205–220.

Lambert, J. E. 1997. Digestive Strategies, Fruit Processing, And Seed Dispersal In The Chimpanzees (*Pan Troglodytes*) And Redtail Monkeys (*Cercopithecus Ascanius*) Of Kibale National Park, Uganda. University of Illinois at Urbana-Champaign.

Lee-Thorpe, J.A., van der Merwe, N.J., 1991. Aspects of the chemistry of modern and fossil biological apatites. Journal of Archaeological Science 18, 343–35.

Lee-Thorp, J.A., Van der Merwe, N.J., Brain, C.K. 1994. Diet of *Australopithecus robustus* at Swartkrans from stable carbon isotopic analysis. Journal of Human Evolution, 27:361–372.

Lee-Thorp, J.A., Thackeray, J.F., van der Merwe, N.J. 2000. The hunters and the hunted revisited. Journal of Human Evolution, 39(6):565–576.

Lee-Thorp, J., Likius, A., Mackaye, H. T., Vignaud, P., Sponheimer, M., and Brunet, M. 2012. Isotopic evidence for an early shift to C_4 resources by Pliocene hominins in Chad. Proceedings of the National Academy of Sciences of the United States of America, 109(50), 20369–72. http://doi.org/10.1073/pnas.1204209109

Luz, B., Kolodny, Y., Horowitz, M. 1984. Fractionation of oxygen isotopes between mammalian bone phosphate and environmental drinking water. Geochimica et Cosmochimica Acta, 48, 1689-1693.

Luz, B., Kolodny, Y., 1985. Oxygen isotope variations in phosphate of biogenic apatites. IV. Mammal teeth and bones. Earth and Panetary Sciences Letters, 75, 29-36.

Luz, B., Kolodny, Y. 1989. Oxygen isotope variation in bone phosphate. Appl Geochem, 4:317–323.

Marshall, J. D., Brooks, J. R., and Lajtha, K. 2007. Sources of variation in the stable isotopic composition of plants. In R. Michener & K. Lajtha (Eds.), Stable isotopes in ecology and environmental science (2nd ed., pp. 22–60). Boston: Blackwell.

Martínez del Rio, C., Wolf, N., Carleton, S. A., and Gannes, L. Z. 2009. Isotopic ecology ten years after a call for more laboratory experiments. Biological Reviews ofthe Cambridge Philosophical Society, 84, 91–111.

Muzuka, A. 1999. Isotopic compositions of tropical East African flora and their potential as source indicators of organic matter in coastal marine sediments. Journal ofAfrican Earth Sciences, 28, 757– 766.

Mitani, J.C., Watts, D.P. 2001. Why do chimpanzees hunt and share meat? Animal Behavior 61:915–924.

Nelson, S. V. 2013. Chimpanzee fauna isotopes provide new interpretations of fossil ape and hominin ecologies. Procedings of the Royal Society, 280(November).

O'Brien, D. M., and Wooller, M. J. 2007. Tracking human travel using stable oxygen and hydrogen isotope analyses of hair and urine. Rapid Communications in Mass Spectrometry, 21, 2422–2430.

Oelze, V. M., Fahy, G., Hohmann, G., Robbins, M. M., Leinert, V., Lee, K., … Kühl, H. S. 2016. Comparative isotope ecology of African great apes. Journal of Human Evolution, 101, 1–16. http://doi.org/10.1016/j.jhevol.2016.08.007

O'Leary, M. 1988. Carbon isotope in photosynthesis. Bioscience, 38, 328-336.

Passey, B. H. and Cerling, T. E. 2002. Tooth enamel mineralization in ungulates: Implications for recovering a primary isotopic time-series. Geochimica et Cosmochimica Acta, 66, 3225–3234.

Passey, B., and Cerling, T. 2006. In situ stable isotope analysis ($\delta^{13}C$, $\delta^{18}O$) of very small teeth using laser ablation GC/IRMS. Chemical Geology, 235(3–4), 238–249. http://doi.org/10.1016/j.chemgeo.2006.07.002.

Passey, B.H., Cerling, T.E., Schuster, G.T., Robinson, T.F., Roeder, B.L., Krueger, S.K. 2005. Inverse methods for estimating primary input signals from time-averaged isotope profiles. Geochimica et Cosmochimica Acta, 69:4101–4116.

Potts, K. B., Watts, D. P., and Wrangham, R. W. 2011. Comparative Feeding Ecology of Two Communities of Chimpanzees (*Pan troglodytes*) in Kibale National Park, Uganda. International Journal of Primatology, 32(3), 669–690. http://doi.org/10.1007/s10764-011-9494-y

Smith, C. C., Morgan, M. E., and Pilbeam, D. 2010. Isotopic ecology and dietary profiles of Liberian chimpanzees. Journal of Human Evolution, 58(1), 43–55. http://doi.org/10.1016/j.jhevol.2009.08.001.

Sponheimer, M., Lee-Thorp, J.A. 1999. Isotopic evidence for the diet of an early hominid, *Australopithecus africanus*. Science, 283(5400):368–370.

Sponheimer, M., Robinson, T., Ayliffe, L., Roeder, B., Hammer, J., Passey, B. 2003. Nitrogen isotopes in mammalian herbivores: hair $\delta^{15}N$ values from controlled feeding study. International Journal of Osteoarchaeology, 13, 80–87.

Sponheimer, M., Lee-Thorp, J., de Ruiter, D., Codron, D., Codron, J., Baugh, A.T., Thackeray, F. 2005. Hominins, sedges, and termites: new carbon isotope data from the Sterkfontein valley and Kruger National Park. Journal of Human Evolution, 48:301–312.

Sponheimer, M., Passey, B. H., de Ruiter, D. J., Guatelli-Steinberg, D., Cerling, T. E., and Lee-Thorp, J.

A. 2006. Isotopic evidence for dietary variability in the early hominin *Paranthropus robustus*. Science, 314, 980–982.

Sponheimer, M., Alemseged, Z., Cerling, T. E., Grine, F. E., Kimbel, W. H., Leakey, M. G., … Wynn, J. G. 2013. Isotopic evidence of early hominin diets. Proceedings of the National Academy of Sciences, 110(26), 1–6. http://doi.org/10.1073/pnas.1222579110

Trudinger, C.M., Enting, I.G., Francey, R.J., Etheridge, D.M., Rayner, P.J., 1999. Long- term variability in the global carbon cycle inferred from a high-precision CO_2 and $\delta^{13}C$ ice-core record. Tellus Series B: Chemical and Physical Meteorology. 51, 233–248.

van der Merwe, N.J., Thackeray, J.F., Lee-Thorp, J.A., Luyt, J., 2003. The carbon isotope ecology and diet of *Australopithecus africanus* at Sterkfontein, South Africa. Journal of Human Evolution, 44, 581–597.

van der Merwe, N.J., Masao, F.T., Bamford, M.K. 2008. Isotopic evidence for contrasting diets of early hominins *Homo habilis* and *Australopithecus boisei* of Tanzania. South African Journal of Science, 104:153–155.

Watts, D. P., Muller, M. N., Amsler, S. J., Mbabazi, G., and Mitani, J. C. 2006. Lethal Intergroup Aggression by Chimpanzees in Kibale National Park , Uganda, American Journal of Primatology, 180 (February 2005), 161–180. http://doi.org/10.1002/ajpa.

Watts, D.P., Potts, K.B., Lwanga, J.S., Mitani, J.C. 2012. Diet of chimpanzees (*Pan troglodytes schweinfurthii*) at Ngogo, Kibale National Park, Uganda, 1. Diet composition and diversity. American Journal of Primatology, 74, 114-129.

Werner, R. A., and Schmidt, H.-L. 2002. The in vivo nitrogen isotope discrimination among organic plant compounds. Phytochemistry, 61, 465–484.

Wiedemann-Bidlack, F. B., Colman, A. S., and Fogel, M. L., 2008, Phosphate oxygen isotope analysis on microsamples of bioapatite: removal of organic contamination and minimization of sample size, Rapid Communications in Mass Spectrometry, 22, 1807–16.

White, T.D., Asfaw, B., Beyene, Y., Haile-Selassie, Y., Lovejoy, C.O., Suwa, G., and Giday, W. *Ardipithecus ramidus* and the Paleobiology of Early Hominids. In: Science, 326 (5949), 2009, pp. 75–86; doi:10.1126/science.1175802

Wood, B. M., Watts, D. P., Mitani, J. C., and Langergraber, K. E. 2017. Favorable ecological circumstances promote life expectancy in chimpanzees similar to that of human hunter-gatherers. Journal of Human Evolution, 105, 41-56. http://doi.org/10.1016/j.jhevol.2017.01.003

Wynn, J. G., Sponheimer, M., Kimbel, W. H., Alemseged, Z., Reed, K., Bedaso, Z. K., and Wilson, J. N. 2013. Diet of *Australopithecus afarensis* from the Pliocene Hadar Formation, Ethiopia. Proceedings of the National Academy of Sciences of the United States of America, 110(26), 10495–500. http://doi.org/10.1073/pnas.1222559110

Chapter 5: Conclusions, Implications and Future Directions

This project investigated the relationships between the dental development, the weaning process, and the diets of wild Ugandan chimpanzees (*Pan troglodytes schweinfurthii*) using three different, but interrelated methods. The first study used histological analysis to measure and compare dental formation and emergence variables from several chimpanzee communities, to assess whether chimpanzees from Ngogo have delayed dental development relative to other populations, and to situate that outcome within life history theory. The second study examined the relationship between trace elemental distributions in chimpanzee dental tissues and structural indicators of developmental pace, to assess whether a peak in M1 root growth rate showed evidence of aligning with weaning completion. The third study attempted to disentangle the numerous sources of variability in chimpanzee dietary inputs, which manifest in various bodily tissues, and which inform studies of dietary reconstruction, paleoecology, and life history for extinct taxa, including fossil hominins.

Chapter 2 Conclusions: The estimated M_1 emergence age range of 2.15-4.10 years in this study's chimpanzee sample, and the similar range of 2.14-3.99 years for the known captive chimpanzee sample, suggests that, instead of being dentally delayed relative to captive chimpanzees (Zihlman et al., 2004; 2007), the range in M1 emergence ages in wild chimpanzees is at least as wide as that for captive ones (Smith et al., 2007). These new data can inform the discussion of the appropriateness of using dental devlopment data from captive chimpanzees in comparative studies of fossil hominins (Smith et al., 2010). Additionally, by using adult

individuals, this study circumvents the issue of using deceased juveniles, whose development may have been atypical, to infer developmental pace for that population (Smith and Boesch, 2011).

It was also predicted that this new sample, made up of small numbers of individuals from four different Ugandan chimpanzee communities would help illustrate the dental developmental variability to be expected within a single *Pan* subspecies, and this was achieved by increasing the previously known *P.t. schweinfurthii* M_1 emergence age range from 9.6 months in three Kanyawara chimpanzees (Machanda et al., 2015), to almost two years when data from this study were included.

For the Ngogo chimpanzees in this study, the M_1 root growth spurts all fell considerably after the age range of Kanyawara M_1 emergence (Machanda et al., 2015), which suggests that the chimpanzee M_1 root growth spurt is more likley to coincide with its attainment of occlusion than with its emergence. Further support of this is that the estimated M1 emergence ages for most of the Ngogo chimpanzees were also somewhat after those at Kanyawara, or on the late end of their range (Malone, Chapter 2 p.35).

The fifth prediction, that the root growth spurt and M_1 occlusion age slightly precede weaning completion, was supported by the growth spurt age range of 3.03 - 4.60 years in the Ngogo chimpanzees in this sample, and the inferred mean age at weaning completion (4.0-4.5 years) from fecal isotope data of Ngogo infant-mother pairs (Badescu et al., 2017).

Results overall suggest that an M_1 root growth spurt, likely coinciding with the attainment of functional occlusion, followed by an abrupt drop in stress episode frequency, may represent a structural proxy for the threshold of nutritional independence/weaning completion in

these Ugandan chimpanzees. However, to more robustly link the root growth spurt/occlusion age to weaning completion, another proxy for weaning in these specific individuals was needed.

Chapter 3 Conclusions: This chapter addressed the need for a proxy of dietary changes during the weaning process by determining the variation in Calcium-normalized barium (Ba/Ca) intensities within the M1 enamel and dentine of these Ugandan chimpanzees, since this variation has been linked to the transition from nursing to adult foods in the teeth of multiple extant and fossil hominoids.

This study found that the changes in Ba/Ca intensity (that presumably reflect dietary changes) do show the same general patterns of increase and decrease through developmental time in chimpanzees as in other primates for which this has been assessed. It was also found that the Ba/Ca values increased at the time of the M_1 root growth spurt, followed by a decrease that continued thereafter, (except in cases of enamel damage), which supported the hypothesis that weaning completion occurred just after the M1 root growth spurt in these chimpanzees. Since the growth spurts of these individuals were found to align well with the inferred ages at nutritional independence in Ngogo chimpanzees as assessed in a fecal isotope study (Badescu et al., 2017), this lends further support to this study's proposed connection between the M_1 root growth spurt and weaning completion.

One of the implications of these findings is that age at weaning completion, an important life history variable, can potentially be directly measured in isolated M1s that are no longer in the mandible, since the growth spurt can be measured in the M1 root and changing Ba/Ca values can be obtained from the root dentine. (We used the M1s and M2s or P4s, but it may be possible, and much simpler, to do this with only the M1s.) These structural and chemical correspondences

should be confirmed in other chimpanzee populations, as well as in other primate taxa to assess whether this association holds true.

Another potential outcome of this study is that this method of determining the M1 root growth spurt age could be applied to dental remains in the fossil record, including those of fossil hominins, though further study into the integrity of the trace elemental signals in fossil enamel is a necessary precursor to such studies. Since this study successfully tracked this structural and chemical proxy for weaning completion in the teeth of adult individuals, it may be possible to significantly increase the sample size for which we can infer weaning completion age in fossil taxa, if we do not have to rely upon using only juvenile remains to infer M_1 emergence age. This also eliminates the potential complication of using dental remains from deceased juveniles whose early deaths may not indicate "typical" developmental patterns, compared with individuals that survived through adulthood (see Smith and Boesch, 2011).

Chapter 4 Conclusions: Our data suggest that there may be a habitat-specific difference in $\delta^{13}C_{\text{bone collagen-hair keratin}}$ offsets, since the values from this study, limited though they are, show a lower offset value than has been recorded for other sites (DeNiro and Epstein, 1981). An overall adult $\delta^{13}C_{\text{enamel apatite}}$ range of -14.3 to -16.0‰ and an $\delta^{18}O_{\text{enamel apatite}}$ range of 1.2 to -1.4‰ was determined for the chimpanzees in this study. Based upon the tissue-specific isotope values of all of these chimpanzees, and the isotopic contents of their food items and percent of time spent feeding on each, we have calculated provisional "total dietary input" values of $\delta^{13}C$ -27.4‰ and $\delta^{15}N$ 4.2‰. This creates numerous diet-to-tissue fractionation factors for these individuals, but the most relevant one for fossil hominin dietary reconstructions is the $\delta^{13}C_{\text{diet-enamel apatite}}$ fractionation factor for the Ngogo chimpanzees, which we estimate as +12.3‰.

Future Directions

In future work seeking to resolve the issue of the co-occurrence of the M_1 root growth spurt and occlusion, it would be beneficial to measure the growth spurt on the intact dental remains of as many juvenile chimpanzees as possible. This would permit the root growth spurt and M_1 emergence age to be measured on the same individual, thereby avoiding the use of pooled M_1 emergence data in favor of direct comparisons. Doing so will allow the verification the 2.5-6.0 month emergence-to-occlusion delay, instead of inferring one parameter from the other and introducing error at each step.

In order to more accurately compare weaning age data between chimpanzee populations and subspecies, further fecal isotope studies should be carried out in populations such as the Taï Forest chimpanzees, those at Mahale and Gombe, as well as at Bwindi and Kanyawara. Doing so will allow consistent measures of "weaning completion" to be compared to see whether the Ngogo chimpanzees do, in fact, wean later than other populations.

Along with such fecal isotope studies for extant primates, it would be worthwhile to characterize the variability in the isotopic offsets between tissues such as hair, which can be collected frequently and non-invasively, and enamel apatite, the critical tool for investigating the diets and environments of fossil taxa.

The use of histological, stable isotopic, and trace elemental analyses, when utilized together, show great promise for future efforts to characterize the variability in diets, dental development, and weaning behavior in wild primates. Such endeavors will, in turn, open new channels of inquiry concerning fossil hominin life history evolution.

Appendix

Appendix Table 23: M1 and M2 Periodic Variable Measurements for the Chimpanzees in theis Study

	M1 mb icdsr	M1 mb mcdsr	M1 mb ocdsr	M1 mb iidsr	M1 mb midsr	M1 mb oidsr	M1 avg mb cdsr	M1 avg mb idsr	M2 mb icdsr	M2 mb mcdsr	M2 mb ocdsr	M2 mb iidsr	M2 mb midsr	M2 mb idsr	M2 avg mb cdsr	M2 avg mb idsr
NG001	4.264	4.346	4.551	5.320	5.352	5.518	4.387	5.397	4.240	4.290	4.340	4.013	4.113	4.213	4.290	4.113
NG002	4.432	4.684	4.887	5.747	5.891	6.747	4.668	6.033	3.449	4.200	5.141	4.462	4.917	4.981	4.263	4.786
NG004	4.796	5.814	5.914	5.864	5.914	5.964	4.796	5.914	4.642	4.679	5.307	4.574	5.093	5.478	4.876	5.048
NG005	4.240	4.922	5.967	4.402	5.860	6.642	5.043	5.635	N/A	N/A	N/A	N/A	N/A	N/A	N/A	N/A
NG012	3.452	5.580	6.358	4.666	4.994	5.887	5.130	5.182	3.601	4.196	5.263	3.341	4.431	5.522	4.353	4.431
NG013	3.652	4.180	5.236	4.176	4.622	5.013	4.356	4.604	3.201	4.003	4.963	3.147	4.031	4.904	4.056	4.027
MUZM	4.002	4.187	4.371	5.244	5.397	5.549	4.187	5.397	N/A	N/A	N/A	N/A	N/A	N/A	N/A	N/A
NG003	N/A	N/A	N/A	N/A	N/A	N/A	N/A	N/A	N/A	N/A	N/A	N/A	N/A	N/A	4.563	4.586
N	N=7	N=7	N=7	N=7	N=7	N=7	N=7	N=7	N=5	N=5	N=5	N=5	N=5	N=5	N=6	N=6
Mean	4.120	4.816	5.326	5.060	5.433	5.903	4.652	5.452	3.826	4.273	5.003	3.907	4.517	5.020	4.400	4.499
min	3.452	4.180	4.371	4.176	4.622	5.013	4.187	4.604	3.201	4.003	4.340	3.147	4.031	4.213	4.056	4.027
max	4.796	5.814	6.358	5.864	5.914	6.747	5.130	6.033	4.642	4.679	5.307	4.574	5.093	5.522	4.875	5.048
Sd σ	0.460	0.662	0.768	0.657	0.497	0.623	0.360	0.480	0.596	0.250	0.394	0.645	0.474	0.531	0.285	0.392

Appendix Table 24: M3 and P4 Periodic Variable Measurements

	M3 mb icdsr	M3 mb mcdsr	M3 mb ocdsr	M3 mb iidsr	M3 mb midsr	M3 mb oidsr	M3 av cdsr	M3 av idsr	P4 mb icdsr	P4 mb mcdsr	P4 mb ocdsr	P4 mb iidsr	P4 mb midsr	P4 mb oidsr	P4 av cdsr	P4 av idsr
NG001	4.086	4.577	5.068	5.580	5.602	6.234	4.577	5.805	N/A	N/A	N/A	N/A	N/A	N/A	N/A	N/A
NG002	4.684	6.104	6.113	4.580	5.099	5.643	5.634	5.107	N/A	N/A	N/A	N/A	N/A	N/A	N/A	N/A
NG004	4.655	4.894	4.463	4.017	4.953	5.007	4.670	4.659	N/A	N/A	N/A	N/A	N/A	N/A	N/A	N/A
NG005	4.114	5.194	5.914	4.395	5.205	5.653	5.074	5.084	4.638	4.791	5.314	4.444	5.687	5.763	4.914	5.298
NG012	5.134	5.234	5.334	5.605	5.705	5.805	5.236	5.705	N/A	N/A	N/A	N/A	N/A	N/A	N/A	N/A
NG013	3.729	4.200	4.668	3.394	4.058	5.139	4.199	4.197	N/A	N/A	N/A	N/A	N/A	N/A	N/A	N/A
MUZM	3.993	4.307	4.649	4.321	4.938	4.963	4.316	4.740	3.948	4.370	4.729	4.196	4.279	4.362	4.349	4.279
NG003	5.179	5.234	5.289	5.064	5.187	5.311	5.234	5.187	4.078	4.168	4.258	4.239	4.338	4.436	4.168	4.338
N	N=8	N=8	N=8	N=8	N=8	N=8	N=8	N=8	N=3	N=3	N=3	N=3	N=3	N=3	N=3	N=3
Mean	4.447	4.968	5.187	4.619	5.093	5.469	4.867	5.061	4.221	4.442	4.767	4.293	4.768	4.853	4.477	4.638
min	3.729	4.201	4.463	3.394	4.058	4.963	4.199	4.197	3.948	4.168	4.258	4.196	4.279	4.362	4.168	4.279
max	5.179	6.104	6.113	5.605	5.705	6.234	5.634	5.805	4.077	4.791	5.314	4.444	5.687	5.763	4.168	5.298
Sd σ	0.544	0.617	0.600	0.765	0.503	0.442	0.503	0.534	0.367	0.318	0.529	0.133	0.797	0.788	0.389	0.572

Tables 24 (top) and 2 (bottom): Inner, middle, and outer cuspal and imbricational enamel daily secretion rates (DSR in μm) of M1-M3. Average values are given by region of each tooth for each individual and overall descriptive statitics by tooth type are given for the whole population.

Appendix Table 25: Descriptive Statistics for periodic variables of all teeth

		CDSR			IDSR			RP			TFT	
	mean	**range**	**σ**	**mean**	**range**	**σ**	**mean**	**range**	**σ**	**mean**	**range**	**σ**
M1 mb	4.65 n=7	4.19-5.13	0.36	5.45	4.60-6.03	0.48	5.38 n=8	5-6	0.52	646	502- 776	85.29
M2 mb	4.40 n=6	4.06-4.88	0.29	4.50	4.03-5.05	0.39	“”	“”	“”	781	661- 857	72.9
M3 mb	4.87 n=8	4.20-5.63	0.50	5.06	4.20-5.81	0.53	“”	“”	“”	963	885- 1111	82.62
P4 mb	4.48 n=3	4.17-4.91	0.39	4.64	4.28-5.30	0.57	“”	“”	“”	N/A	N/A	N/A
χ	4.64	3.15-6.75	N/A	5	N/A	N/A	5.38	N/A	N/A	N/A	N/A	N/A

Means, ranges and standard deviations of M1-M3 periodic variables (CDSR= cuspal daily secretion rate, IDSR= imbricational daily secretion rate, RP= Retzius Periodicity, TFT= total formation time)

Appendix Table 26: Measures of M1 periodic variables

	Tooth/	Cusp	AVG CDSR (µm)	CFT (min days)	CFT (min yrs)	AVG IDSR (µm)	RP (days)	R# (min)	IFT (min days)	IFT (min yrs)	TFT (min days)	TFT (min yrs)
NG001	RM1	mb	4.39	177	0.48	5.40	5	65	325	0.89	502	1.38
NG002	RM1	mb	4.67	226	0.62	6.03	5	72	360	0.99	586	1.61
NG003	LP4	mb	4.17	N/A	N/A	4.34	6	N/A	N/A	N/A	N/A	N/A
NG004	RM1	mb	4.80	224	0.62	5.92	5	98	490	1.34	714	1.96
NG005	RM1	mb	4.36	187	0.51	5.26	5	80	400	1.10	587	1.61
NG012	LM1	mb	5.13	193	0.53	5.18	6	70	420	1.15	613	1.68
NG013	RM1	mb	4.90	268	0.73	4.34	5	78	390	1.07	658	1.80
MUZM	RM1	mb	4.19	225	0.6	5.40	6	92	552	1.51	777	2.13

Measures and counts of periodic structures, in #s or µm, of the M1 for all eight chimpanzees (except for the P3 in NG003) in both days and years. (CDSR= cuspal daily secretion, CFT= cuspal formation time, IDSR= imbricational daily secretion rate, RP= Retzius Periodicity, R#= Retzius #, IFT= imbricational formation time, TFT= total formation time)

Appendix Table 27: Measures of M2/P4 periodic variables

	Tooth/	Cusp	AVG CDSR (µm)	CFT (min days)	CFT (min yrs)	AVG IDSR (µm)	RP (days)	R# (min)	IFT (min days)	IFT (min yrs)	TFT (min days)	TFT (min yrs)
NG001	RM2	mb	4.29	231	0.63	4.11	5	86	430	1.18	661	1.81
NG002	LM2	mb	4.26	278	0.76	4.79	5	61	305	0.84	583	1.60
NG003	LM2	mb	4.56	N/A	N/A	4.586	6	133	798	2.19	N/A	N/A
NG004	LM2	mb	4.88	171	0.47	5.05	5	113	565	1.55	736	2.02
NG005	RP4	mb	4.91	234	0.64	5.30	5	103	515	1.41	749	2.05
NG012	LM2	mb	4.35	246	0.67	4.43	6	118	708	1.94	954	2.61
NG013	RM2	mb	4.68	199	0.55	4.59	5	94	470	1.29	669	1.83
MUZM	RP4	mb	4.35	202	0.55	4.28	6	120	720	1.97	922	2.53

Measures and counts of periodic structures, in #s or µm, of the M2 for all eight chimpanzees (except for P4 in NG005 and MUZM2625) in days and years.

Appendix Table 28: Measures of M3 periodic variables

	Tooth/	Cusp	AVG CDSR (µm)	CFT (min days)	CFT (min yrs)	AVG IDSR (µm)	RP (days)	R# (min)	IFT (min days)	IFT (min yrs)	TFT (min days)	TFT (min yrs)
NG001	RM3	mb	4.58	322	0.88	5.81	5	120	600	1.64	922	2.53
NG002	RM3	mb	5.63	208	0.57	5.11	5	68	340	0.93	548	1.50
NG003	LM3	mb	5.23	N/A	N/A	5.19	6	N/A	N/A	N/A	N/A	N/A
NG004	LM3	mb	4.67	140	0.38	4.66	5	91	455	1.25	595	1.63
NG005	RM3	mb	5.07	204	0.56	5.08	5	106	530	1.45	734	2.01
NG012	LM3	mb	5.23	261	0.71	5.71	6	93	558	1.53	819	2.24
NG013	RM3	mb	4.20	330	0.90	4.20	5	126	630	1.73	960	2.63
MUZM	RM3	mb	4.32	199	0.55	4.74	6	85	510	1.40	709	1.94

Measures and counts of periodic structures, in #s or µm, of the M3 for all eight chimpanzees in both days and years.

Appendix Figure 30: Supplemental Ba/Ca values from all eight red-tailed monkey M1s